Best Available
Copy
for all Pictures

AD-772 947

UH-1D FILAMENT-WOUND TUBULAR-REINFORCED ROTOR BLADE

David Wall, et al

Fiber Science, Incorporated

Prepared for:

Army Air Mobility Research and Development Laboratory

October 1973

DISTRIBUTED BY:

NTIS

National Technical Information Service
U. S. DEPARTMENT OF COMMERCE
5285 Port Royal Road, Springfield Va. 22151

Unclassified
Security Classification

AD 772 947

DOCUMENT CONTROL DATA - R & D

(Security classification of title, body of abstract and indexing annotation must be entered when the overall report is classified)

1. ORIGINATING ACTIVITY *(Corporate author)* Fiber Science, Inc. 245 East 157th Street Gardena, California	2a. REPORT SECURITY CLASSIFICATION Unclassified 2b. GROUP

3. REPORT TITLE

UH-1D FILAMENT-WOUND TUBULAR-REINFORCED ROTOR BLADE

4. DESCRIPTIVE NOTES *(Type of report and inclusive dates)*

Final Report

5. AUTHOR(S) *(First name, middle initial, last name)*

David Wall
Dale Abildskov
Larry Ashton

6. REPORT DATE	7a. TOTAL NO. OF PAGES	7b. NO. OF REFS
October 1973	~~112~~ 115	

8a. CONTRACT OR GRANT NO. DAAJ02-72-C-0013 b. PROJECT NO. Task 1F162208A17001 c. d.	9a. ORIGINATOR'S REPORT NUMBER(S) USAAMRDL Technical Report 73-61 9b. OTHER REPORT NO(S) *(Any other numbers that may be assigned this report)*

10. DISTRIBUTION STATEMENT

Approved for public release; distribution unlimited.

11. SUPPLEMENTARY NOTES	12. SPONSORING MILITARY ACTIVITY Eustis Directorate U. S. Army Air Mobility R&D Laboratory Fort Eustis, Virginia

13. ABSTRACT

The results of engineering design, fabrication and testing of filament-wound tubular-reinforced composite main rotor blades for the UH-1D helicopter are reported herein. Three blades were fabricated using wet winding, two using principally S-glass roving/epoxy and one using principally PRD-49 roving. In the course of the program, a design concept for making a highly redundant root-end attachment was developed and the fabrication feasibility was proven. The ability to calculate the structural characteristics was verified within the testing and fabrication tolerances.

DD FORM 1 NOV 65 1473 REPLACES DD FORM 1473, 1 JAN 64, WHICH IS OBSOLETE FOR ARMY USE.

Unclassified
Security Classification

14 KEY WORDS	LINK A		LINK B		LINK C	
	ROLE	WT	ROLE	WT	ROLE	WT
Main rotor blades						
Filament-wound tubular-reinforced rotor blades						
UH-1D helicopter						

DEPARTMENT OF THE ARMY
U. S. ARMY AIR MOBILITY RESEARCH & DEVELOPMENT LABORATORY
EUSTIS DIRECTORATE
FORT EUSTIS, VIRGINIA 23604

This program was carried out under Contract DAAJ02-72-C-0013 with Fiber Science Inc.

The report presents the results of the design, fabrication, and limited testing of full-scale filament-wound tubular spar UH-1D main rotor blades.

The report has been reviewed by the Eustis Directorate, U.S. Army Air Mobility Research and Development Laboratory and is considered to be technically sound. It is published for the exchange of information and the stimulation of future research.

This program was conducted under the technical management of Messrs. Kenneth Bauman and Irving E. Figge, Technology Applications Division.

Task 1F162208A17001
Contract DAAJ02-72-C-0013
USAAMRDL Technical Report 73-61
October 1973

UH-1D FILAMENT-WOUND TUBULAR-REINFORCED ROTOR BLADE

Final Report

By

D. Wall
D. Abildskov
L. Ashton

Prepared by

Fiber Science, Inc.
Gardena, California

for

EUSTIS DIRECTORATE
U.S. ARMY AIR MOBILITY RESEARCH AND DEVELOPMENT LABORATORY
FORT EUSTIS, VIRGINIA

SUMMARY

The results of engineering design, fabrication and testing of filament-wound tubular-reinforced composite main rotor blades for the UH-1D helicopter are reported herein. Three blades were fabricated using wet winding, two using principally S-glass roving/epoxy and one using principally PRD-49 roving.

In the course of the program, a design concept for making a highly redundant root-end attachment was developed and the fabrication feasibility was proven. The ability to calculate the structural characteristics was verified within the testing and fabrication tolerances.

The first and third blades fabricated, serial numbers 001 and 003, respectively, and a conventional metallic blade were tested, statically and dynamically, to evaluate their stiffnesses and natural frequencies--each being supported as a simple cantilever beam. Table I summarizes the results of this testing.

Figure 1 shows a complete filament-wound tubular-reinforced composite rotor blade.

The objectives of the program were (1) to establish the feasibility of designing and constructing a filament-wound tubular-element-reinforced composite rotor blade and (2) to perform simple static and dynamic testing to verify the accuracy of analysis and to prove the tailorability of the new composite approach.

These objectives were satisfactorily met, although, in the effort to duplicate the stiffness characteristics of the existing aluminum rotor blade, a design using all fiberglass materials was determined very early in the program to be short of the stiffness requirements because of the low modulus of glass fibers.

A significant achievement in the program was the development of computer program design and analysis techniques compatible with the inherent tailorability of the rotor blade. The concept promises to offer advantages in design and method of manufacture--both important in low-cost construction.

FOREWORD

This report was prepared by Fiber Science, Inc., a subsidiary of the Edo Corporation, for the Eustis Directorate, U.S. Army Air Mobility Research and Development Laboratory, Fort Eustis, Virginia. Mr. Kenneth Bauman and Mr. I. E. Figge were the U.S. Army program monitors.

The activities reported herein cover the period from October 1971 to January 1973. The project engineer was Mr. David Wall. Other significant contributors to the program include Messrs. D. Abildskov, M. Rivera and L. Ashton of Fiber Science, Inc.

The work was authorized by DA Task 1F162208A17001.

TABLE OF CONTENTS

LIST OF ILLUSTRATIONS

LIST OF ILLUSTRATIONS - CONTINUED

LIST OF TABLES

LIST OF SYMBOLS

A	area (in.^{2})	
AE	spanwise stiffness (lb)	
C	coefficient of damping	
CG	center of gravity, dist. aft of leading edge (in.)	
c	dimension measured from NA (in.)	
d	dimension (in.)	
E	modulus of elasticity (psi)	
EI_x	bending stiffness about x axis (lb-in.^{2})	See Figure 32
EI_y	bending stiffness about y axis (lb-in.^{2})	See Figure 32
F	allowable strength (psi)	
G	modulus of rigidity (psi)	
I	moment of inertia (in.^{4})	
K	torsional constant (in.^{4})	
KG	torsional stiffness (lb-in.^{2})	
M	bending moment (in.-lb)	
MS	margin of safety	
P	load (lb)	
QE	moment area times modulus (lb-in.)	
t	thickness (in.)	
V	shear (lb), volume ratio	
W	weight ratio, unit weight (lb/in.)	
x	dimension measured from leading edge, in.	
α	coefficient of thermal expansion (in./in./°F), angle (deg)	
μ	Poisson's ratio	

LIST OF SYMBOLS - CONTINUED

ρ	density (lb/in.^{3})
σ	unit stress (psi)
τ	unit shear stress (psi)

Subscripts

b	denotes beamwise direction
bru	denotes bearing ultimate
c	denotes chordwise direction, denotes composite
cu	denotes compression ultimate
r	refers to resin
su	denotes sheer ultimate
t	denotes torsion
tu	denotes tension ultimate

INTRODUCTION

Fiber-reinforced plastic materials have been considered for use in helicopter rotor blades for some time. The interest centers around the high strength-to-weight ratio of composites--especially unidirectional composites. The fiber/matrix combinations offer advantages of high fatigue life and field repairability. Helicopter engineers have been quick to recognize the advantages of glass and other fiber composites in extending rotor blade life; therefore, several manufacturers in the United States and Europe have developed data on the use of glass-reinforced rotor blades supporting the goal of improved blade life and the potential weight advantages of composite construction.

The building of an all-composite reinforced rotor blade can be a costly operation if conventional hand-layup or tape-layup systems are utilized in the construction technique. The use of hand-layup for building composites adds the human variable to the manufacturing technique. Stringent quality assurance cannot prevent workmanship from being a significant contribution in affecting the performance and cost of the blade.

The study and work performed herein was undertaken to prove the manufacturing feasibility of building a complicated rotor blade using wet filament winding as the manufacturing technique. In the work performed, filament winding is the predominant method of manufacture for fabricating the rotor blade spar (a series of tubular filament-wound elements and wound "pultrusions"), the blade trailing-edge spine, and the blade skin. Filament winding using the wet impregnation process was chosen because the operation allows the deposition, placement and control of glass filament and epoxy resin at the very lowest possible material cost while providing a very high degree of reproducibility and quality control.

This report represents the results of a research and development program to design, fabricate and test a full-scale tubular-reinforced composite blade having the configuration and structural capability of the UH-1D main rotor blade. The primary objectives of the program were to demonstrate fabrication feasibility and predictability of the design.

The blade is 24 feet long from the center of rotation to its tip, has a chord length of 21 inches, and has a basic NACA-0012 airfoil shape except in the root-end fitting area.

The design goal was to match the characteristics of the existing metal blade as closely as possible; however, it was recognized

that it would be impossible to match the stiffnesses using glass fibers. The use of PRD-49 fibers in the skins would enable a much closer match of the stiffnesses.

A computer program was developed as a design aid for calculating the cross-sectional properties of the tubular reinforced composite blade. A copy of this program is included in Appendix I.

The main body of this report is primarily concerned with reporting the design, fabrication techniques and test results. The drawings are presented in Appendix II.

BLADE DESIGN

DESIGN CRITERIA

The structural design goal was to match, as nearly as possible, the properties of the existing UH-1D rotor blade using the FSI tubular-reinforced composite concept. Also, the material selection was to be made with the goal of not adversely affecting the inherent radar cross section of the rotor blade.

The order of importance assigned to the various criteria was as follows:

1. The blade weight should be equal to the weight of the current metal blade.

2. The center of gravity should be at the same location as it is in the current metal blade.

3. The torsional stiffness should be the same as it is in the current metal blade.

4. The chordwise stiffness should be the same as it is in the current metal blade.

5. The spanwise stiffness should be the same as it is in the current metal blade.

The design parameters and loads were taken from the current metal blade and used as criteria for the tubular-reinforced composite blade. These criteria are given in Tables II, III and IV.

MATERIAL SELECTION

The materials were selected on the basis of strength, density, moduli and radar reflectivity. The properties of the basic materials used in the design analysis are shown in Table V.

The theoretical properties of S-glass and PRD-49/epoxy used for the rotor blade skins are shown in Figures 2 and 3.

The resin volume, weight and composite density relations of E-glass, S-glass and PRD-49/epoxy are shown in Figures 4, 5 and 6.

The composite properties of the various items making up the blade (skin, nose fill, tubes, trailing-edge tip and foam material) are shown in the computer output cross-sectional

property data tables (Tables VIII through X). NOTE: The density used with the aft (trailing edge) skin accounted for a .005 inch thickness of adhesive to bond the skin to the PVC foam.

STRUCTURAL DESIGN

The UH-1D filament-wound tubular-reinforced composite rotor blade has the same airfoil configuration as the current metallic UH-1D rotor blade except that the root-end buildup has been extended 4.25 inches inboard and given a smooth taper. (See Appendix II, drawing 48-XB-001.)

The design concept was based on using a fabrication concept which is amenable to low-cost automated (machine) fabrication techniques and minimizes any interlaminar shear requirements on the resin. The root-end fitting is highly redundant with the longo material wrapping around the root-end fitting.

Blade configuration, cross-sectional properties and stresses are presented in Figures 7 through 10, Tables VI through X and Appendix III.

BLADE FABRICATION

Three UH-1D main rotor blades were fabricated during the program. The tool design and manufacturing methods were oriented to the limited quantity of prototype rotor blades to be built.

Fabrication of the blade can be separated into five disciplines: (1) filament winding, (2) laminating, (3) foam machining, (4) steel machining and (5) assembly of components. The fabrication flow chart including the tools and equipment used is shown in Figure 11.

FILAMENT WINDING

The tubes, longo material and skin material were all fabricated by the filament wet-winding process. With the exception of the nose rod, which was constructed by the "pultrusion" process, and the number 2 tube, which was wound over a "pultruded" rod, the tubes were all initially wound on 65-inch-long steel mandrels to a wall thickness of .0123 inch. See Figure 12. Removal of the wound tubes from their mandrels (polished steel) was accomplished as follows: The mandrels were made in three pieces--two removable end domes and one hollow cylindrical center section. When the windings around one of the end domes were cut off and the end dome removed, water was pumped (p = 2,500 psi) into the cylindrical mandrel which pushed against the end fitting, still held by the windings, driving it off and pulling with it the wound tube. Five of these short thin-wall tubes were then bonded together (overlapping shear joint), making up the full-length tubular element. These tubular elements were then overwrapped to the desired wall thickness. The long tubes used in S/N 001 were supported at five intermediate points in addition to end supports during the overwinding operation (see Figure 13); however, considerable damage was done to the windings by the intermediate supports. A technique of applying axial tension to the tube was developed which eliminated the requirement of intermediate supports.

The thick-wall tubes used in the nose section were kept in the uncured condition until they were combined with the longo material in the main mold. The thin-wall tubes in the aft portion of the blade were cured prior to final assembly.

The longo material was wound under tension into a loop. See Figure 14. While still in the wet condition, the resin was gradually squeezed out until the proper weight was reached. The longo material was then positioned in the main mold and wrapped around the root end fitting. Unidirectional (style 143) fabric was interspersed with the longo material in the fitting wrap-

around area. The root-end fitting was secured to the mold and was configurated to the proper shape by pulling it through a "pultrusion" type die. Once configurated and properly positioned, a tension load was applied to the longo material at the blade tip end. The mold was closed and the resin was cured. See Figure 15.

The skin material was wound onto a mandrel having a surface area slightly larger than the surface area of the blade. See Figure 16. While still in the wet condition, it was removed from the mandrel by making a longitudinal cut through the wet fibers (see Figure 17) and placed into the main mold. Once in the mold, it was covered with a plastic film, a vacuum was drawn, the excess resin was rubbed out and the skins were cured at elevated temperature. The equipment used did not meter the resin precisely onto the roving nor was it possible to check the resin content prior to curing the skins. This is one of the areas requiring further development.

LAMINATING

The skin material and the skin reinforcing fabric used in the root-end buildup were laminated using conventional practices. See Figure 18.

FOAM MACHINING

The PVC foam used to support the aft tubes and skin was purchased in sheets measuring 37 inches x 16 inches x 1-1/4 inches. These sheets were machined to match the configuration of the tubes and the outside skin using a simple routing setup similar to the type used for routing wood. Two sections of foam were used to encapsulate the tubes with a bond line running down the mid plane of the blade. See Figures 19 and 20.

STEEL MACHINING

The root-end fitting was machined from bar stock using conventional equipment. Prior to being bonded into the assembly, the root-end fitting and the steel bearing plate were cleaned and primed with Prebond 700 (a product of American Cyanamid Company). See Figure 21.

ASSEMBLY OF COMPONENTS

There were two major assembly operations. The first was the nose section assembly, which consisted of combining the first four tubular elements and the longo material between them with the root-end fitting. See Figure 22. The second was the

assembly of the nose section and root-end fitting with the remaining tubes, PVC foam, trailing-edge longo material with the skins, and skin root-end reinforcing material. See Figure 23.

RESULTS

FABRICATION

Three filament-wound tubular-reinforced UH-1D rotor blades were fabricated. The significant results of fabrication are:

1. A method was developed for extracting very thin wall, filament-wound tubes from steel mandrels.

2. The technique used to fabricate the thick-wall tubes was to assemble (overlapping bonded joints) five thin-wall short tubes and then to overwind them as a unit.

3. Filament-wound skins were found to be practical; however, additional development of resin content control is needed.

4. PRD-49 Type III fiber can be handled similarly to glass roving.

5. Applied Plastics Company resin system number APCO 2445/2345 (research number) was found to be a very good system for use with PRD-49; however, some difficulty was experienced with the PVA mold release used in the main skin mold.

6. PVC foam was found to be easily machinable using equipment similar to woodworking equipment.

7. The density variation of the PVC foam was much worse than anticipated; also, it was found to have local high-density hard spots.

8. Wet winding appears to be a practical method of fabrication; and, with minor development, it is expected that resin content control would be equal to the prepreg winding.

9. The E-glass (OCF Type 30 E-glass roving) used as nose fill material in S/N 001 was difficult to handle; S-glass was used in subsequent blades.

10. PRD-49/epoxy was found to be difficult to machine; however, the best results were achieved with high-speed carbide grinding wheels.

11. The blades were all found to have little warpage except for approximately 1/2 inch of chordwise deflection at the blade tip. The chordwise warpage can be attributed to the trailing-edge tip fill material's not being precured prior to assembly with the skins and leading-edge spar assembly.

12. Blade S/N 001 was assembled using only the lower half of the main mold with a vacuum bag over the upper skin. This procedure did not yield the proper blade contour, and the subsequent blades were final-assembled using both halves of the mold bolted together.

The inspection reports for the three blades are shown in Tables XI, XII and XIII. Table XIV summarizes the weight and c.g. location measurements.

TESTING

Blades S/N 001 and S/N 003 and the metallic UH-1D rotor blade were subjected to static loading and dynamic (natural frequency) testing.

The results of the static loads testing are shown in Figures 24, 25 and 26. Also plotted on the graphs are the calculated deflections. The deflections were calculated by the computer using the cross-sectional property data shown in Figures 8, 9 and 10. Figures 27, 28, 29 and 30 show the root-end attachment and the test setup for beamwise/chordwise/torsional static testing.

The deflections and natural frequencies of blade S/N 001 were calculated using a finite element computer program (Mechanics Research, Inc., program STARDYNE) and the theoretical blade cross-sectional properties shown in Figure 8 through 10.

Blade S/N 001 tip-end deflections--both calculated and measured and the percentage differences measured and calculated--are:

	Calculated	Measured	% Difference
Static beamwise, in.	16.67	18.28	+ 9.68
50 lb @ tip beamwise, in.	15.44	14.50	- 6.08
250 lb @ tip chordwise, in.	1.80	2.01	+11.65
10,000 in.-lb torsion, rad	.178	.134	-24.70

Possible differences between the measured and calculated deflections for blade S/N 001 are:

1. The blade was from .07 to .12 inch thicker (see Table XI) than the design value, which would increase its beamwise and torsional stiffnesses slightly.

2. A root-end rotation of only ten minutes would cause a tip deflection of 0.767 inch.

3. The torsional stiffness contribution of all the nose fill and tip fill longitudinal fibers was neglected in the

analysis. Also, the interaction of the tubes and skin and differential bending effects of the blade were neglected in the analysis.

4. The material properties of the composites were all based on calculated values assuming resin properties and taking manufacturers' published fiber properties.

5. The resin content of the actual composite may have varied from the design value.

6. A portion of the testing was conducted outside on a very warm day (T = 95°F); the side of the blade exposed to the sun was too hot to hold bare-handed, while the unexposed side was relatively cool.

7. The accuracy of measurements is estimated at ± 5% or 1/16 inch, whichever is larger.

The measured tip-end deflections for blades S/N 001, S/N 003 and the current metal blade are:

	S/N 001	S/N 003	Metal
Static beamwise, in.	18.28	8.88	6.66
50 lb @ tip beamwise, in.	14.50	9.06	5.75
250 lb @ tip chordwise, in.	2.01	2.97	1.31
10,000 in.-lb torsion, rad	.134	.118	.089

Comparing the measured values of blades S/N 001, S/N 003 and the metal blade, the following observations are made:

1. The static beamwise deflection of S/N 003 was considerably less than expected.

2. The 50-pound load at tip deflection (static + 50-pound load - static) of S/N 003 was greater than the static deflection alone. Blade S/N 001 and the metal blade showed opposite results.

3. The chordwise deflection of S/N 003 was higher than S/N 001, whereas it should have been less.

4. The torsional rotations of both S/N 001 and S/N 003 were within approximately 25% of their calculated values.

The measured natural frequencies are shown in Table XV. During the testing it was noted that the root-end support structure was visually deflecting but was not measured. The root-end flexibility was one possible source of difference between the measured and calculated natural frequencies of S/N 001.

The beamwise and chordwise natural frequencies were determined with the blade supported by flexures at the root end. This method of support would allow lateral deflections in the test plane but resist rotations and lateral deflections in the other plane. (See Figure 31.) It was excited by a hydraulic motor attached to an eccentric cam which would impart $\pm$ 1/4-inch sinusoidal lateral deflection at the blade's root end. The excitation frequency was varied until the maximum blade deflection amplitude was reached. As would be expected, the beamwise deflection amplitude of the metal blade was approximately 1.7 times larger than the fiberglass blade--each being excited at equal displacements at their natural frequency.

Note: Amplitude = $\frac{\sqrt{EI}}{C}$

where EI = flexural stiffness
C = coefficient of damping

The torsional natural frequency was determined with the blade fixed at its root end and supported laterally at its tip end. A 120-pound, 12-foot-long beam was attached to its tip end and was used to "twang" the blade.

PRD-49 EVALUATION

Before the third blade was constructed, a program was implemented to establish handling procedures for PRD-49. Some problems were encountered with the recommended resin systems and the published values for the material properties. Out of this effort came a new and very effective resin system (APCO 2445/2345, a product of Applied Plastics Company).

Because of the high degree of molecular alignment in PRD-49 Type III fibers, the modulus in the radial direction and shear modulus are very low (1.42×10^6 psi and 0.27×10^6 psi respectively) compared to the modulus in the axial direction (19.0×10^6 psi). These differences must be accounted for in predicting the stiffnesses of a PRD-49/epoxy composite.

Although not documented, it would appear that the inner-fiber radial tensile strength is also very low compared to its axial tensile strength. A low radial tensile strength would explain the low compressive strength and high knot strength. (Knot strength is approximately 60 percent of the strength of straight dry fibers of PRD-49.)

COST ANALYSIS

One of the major objectives in the program was the development of the system of manufacturing tubular-element filament-wound blades to show fabrication feasibility. The fabrication feasibility is to be extrapolated to an analysis of the anticipated production cost of building a UH-1D rotor blade in the manner described.

There is no attempt to compare the cost of building the filament-wound tubular-element blade versus the existing aluminum blade. Quantities of metal blades produced in the UH-1 program are used to establish the basis for a cost analysis of the filament-wound blade. It has been reported that approximately 10,000 metal blades have been built for the Bell UH-1 models. For the purposes of this study, a production of 5,000 blades is utilized to establish the costing base. The costs outlined are those to be anticipated on the 2,000th blade.

The production costs for the design and fabrication are difficult to estimate since the fledgling composites industry has had virtually no experience in high-volume quantity production. The experience and advantages gained in high-volume production of metallic blades cannot be adequately applied to the cost analysis of composite rotor blades. The numbers provided are considered to be somewhat conservative because of the overall lack of high-volume production experience and know-how. The influence of a continuous production line on the operation of filament winding and other production techniques described in this report cannot be accurately anticipated.

The cost analysis is based upon a number of changes in the design and fabrication of the blade--differing from that reported herein--to take advantage of the knowledge and experience gained in the course of this early and somewhat limited program. A number of the changes anticipated in the design to develop a production blade are indicated below.

1. A redesign of the root-end buildup or doubler area, eliminating the requirement for the separate leaves or reinforcing plates as duplicated from the existing UH-1D blade.

2. Reinforcement of the root-end buildup area with a series of filament-wound shims of a configuration more compatible with the overall winding and laminating operation.

3. A redesign of the root-end bar to eliminate the costly and complicated configuration described in the report. This bar may be reduced significantly or eliminated with the anticipated improvements.

4. In the production of the UH-1D blade, elimination of hand work by winding on an inflated bladder, thereby building the skin directly into the mold in one operation. The fabrication of the skin reported herein consisted of winding a specific number of plies at predetermined winding angles to an exact thickness on a hard mandrel. The material was slit and hand-laid into the blade mold.

5. The design and use of automated tooling and winding for providing all of the items to reach the final assembly at one point in time, therefore greatly influencing and reducing the labor elements in spar and blade assembly.

The cost estimate for the production of UH-1D rotor blades utilizing the filament-wound tubular element concept is shown below. The estimate is based on a quantity of 5,000 blades, and the base is on the 2,000th blade.

The following rates are the estimated 1972 level for production-oriented shops:

Shop labor	\$4.00/hour
Quality control labor	\$5.00/hour
Inspection	\$5.00/hour
Support	\$3.00/hour
Overhead rate	120%
G & A rate	15%

DIRECT MATERIALS

1.	Purchased parts - root-end bar (redesigned)		$ 200.00
2.	Raw material		
	"S" glass roving - 118 lb @ $4.25	$ 502.00	
	"E" glass roving - 31 lb @ $1.05	33.00	
	Epoxy resin - 84 lb @ $1.50	118.00	
	PVC foam - 15 pieces @ $3.75 sq ft x 1.00	56.00	
	"Pultrusion" bar - 528 in. @ $.0833	44.00	
	Environmental protection	13.00	
	Leading-edge protection (urethane cover)	150.00	916.00
3.	Subcontracted items - balance system materials		25.00
	Total materials		$ 1,141.00
4.	Material burden - 10%		114.00
			$ 1,255.00
5.	Less quantity buys - 15%		188.00
	Net materials		$ 1,067.00

LABOR

Manufacturing labor - 72 hours @ $4.10

Preparing of molds and mandrels	2 hours	
Winding	12 hours	
Spar fabrication	12 hours	
Spar cleanup	2 hours	
Foam machining	1 hour	
Blade fabrication	30 hours	
Trim	1 hour	
Assembly	2 hours	
Cleanup	2 hours	
Quality assurance inspection	8 hours	
	72 hours	
Total manufacturing labor		295.00

OVERHEAD

As applied to labor - 120% for production-oriented shop ($295.00 x 1.2)	354.00
Total direct costs	$ 1,716.00

G & A

As applied to direct costs - 15% for production-oriented shop ($1,716.00 x .15)	257.00
Total cost	$ 1,973.00

The best estimate for the UH-1D blade using PRD-49 fiber material in the skin only is based upon replacing the "S" glass fiber in the skin with PRD-49 Type III fiber.

From the computer program, PRD-49 will account for .1416 + .008 = .15 lb/in.

Assuming straight replacement and PRD-49 Type III at $18.00/pound (present price), direct materials would increase by the following:

.15 x 264 in. = 39.6 lb

Assume that 40 pounds of PRD-49 will replace 40 pounds of "S" glass:

40 (18 - 4.25) =	$ 550.00
Burden - 10%	55.00
	$ 605.00
Less quantity buy - 15%	91.00
	$ 514.00

A direct material cost of $514.00 adds $591.00 ($514 x 1.15 (G & A)) to the total cost; therefore, the blade total cost utilizing PRD-49 is $2,564.00.

NOTE: The cost of PRD-49 Type III is expected to be $9.00 to $12.00 per pound in the 1978 time frame.

CONCLUSIONS

1. Three filament-wound tubular-reinforced UH-1D rotor blades were constructed which demonstrated the fabrication feasibility.

2. The predictability of a filament-wound tubular-reinforced rotor blade was demonstrated within the accuracy of the testing and manufacturing procedures used.

3. A highly redundant root-end attachment was developed which minimizes the interlaminar shear stresses in the root-end area.

4. A new resin system was developed for use with PRD-49 which appears to be much better than previously used wet-winding systems.

5. Experience was gained using PRD-49 fibers, which enhance the analyst's ability to predict the blade's performance.

6. Fabrication of the blades was less difficult than anticipated at the start of the program.

7. The fabrication concept is amenable to low-cost production.

8. Blade warpage caused by residual stresses was very low, even in the blade utilizing PRD-49, due to the resin systems and curing techniques used.

RECOMMENDATIONS

1. The three blades fabricated should be subjected to extensive testing in order to more fully evaluate the full structural potential of the concept.

2. The root-end attachment should be more fully developed and a more rigorous analysis performed.

3. The root-end buildup area should be redesigned to be more compatible with the filament-wound composite approach.

4. The filament-wound tubular-reinforced rotor blade concept should be advanced to the next stage of development--ultimately flown on a helicopter.

5. Core materials such as epoxy foam and honeycomb should also be evaluated along with further evaluation of PVC foam.

6. High-modulus materials such as graphite and boron should be evaluated in the filament-wound tubular-reinforced rotor blade concept.

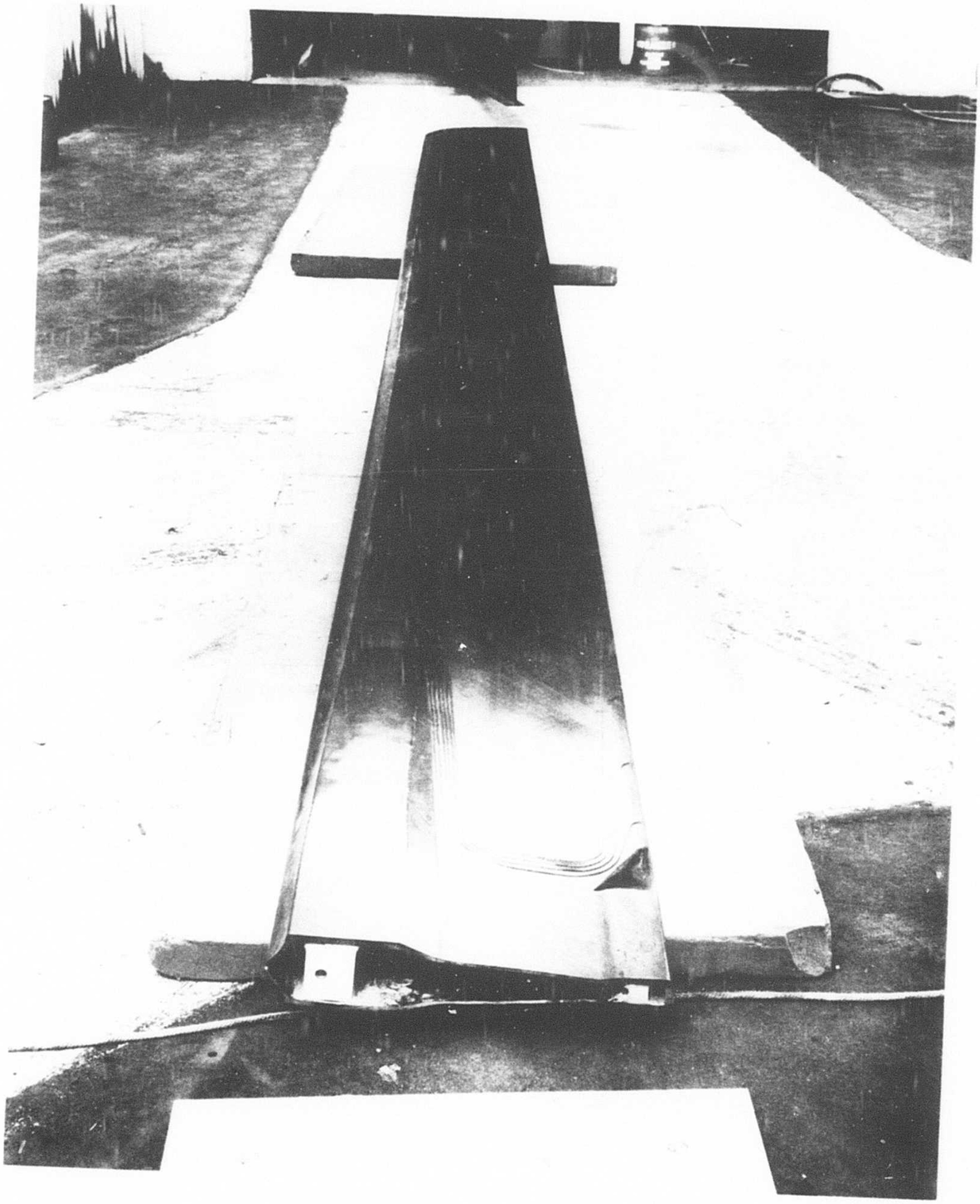

Figure 1. Completed Filament-Wound Tubular-Reinforced Composite Rotor Blade (UH-1D S/N 001).

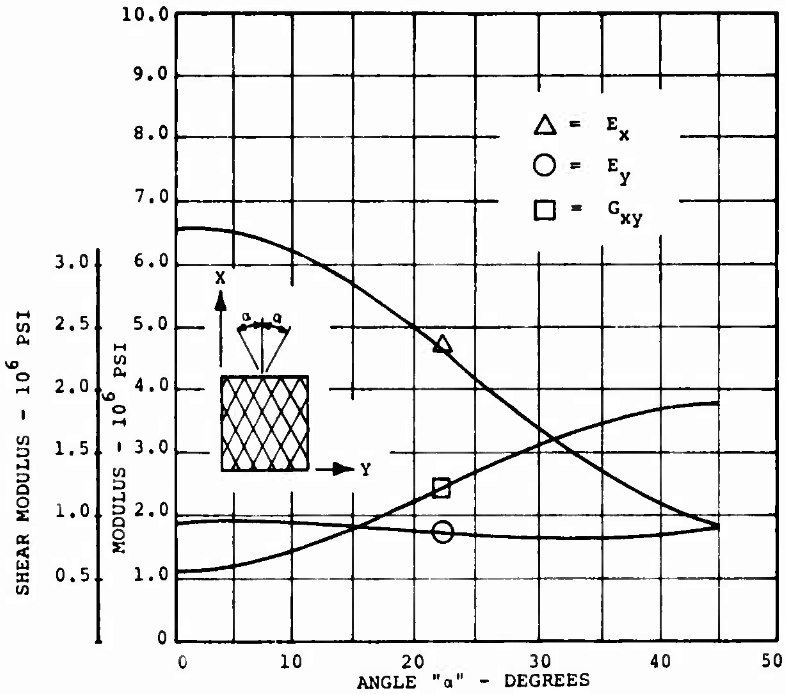

Figure 2. Theoretical Properties of "S" Glass/Epoxy.

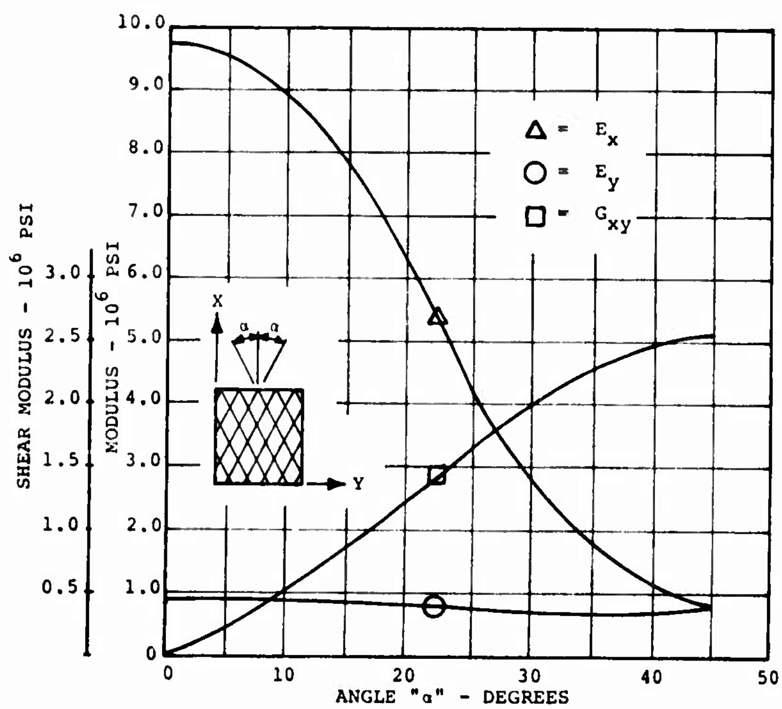

Figure 3. Theoretical Properties of PRD-49/Epoxy.

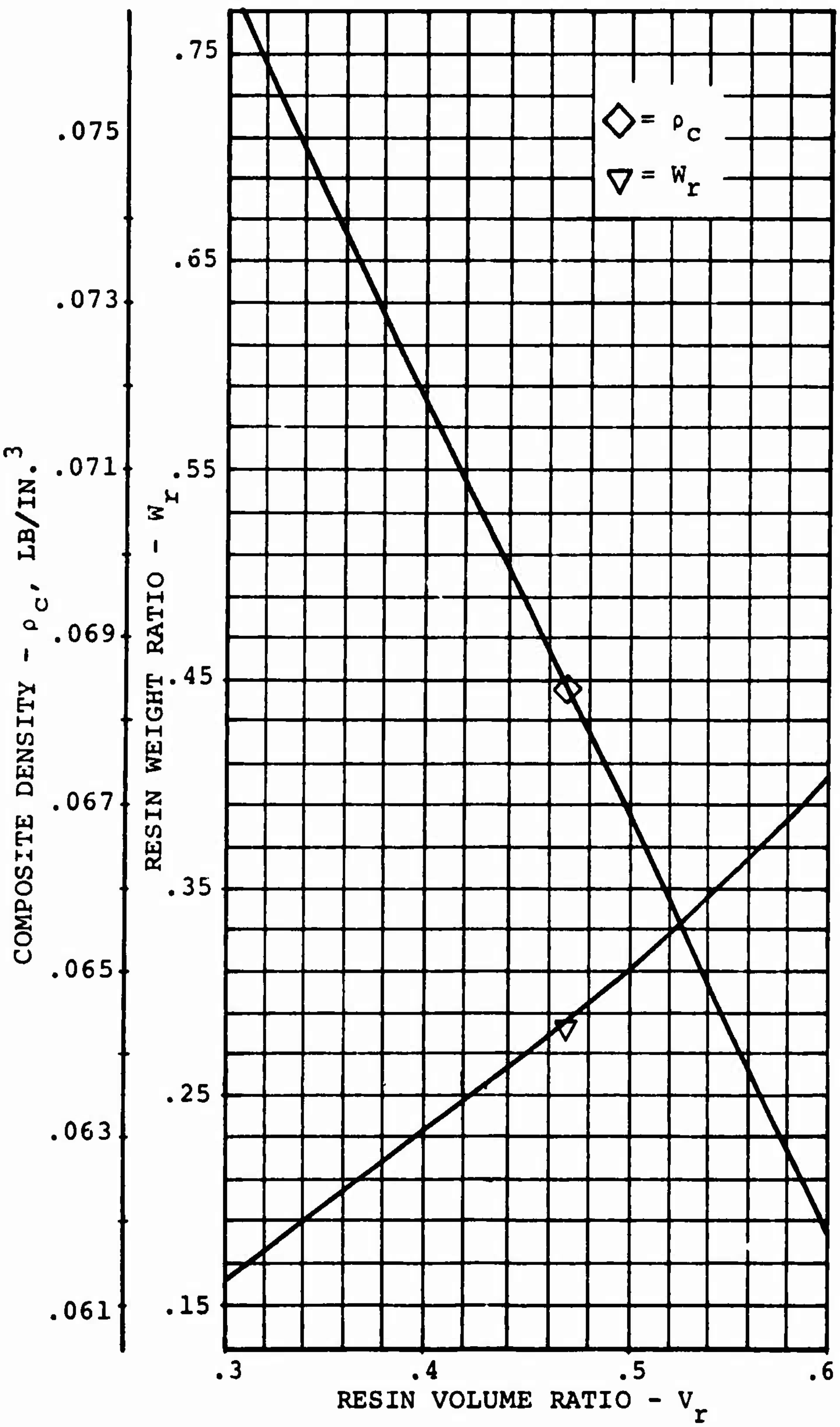

Figure 4. Resin Volume Ratio vs Resin Weight Ratio and Composite Density for "E" Glass/Epoxy.

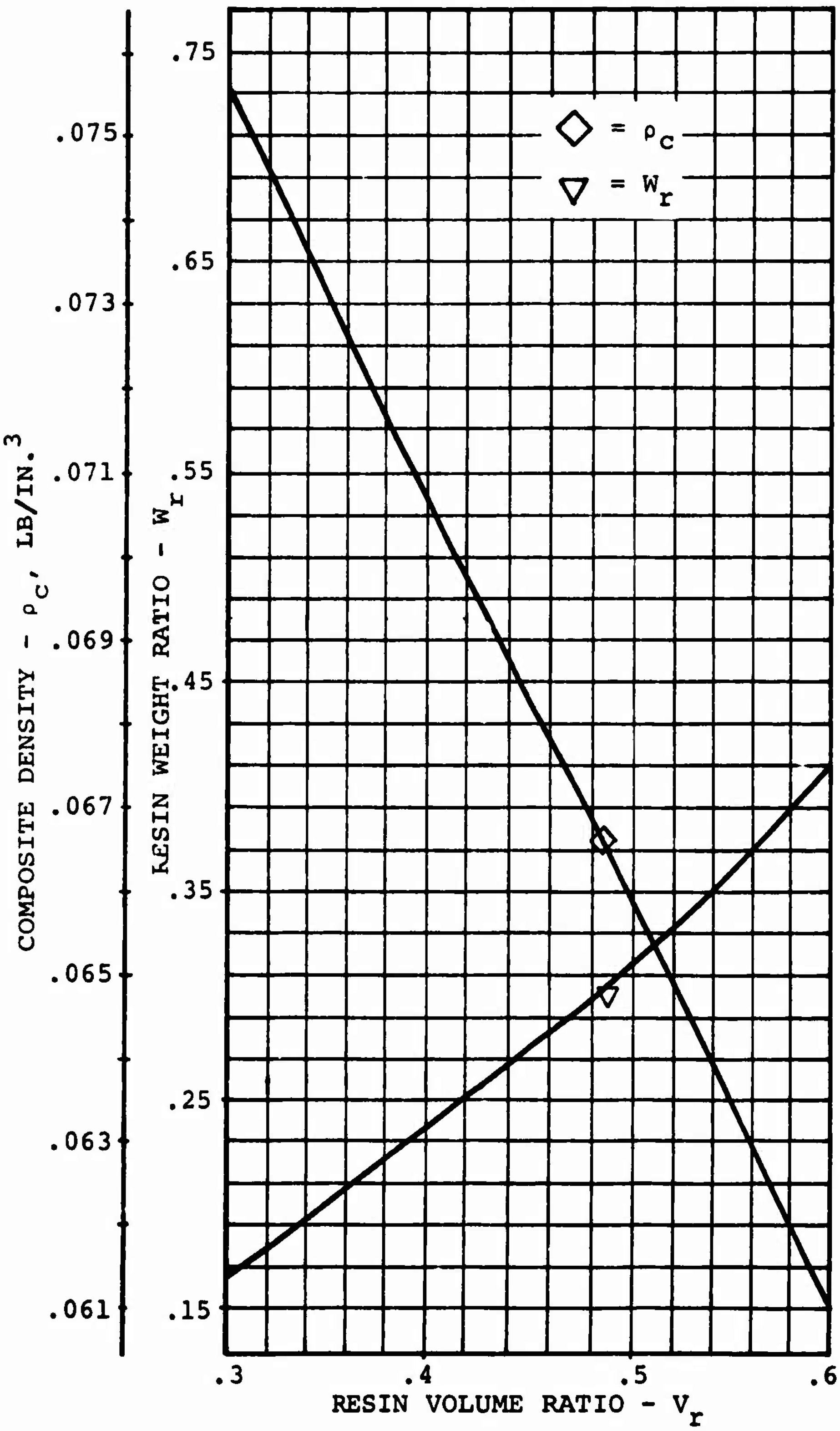

Figure 5. Resin Volume Ratio vs Resin Weight Ratio and Composite Density for "S" Glass/Epoxy.

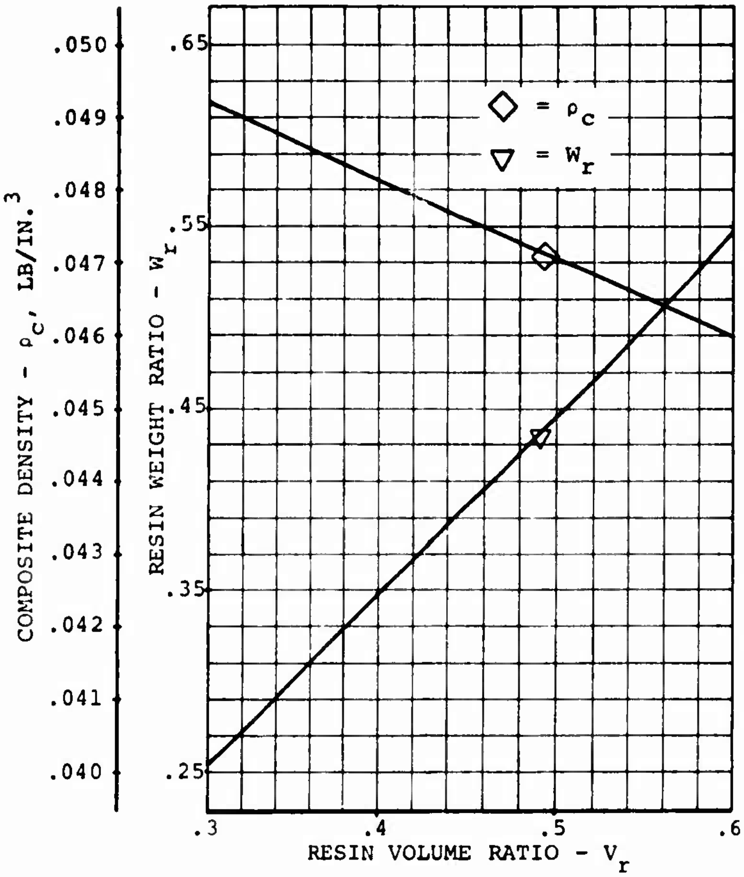

Figure 6. Resin Volume Ratio vs Resin Weight Ratio and Composite Density for PRD-49/Epoxy.

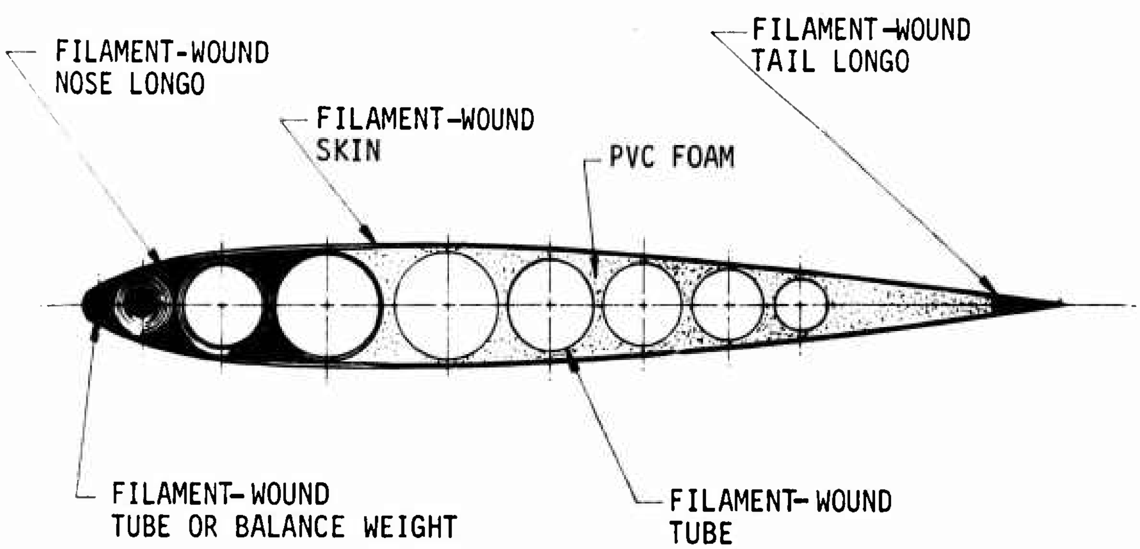

Figure 7. UH-1D Tubular-Reinforced Composite Main Rotor Blade Configuration.

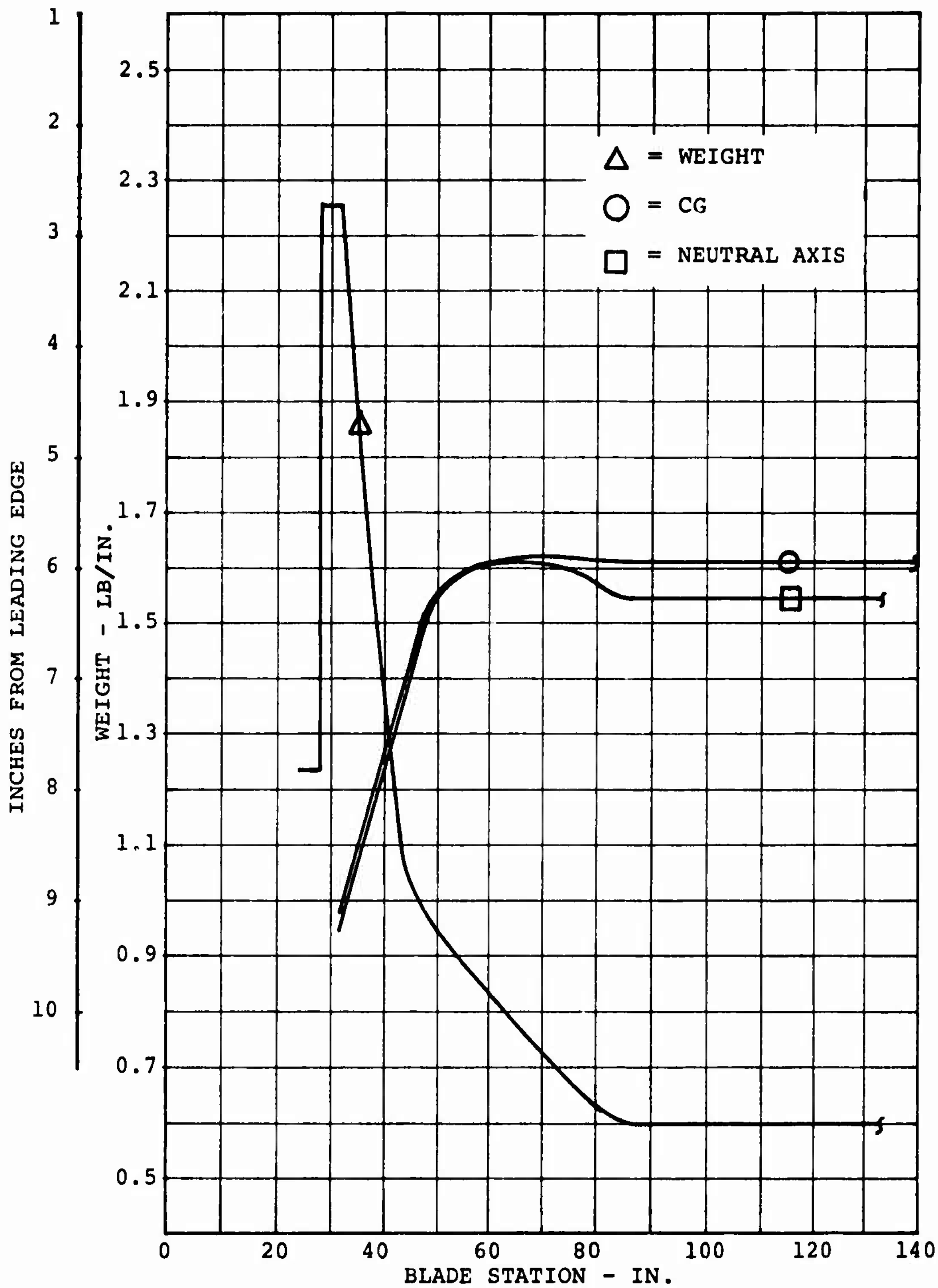

Figure 8. Unit Weight and Distance From Leading Edge to Neutral Axis and CG vs Blade Section, S/N 001.

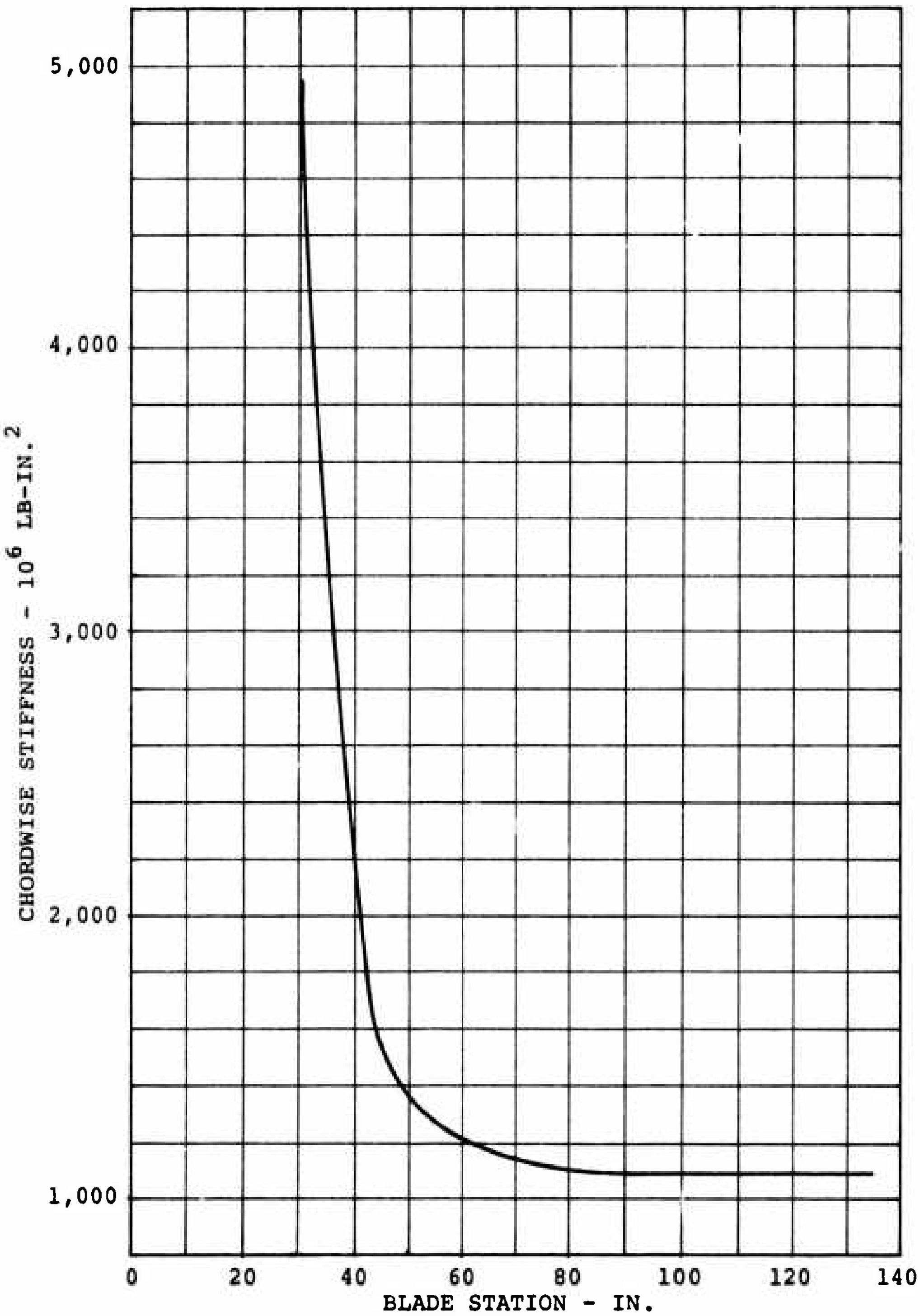

Figure 9. Chordwise Bending Stiffness vs Blade Section, S/N 001.

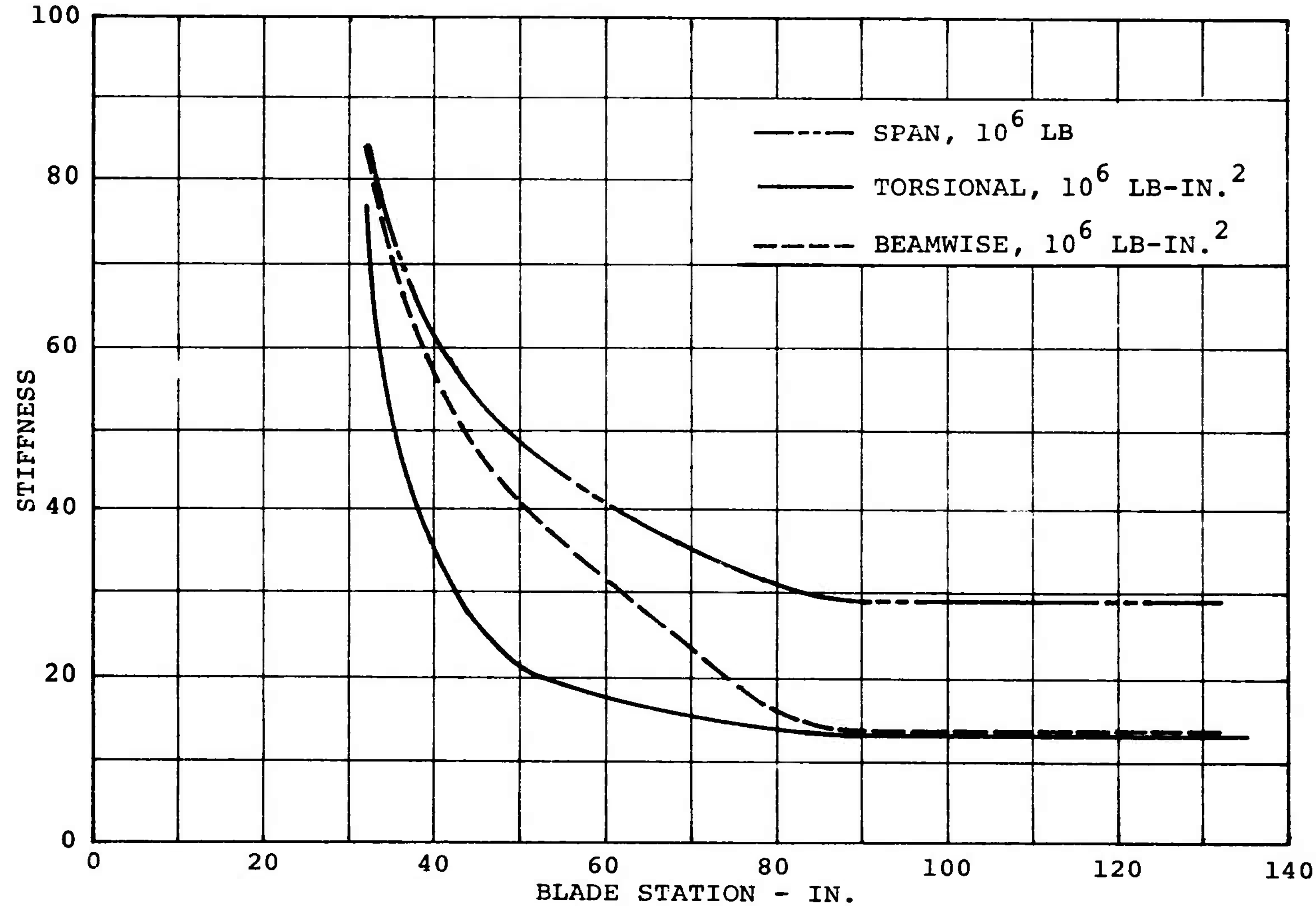

Figure 10. Beamwise Bending, Torsional and Span Stiffness vs Blade Section, S/N 001.

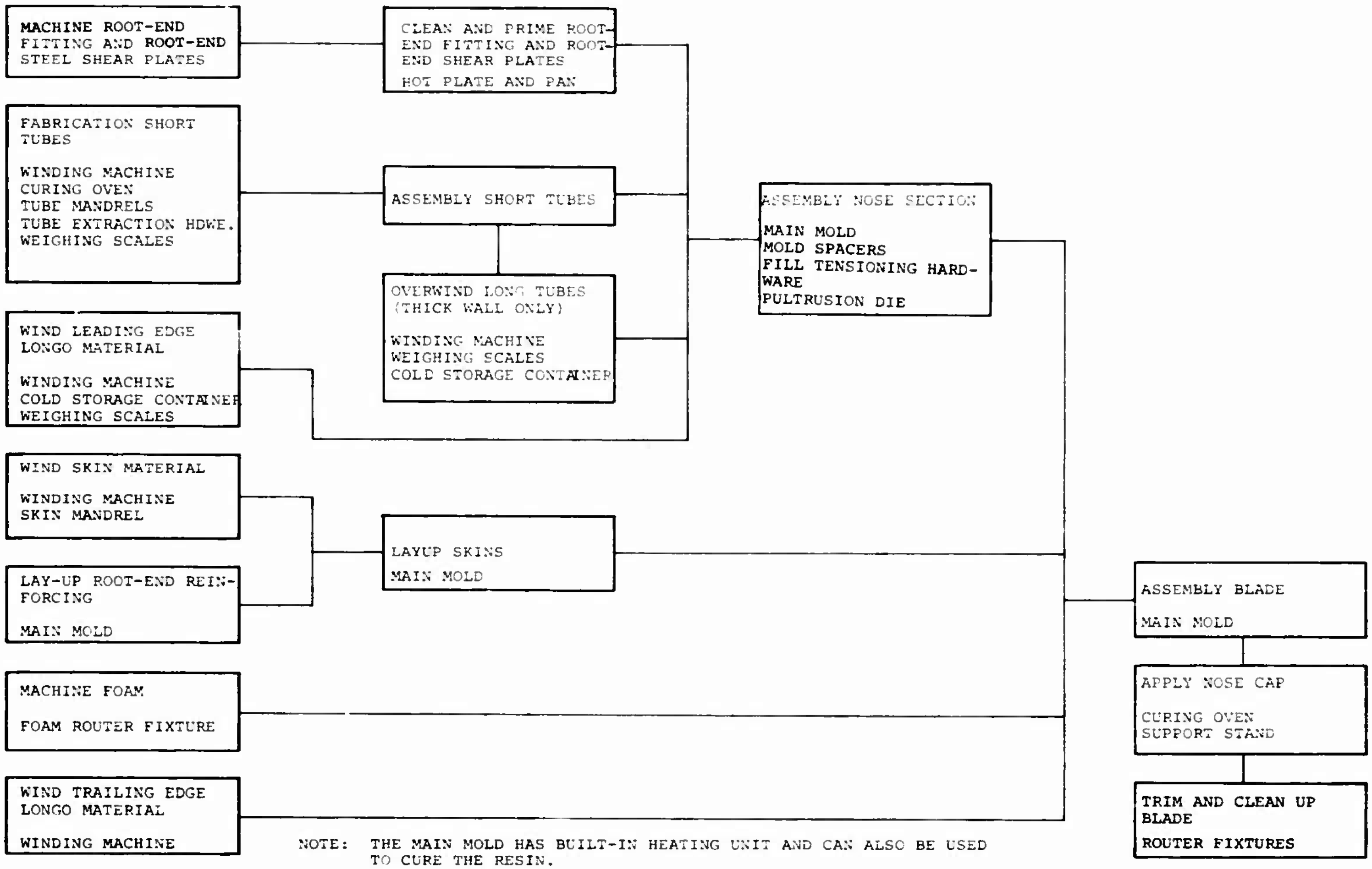

NOTE: THE MAIN MOLD HAS BUILT-IN HEATING UNIT AND CAN ALSO BE USED TO CURE THE RESIN.

Figure 11. Fabrication and Tooling Flow Chart.

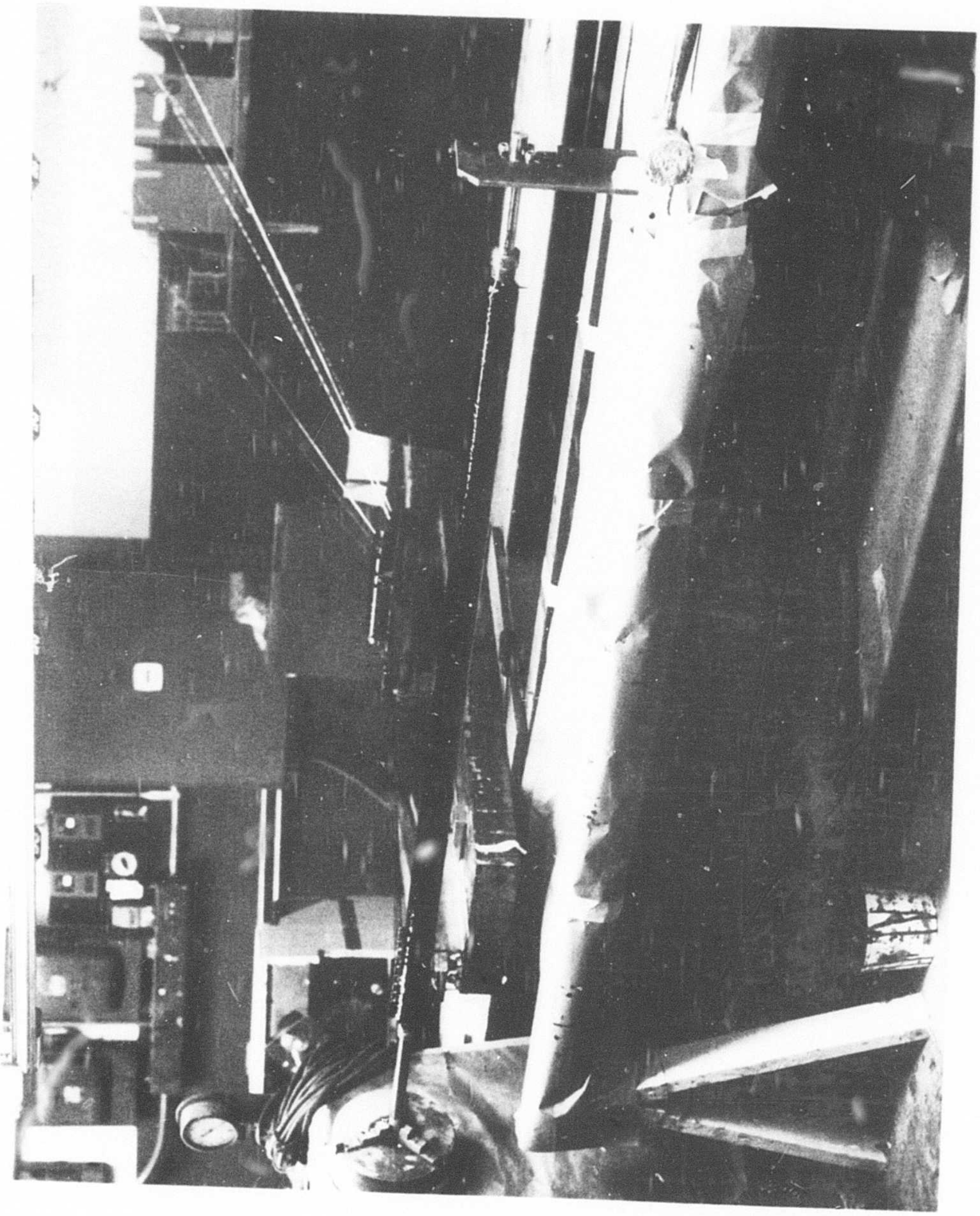

Figure 12. Rotor Blade Tube Winding.

Figure 13. Winding of Long Tubes Used in S/N 001.

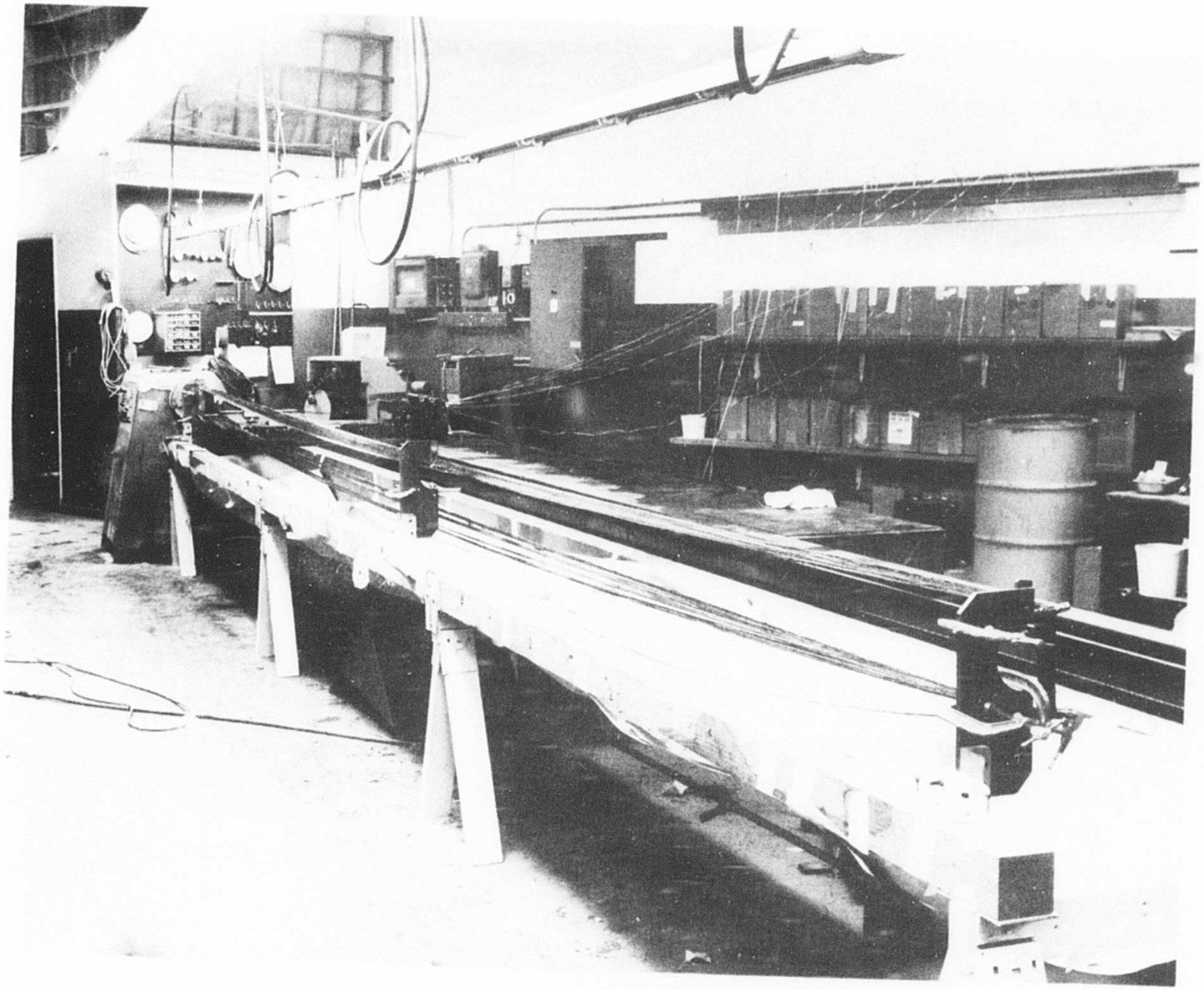

Figure 14. Winding Longo Material.

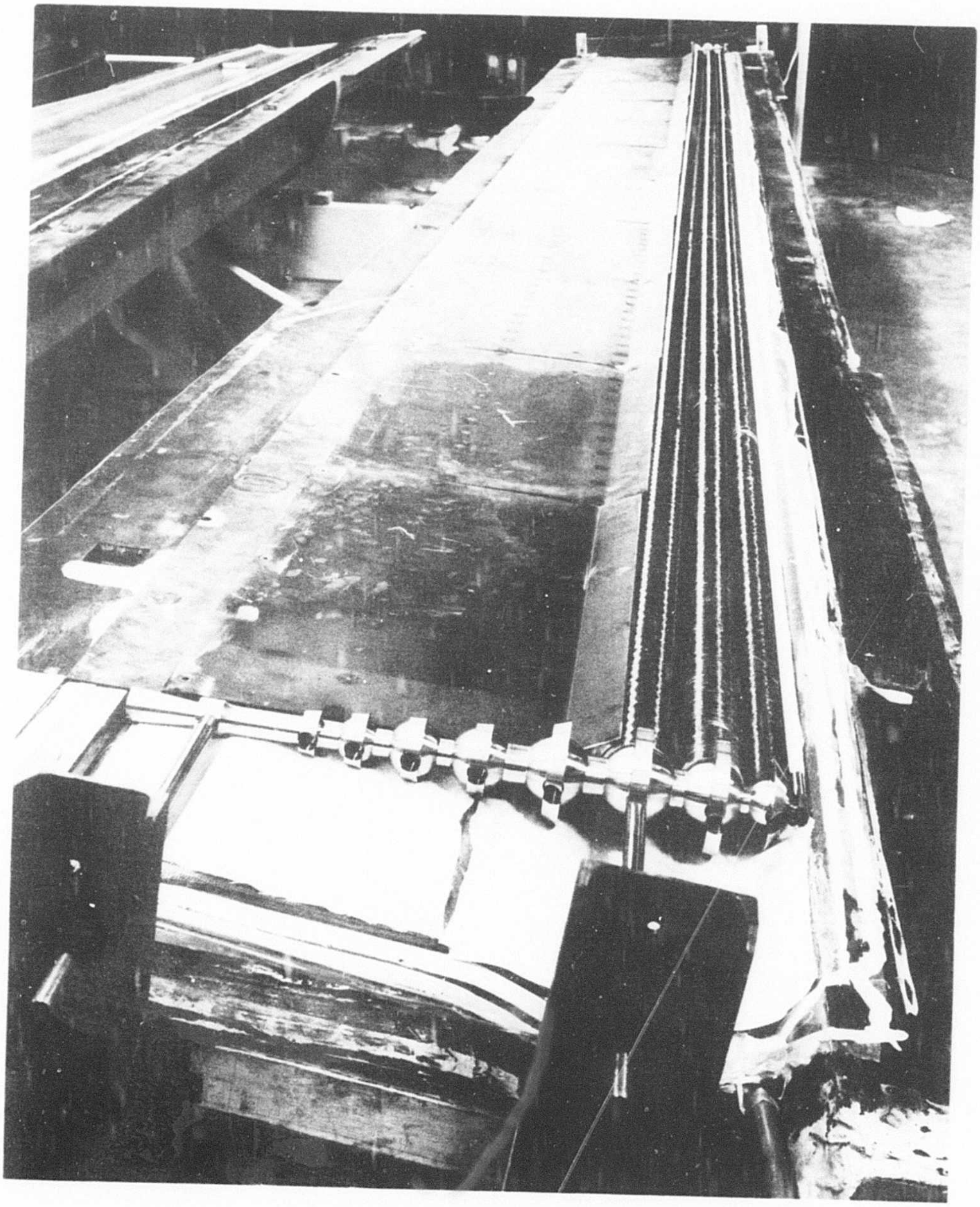

Figure 15. Fabrication of Nose Assembly Prior to Addition of Longo Material.

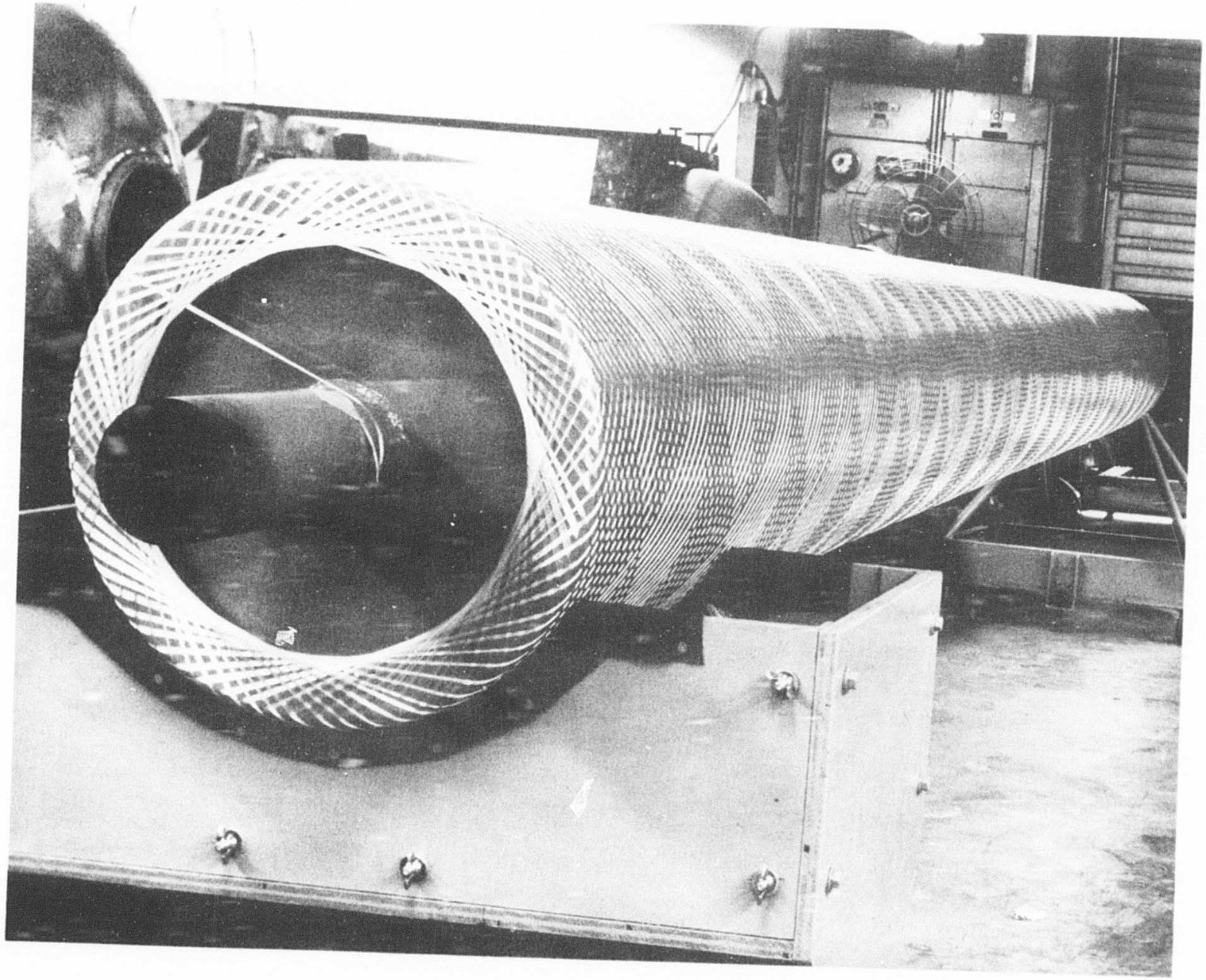

Figure 16. Trial Winding of Skin Material Using Dry Glass.

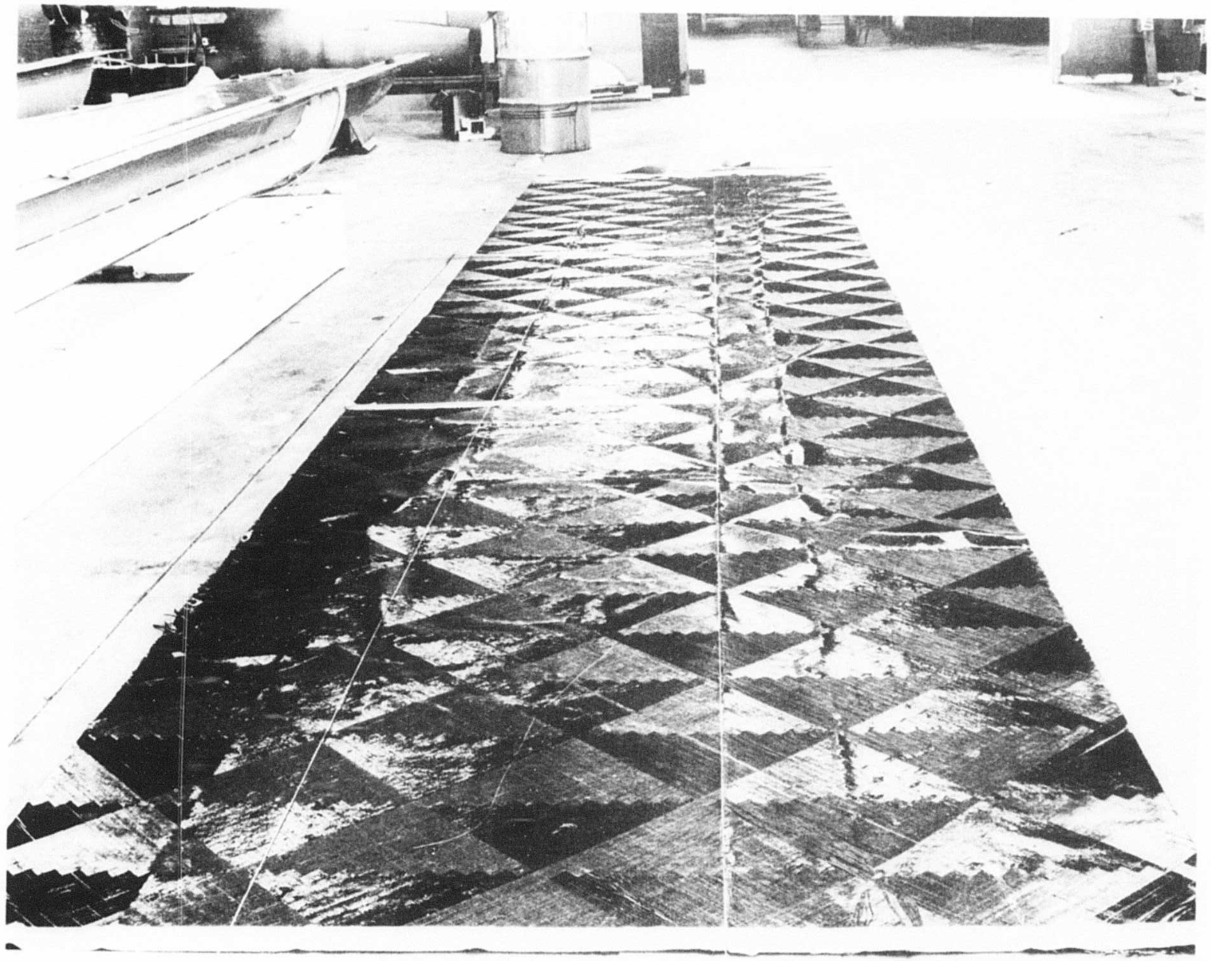

Figure 17. Skin Material Removed From Mandrel.

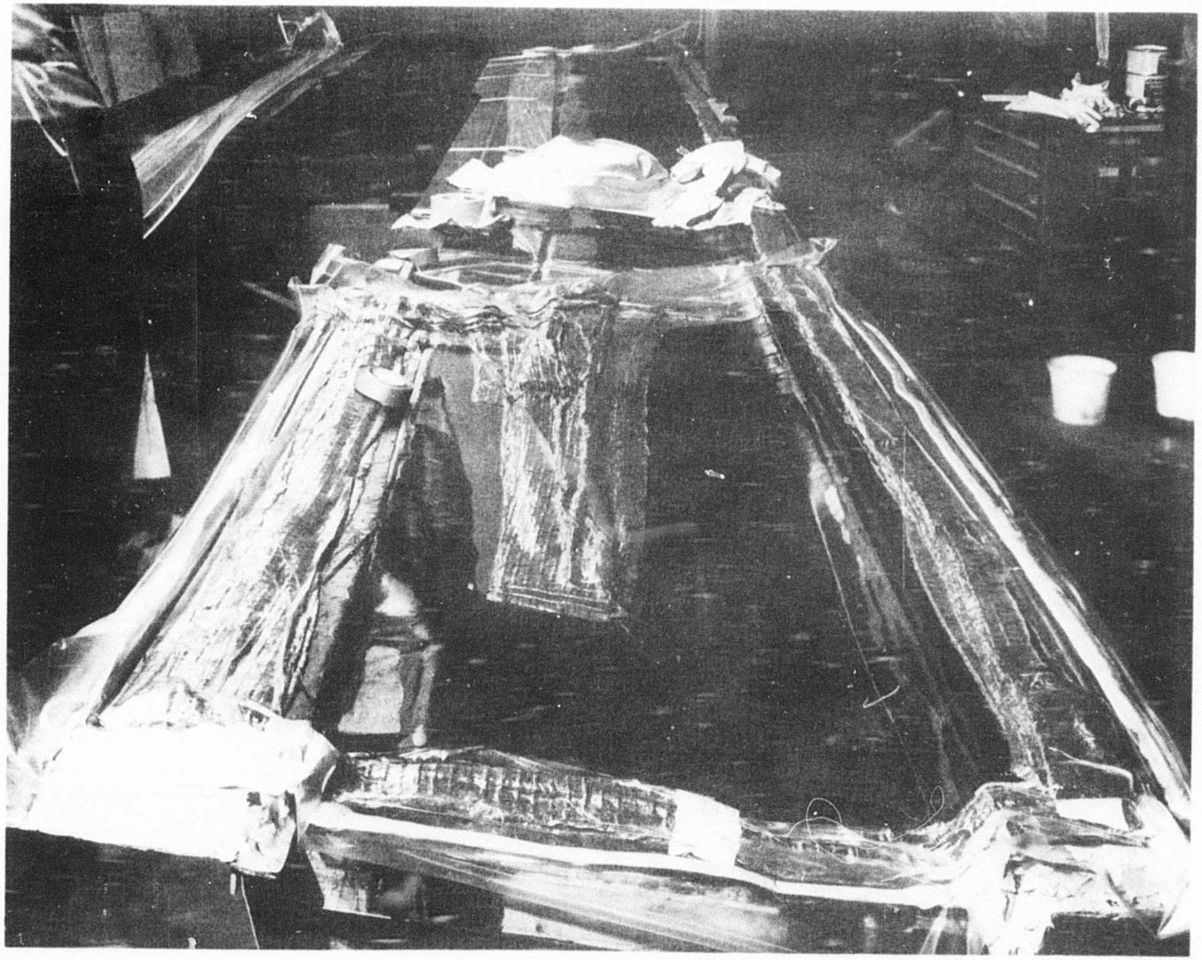

Figure 18. Skin Reinforcing Material.

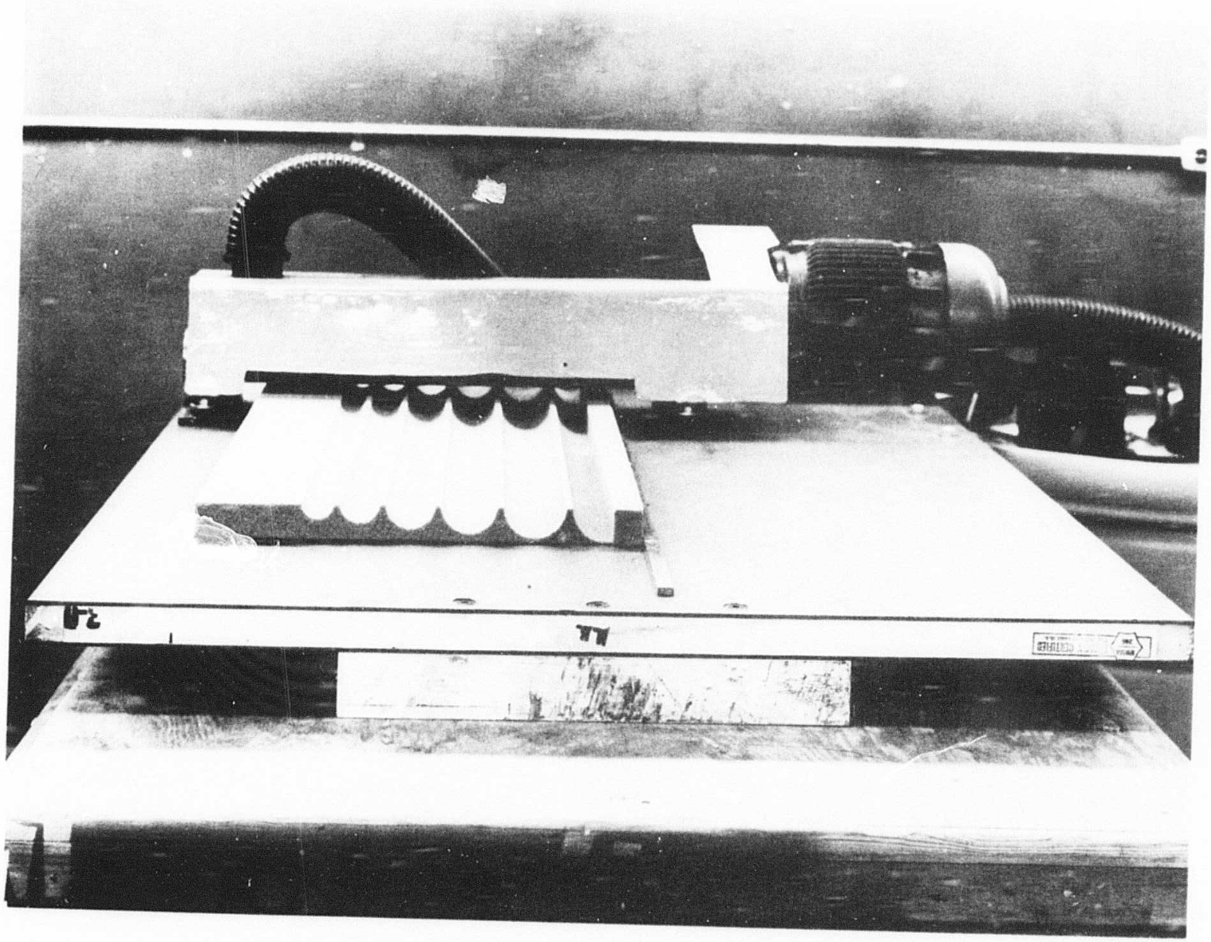

Figure 19. Machining of PVC Foam.

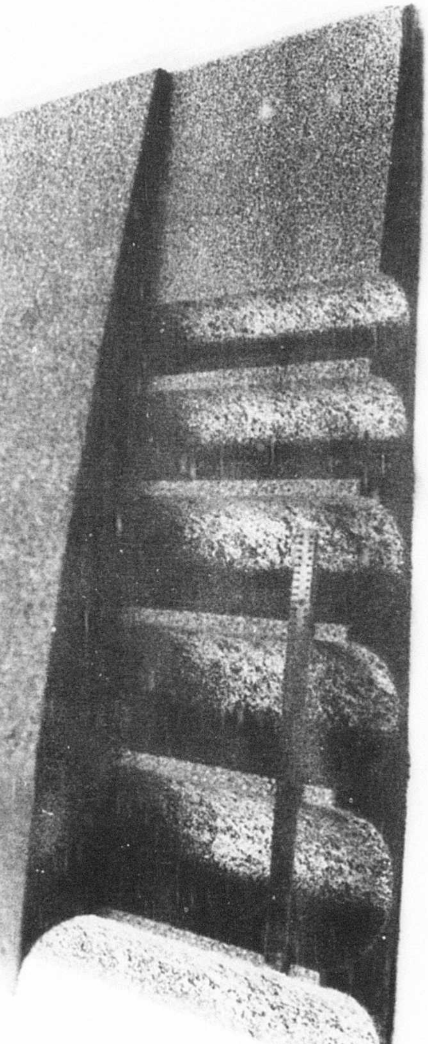

Figure 20. Completed PVC Foam Sections.

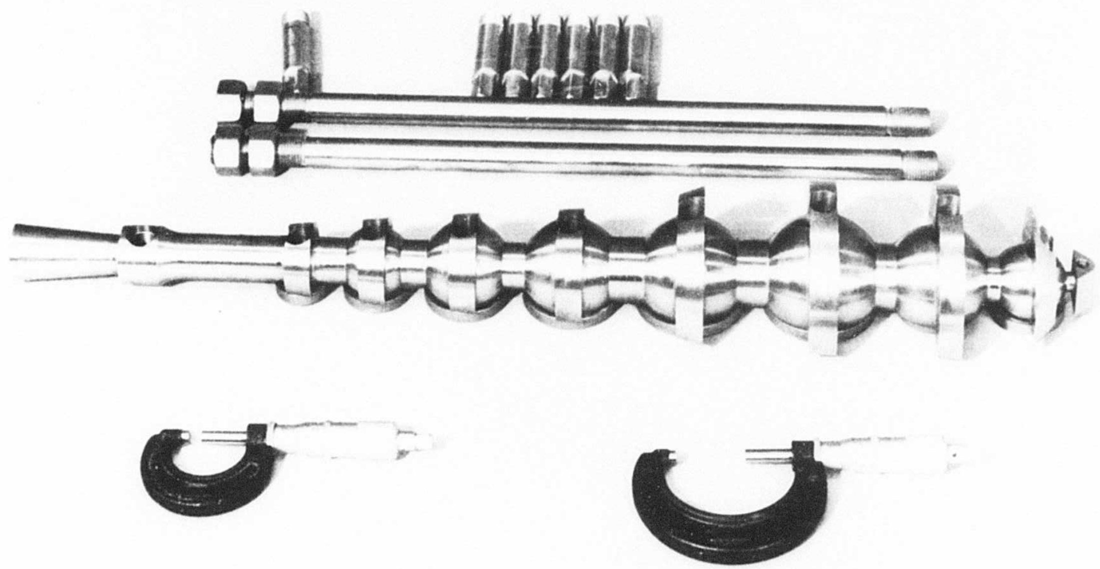

Figure 21. Root-End Fitting Machined Parts and Tooling Studs.

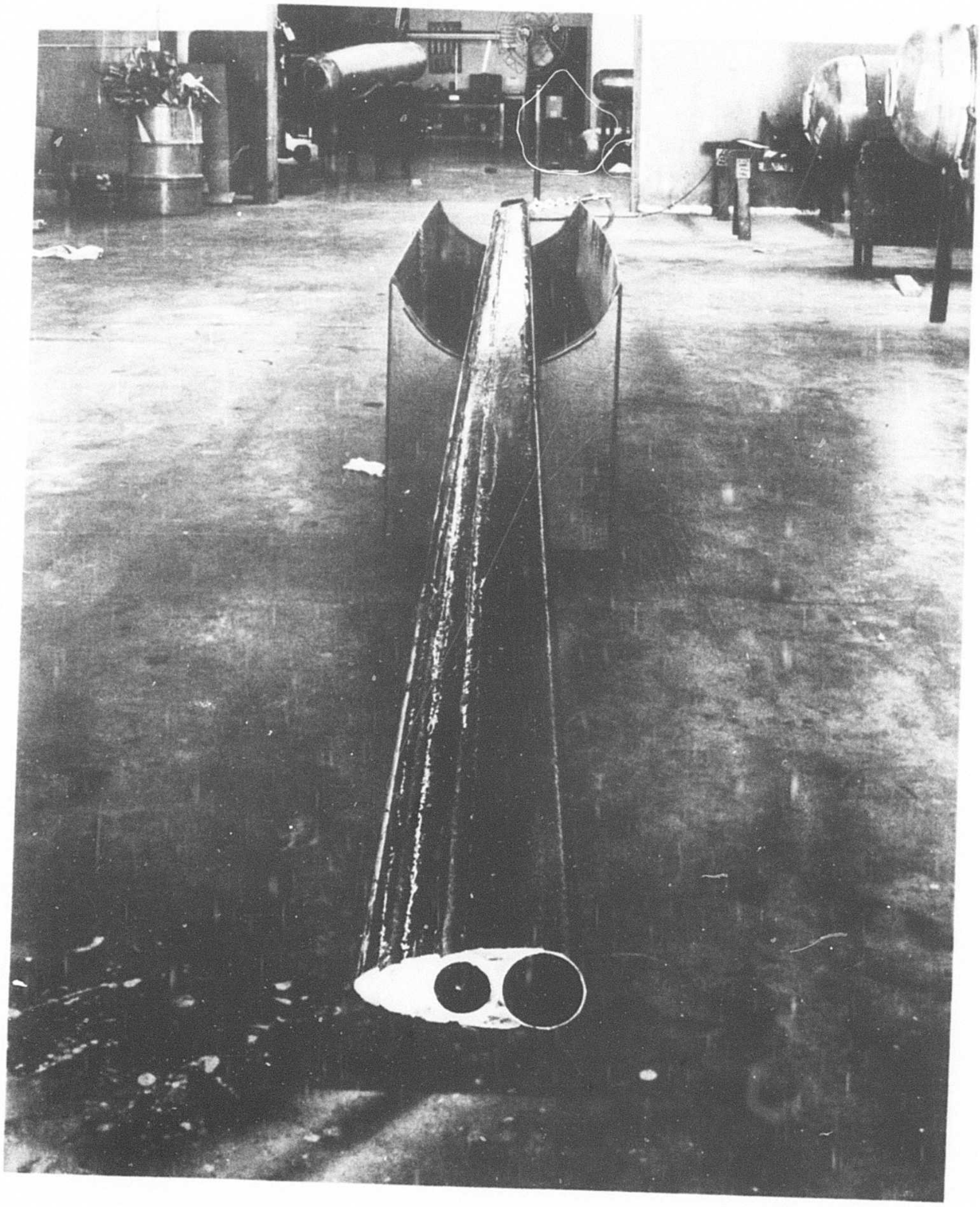

Figure 22. Nose Section Assembly.

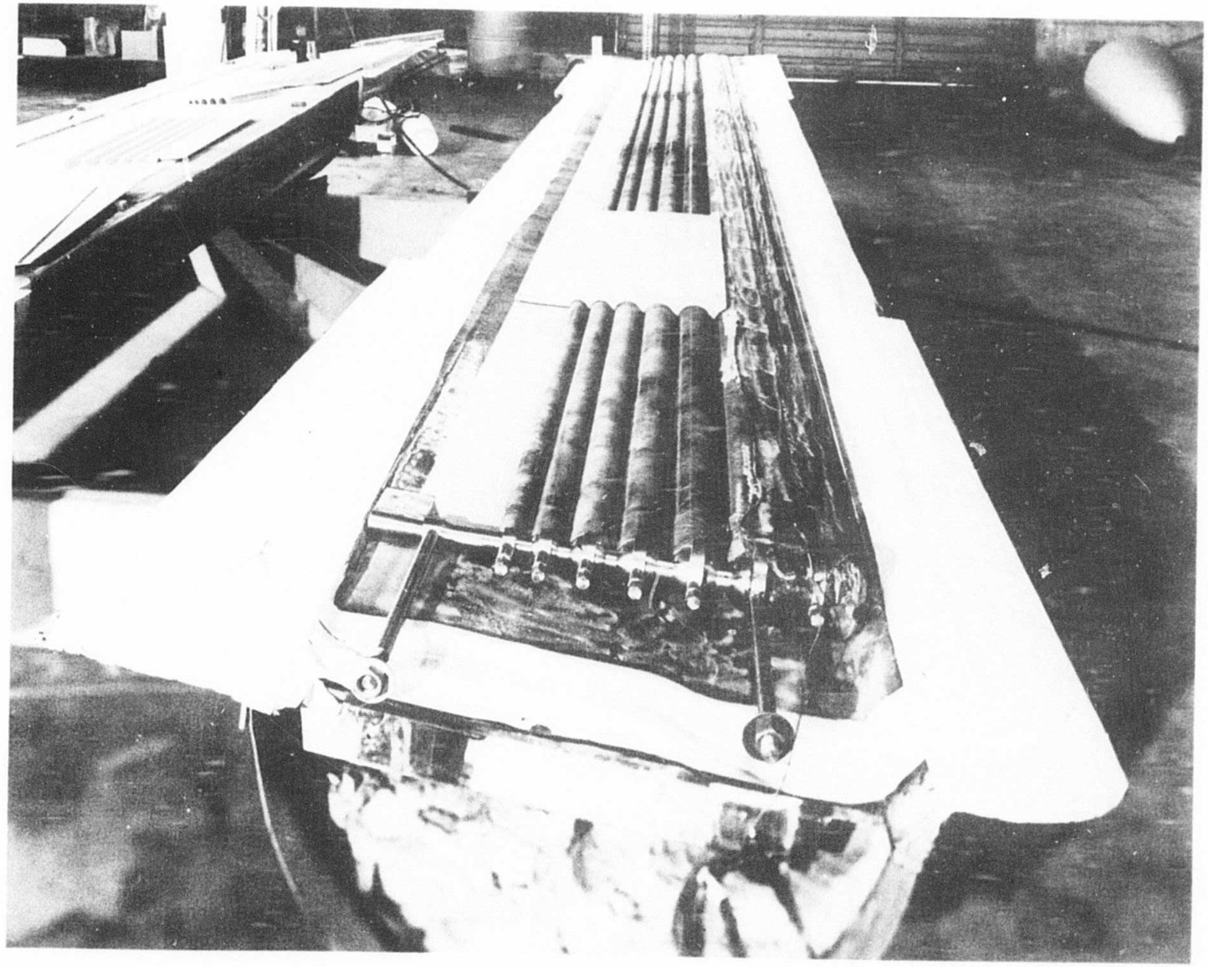

Figure 23. Final Blade Assembly.

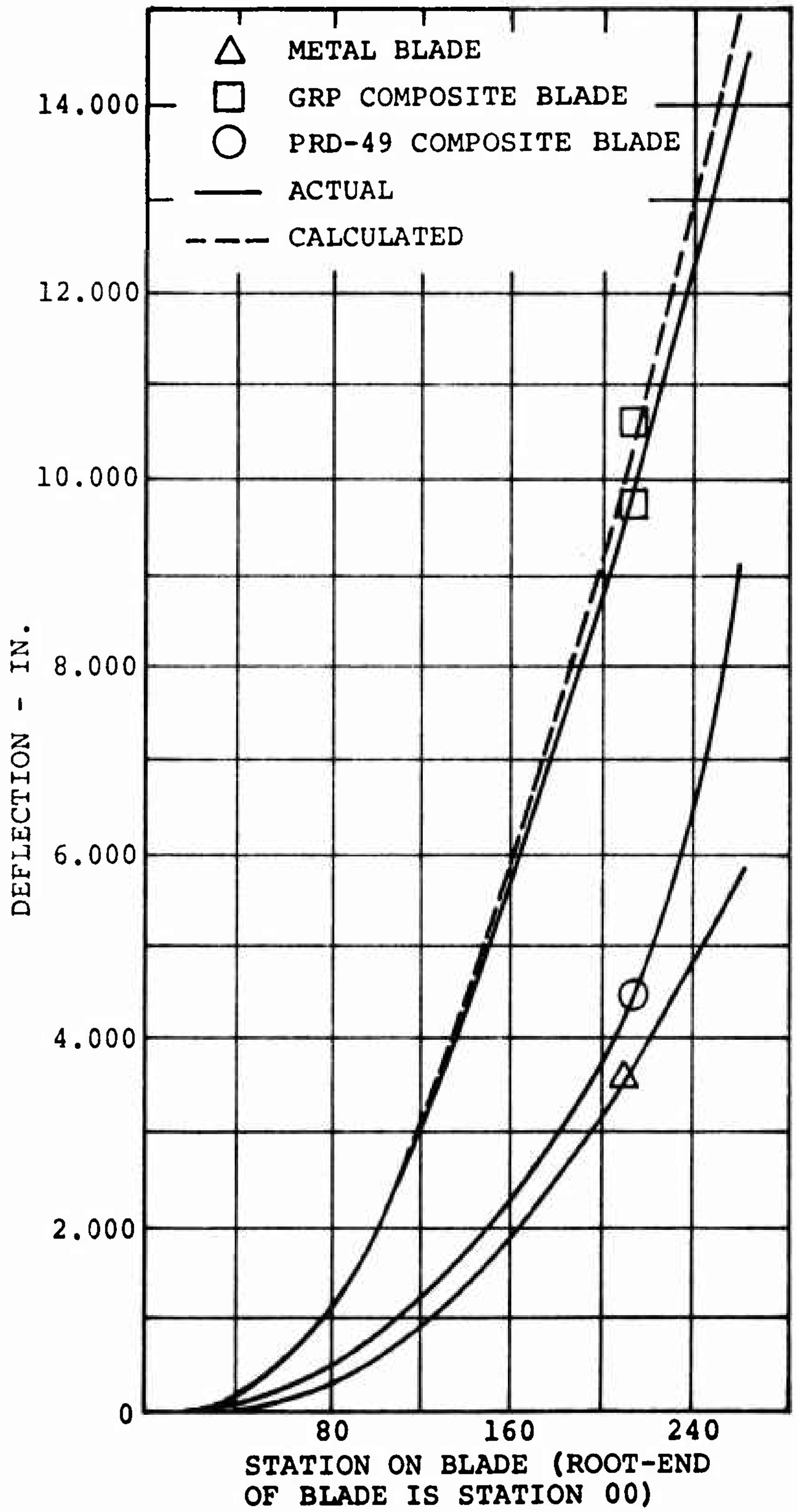

Figure 24. Beamwise Deflection of Blade/ 50-Pound Weight at Tip End Less Natural Deflection.

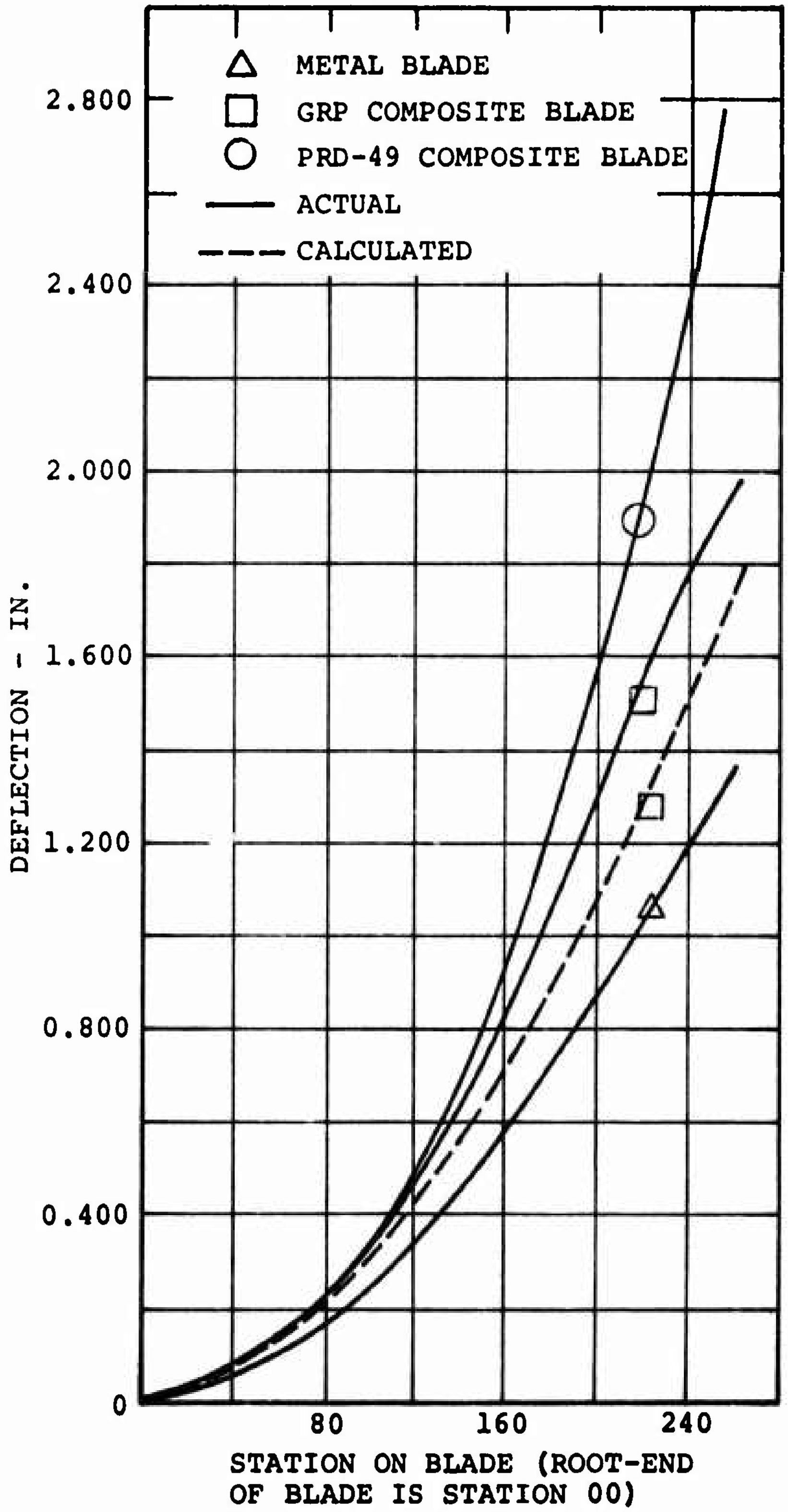

Figure 25. Chordwise Deflection of Blade/250-Pound Weight at Tip End Less Natural Deflection.

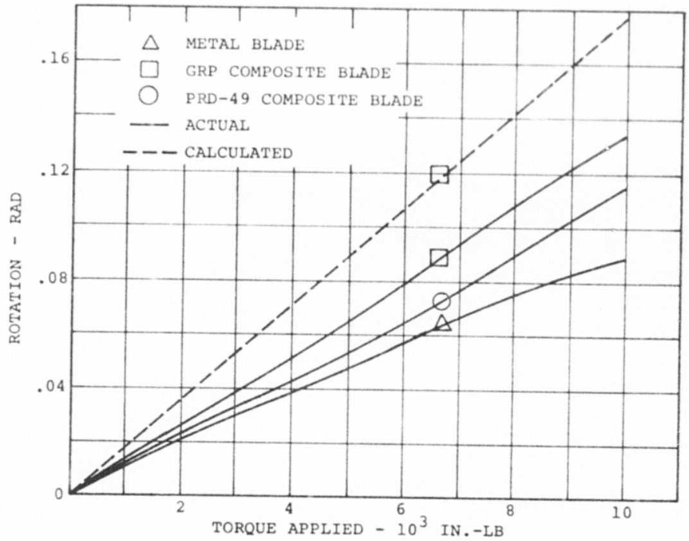

Figure 26. Torsional Deflection of Blade vs Torque Applied at Tip End.

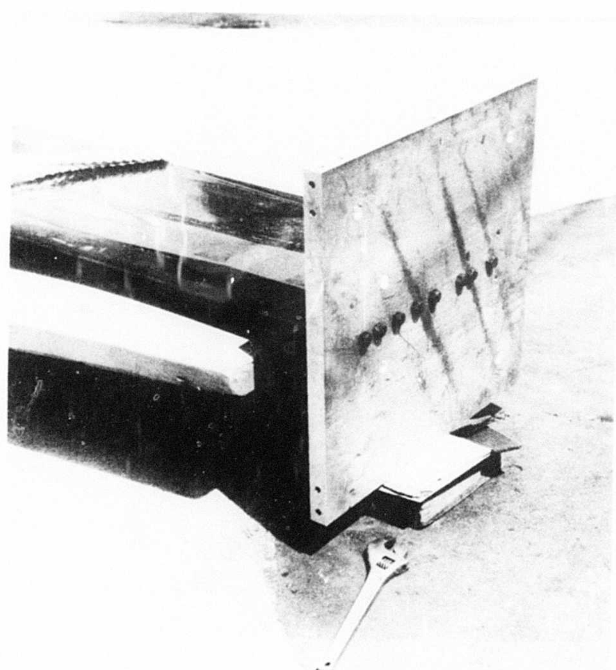

Figure 27. Root-End Mounting Adapter.

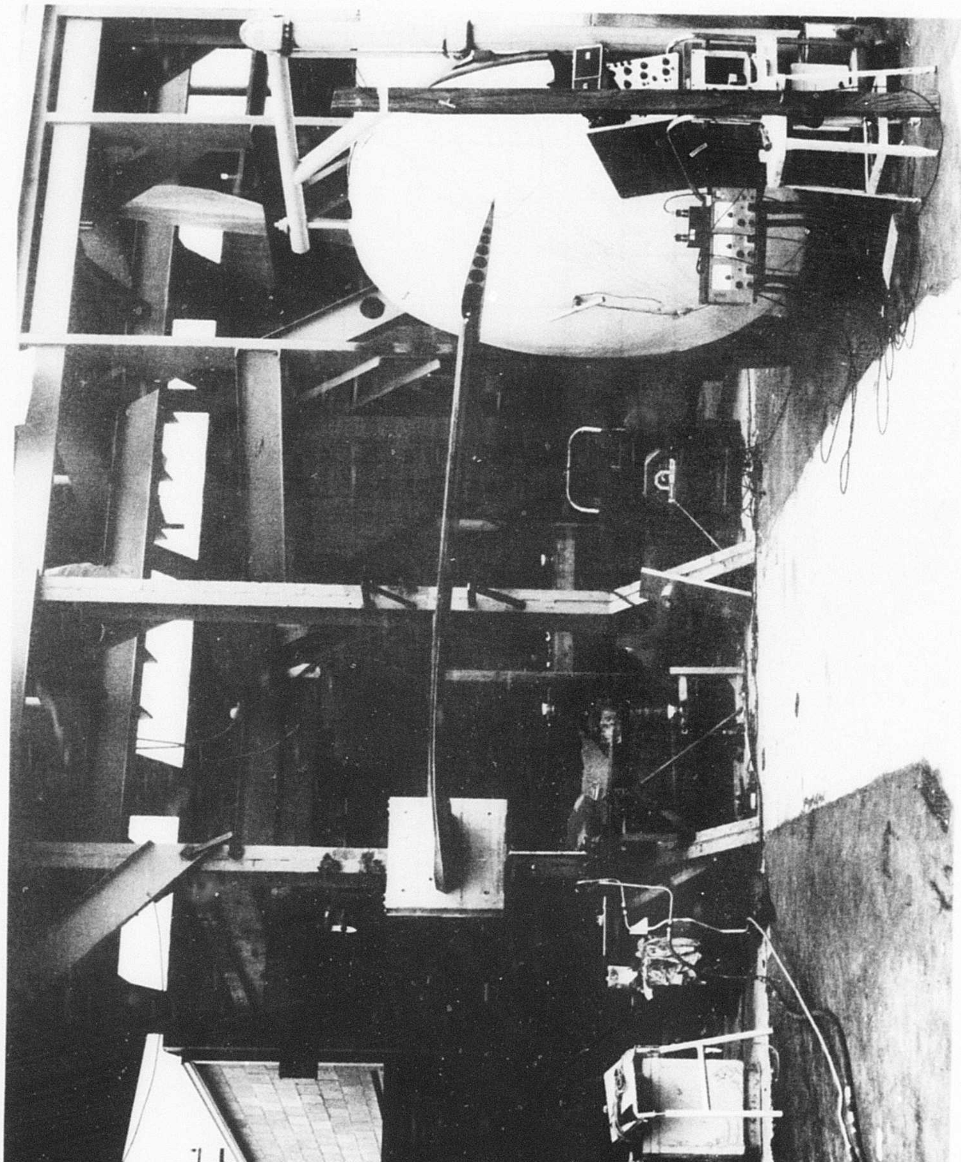

Figure 28. Mounting Position for Beamwise Testing.

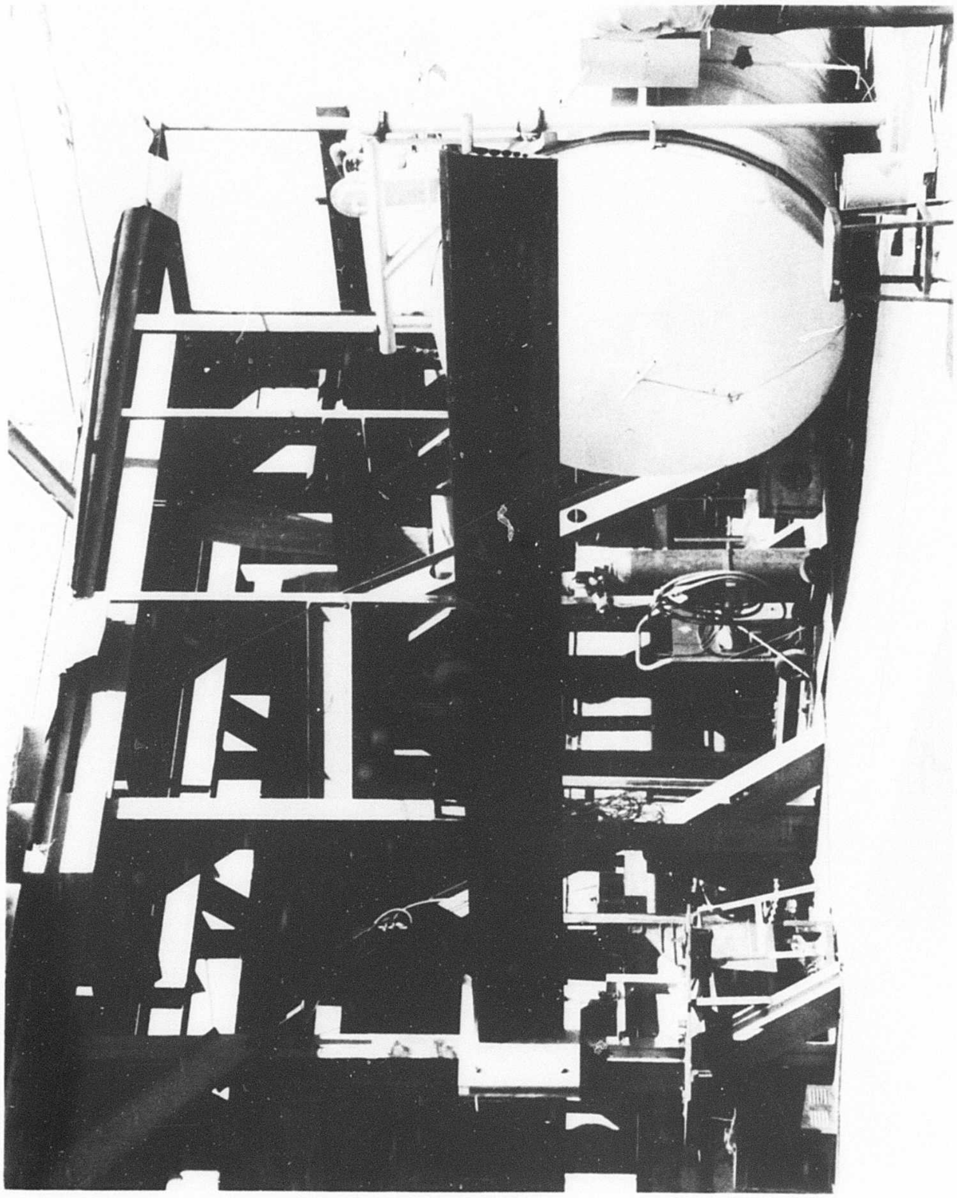

Figure 29. Mounting Position for Chordwise Testing.

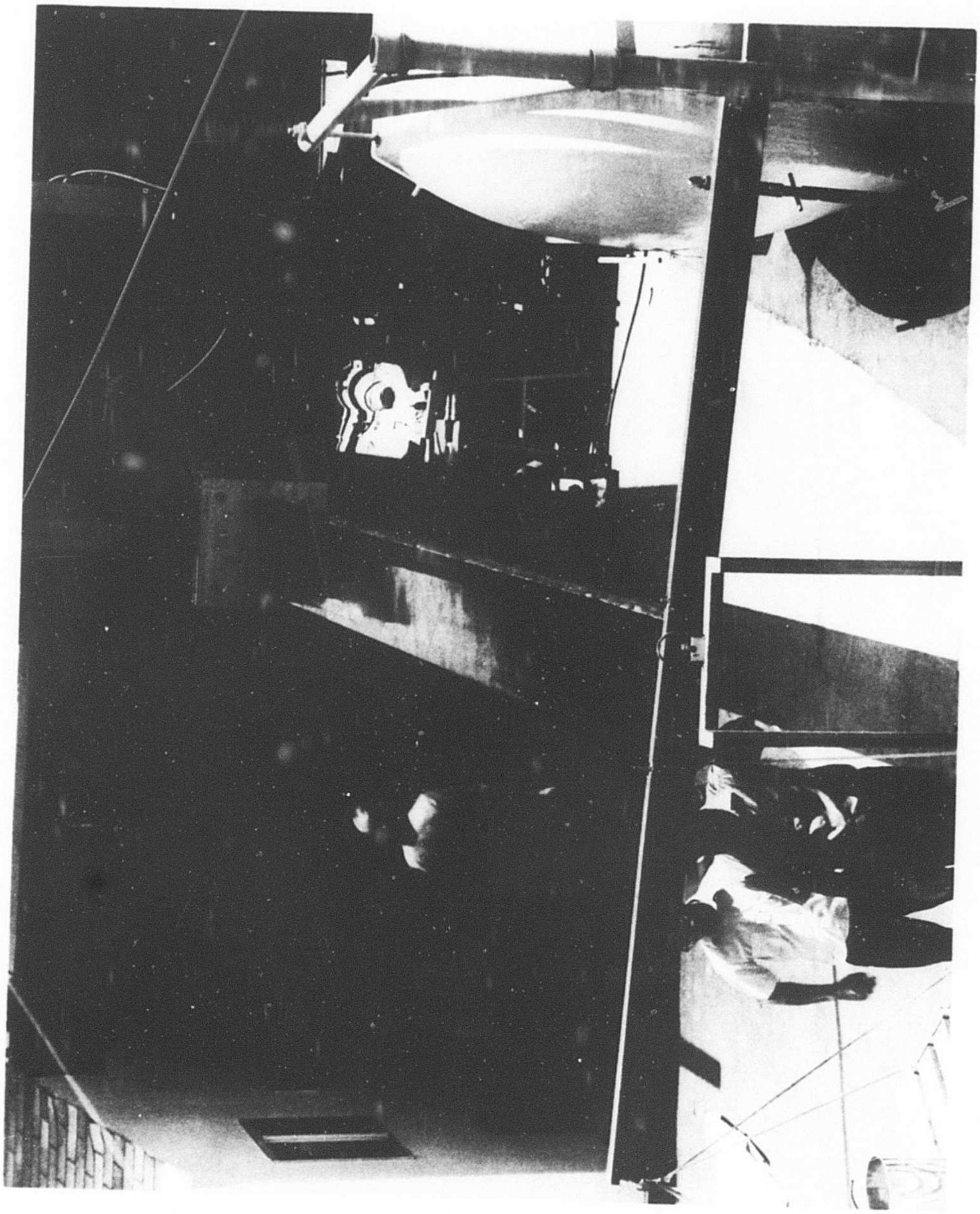

Figure 30. Mounting Position for Torsional Testing.

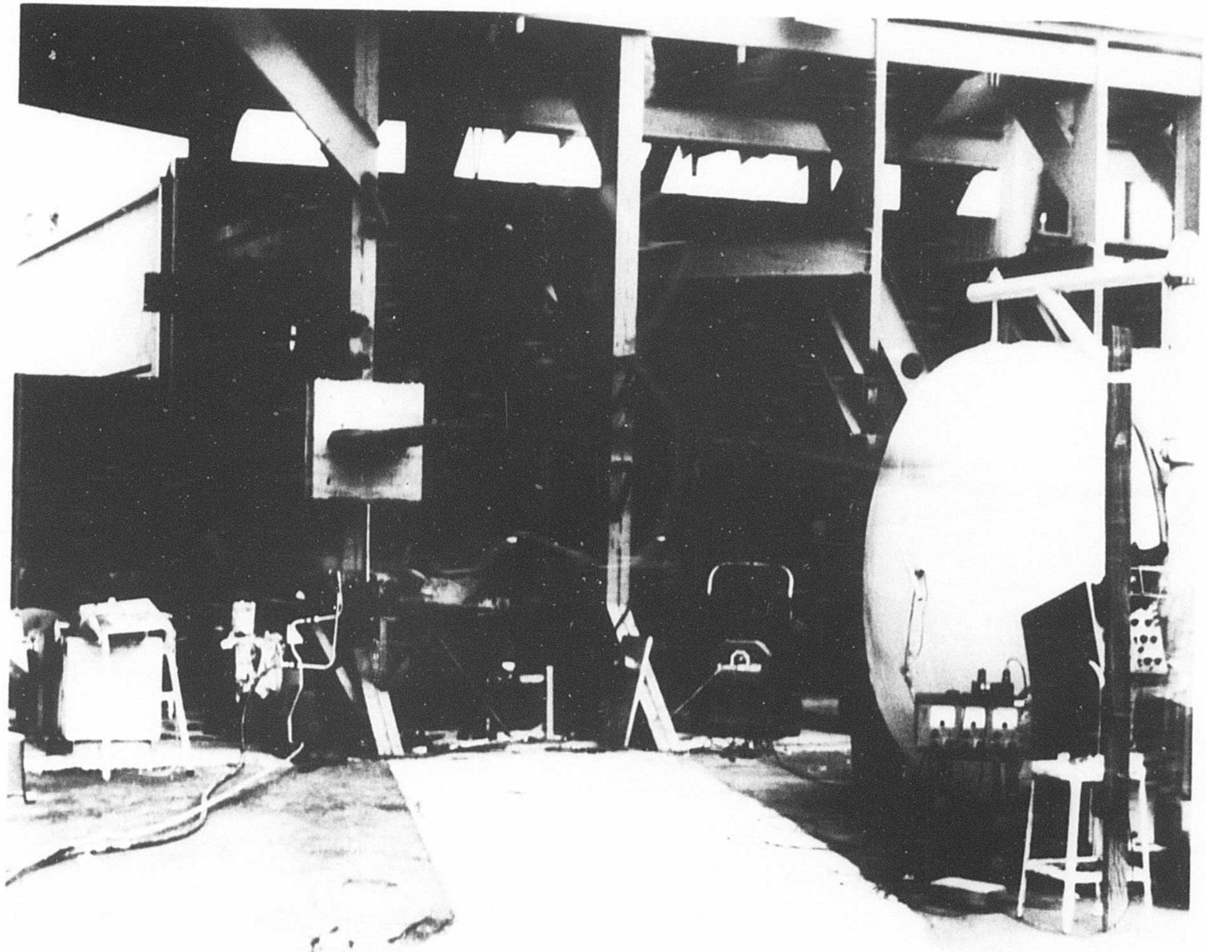

Figure 31. Beamwise Natural Frequency Test.

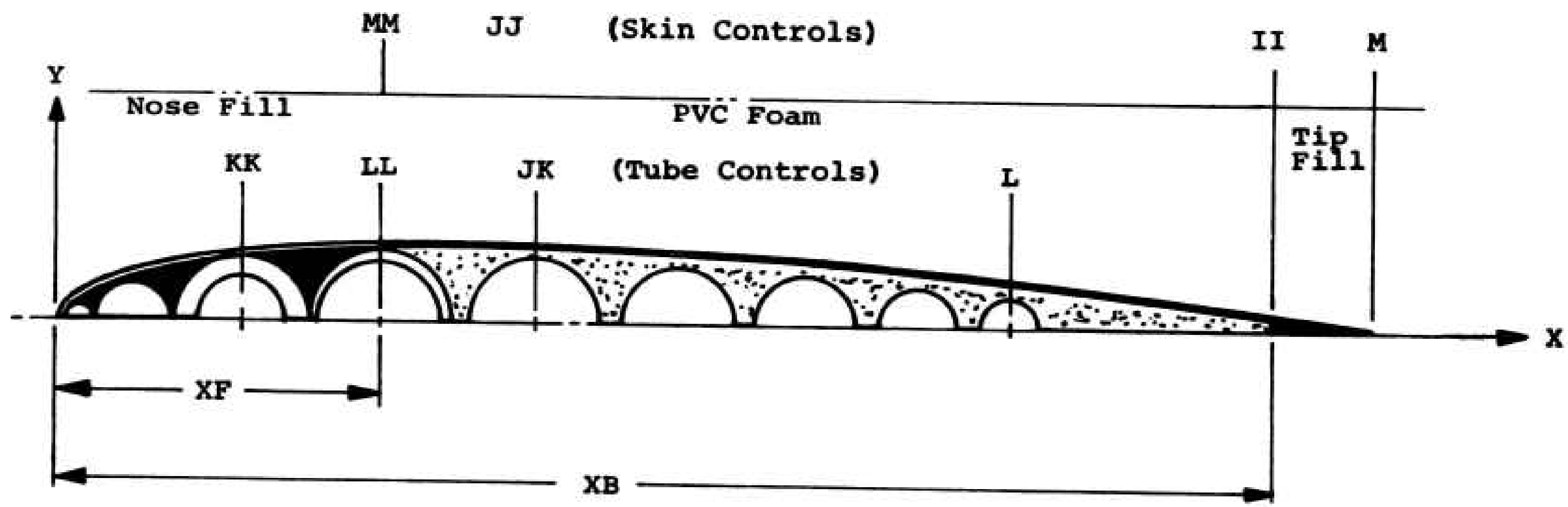

Figure 32. Computer Model.

TABLE I. TEST RESULTS SUMMARY FOR THE UH-1D FILAMENT-WOUND MAIN ROTOR BLADE

Condition	Metal Blade	S/N 001 GRP Composite Blade Test	S/N 001 GRP Composite Blade Calculated	S/N 003 PRD Composite Blade Test
Natural Frequency Results				
1st beamwise, cps	1.20	1.05	.95	1.14
2nd beamwise, cps	8.69	6.66	5.51	6.66
1st chordwise,cps	6.25	5.26	7.78	5.70
1st torsional, cps*	5.00	4.50	3.65	3.60
Static Deflection/1 g Load				
Beamwise, in.	6.66	18.28	16.666	8.88
Static Deflection Load at Tip				
Beamwise, 50-lb load, in.	5.75	14.50	15.44	9.06
Chordwise, 250-lb load, in.	1.31	2.01	1.80	2.97
Torsional torque, 10,000 in-lb, radians	.089	.134	.178	.118

*The testing laboratory mounted a 23.5-pound, 142.5-inch-long wood beam on the blade tip end.

TABLE II. METAL BLADE PARAMETERS (STATION 85.25 AND OUTBOARD)

Unit weight "W"	0.6 lb/in.
Center of gravity (dist. aft of l.e.) "CG"	5.25 in.
Torsional Stiffness "KGK"	31.0×10^6 lb-in.^{2}
Chordwise bending stiffness "EI_y"	$1{,}500.0 \times 10^6$ lb-in.^{2}
Spanwise bending stiffness "EI_x"	30.0×10^6 lb-in.^{2}
Spanwise extentional stiffness "EA"	47.0×10^6 lb

TABLE III. ROTOR BLADE LOADS AT STATION 85.25

Load	ROTOR SPEED - RPM 280	356
Centrifugal force, lb "P"	52,500 1 2 ***	91,000 3 4
Beamwise moment, in.-lb "M_b"*	+ 45,000 1 - 30,000 2	+ 25,000 3 - 20,000 4
Beamwise shear, lb "V_b"	+ 1,400 1 - 925 2	+ 725 3 - 640 4
Chordwise moment, in.-lb "M_c"**	+ 330,000 1 - 102,000 2	+ 365,000 3 - 95,000 4
Chordwise shear, lb "V_c"	+ 4,040 1 - 720 2	+ 4,750 3 - 1,400 4

*$+M_b$ denotes tension in lower side of blade.

**$+M_c$ denotes tension in leading edge of blade.

*** O denotes loading condition.

TABLE IV. ROTOR BLADE ROOT-END ATTACHMENT LOADS (STATION 28.0)

Load	Rotor Speed - RPM 280	Rotor Speed - RPM 356
Centrifugal force, lb "P"	63,000 1 2 ***	103,000 3 4
Beamwise moment, in.-lb "M_b"*	+ 250,000 1 - 175,000 2	+ 145,000 3 - 180,000 4
Beamwise shear, lb "V_b"	+ 5,630 1 - 4,210 2	+ 3,710 3 - 5,930 4
Chordwise moment, in.-lb "M_c"**	+ 510,000 1 - 195,000 2	+ 550,000 3 - 150,000 4
Chordwise shear, lb "V_c"	+ 4,070 1 + 560 2	+ 5,400 3 + 1,570 4

*$+M_b$ denotes tension in lower side of blade.

**$+M_c$ denotes tension in leading edge of blade.

*** O denotes loading condition.

TABLE V. MATERIAL PROPERTY SUMMARY

PROPERTY	E-Glass	S-Glass	PRD-49	Epoxy***	Poly-ester	PVC Foam	Syn-tactic Foam	Ceramic EC-TO
F_{tu}, psi	250,000	325,000	325,000	10,000	8,000	110	3,000	-
F_{cu}, psi	250,000	325,000	50,000	15,000	12,000	80	15,000	-
F_{su}, psi	-	-	-	8,000	6,500	70	10,000	-
E , 10^6 psi	10.5	12.6	19.0(L)* 1.42(T)**	0.5	0.4	.0025	.6	9.31
G , 10^6 psi	4.3	5.2	.27	.185	.148	.0025	.2	3.58
μ ,	.22	.22	.22	.35	.35	.3	.34	.3
α , 10^{-6} in./in./°F	2.8	2.2	-3.44	35.0	35.0	45.0	25.0	-
ρ , lb/in.^{3}	.0920	.0900	.0524	.0417	.0448	.001736	.0243	.2691

*L = in direction of fiber

**T = transverse to direction of fiber

***Resin system = Dow DER 332 (100 pbw)/APCO 320 (17.4 pbw)

TABLE VI. ROTOR BLADE CONSTRUCTION

Unit	Rotor Blade Units S/N 001	S/N 002	S/N 003
Leading Edge Skin			
Material	S-glass	S-Glass	PRD-49
Fiber orientation	20% @ 0° 80% @ 45°	20% @ 0° 80% @ ±45° + 1 ply #113	100% @ ±30° + 3 plies #181 -
Resin volume/weight	.500/.317	.500/.317	.500/.443
Thickness, in.	.0668	.0668	.0668
Skin			
Material	S-glass	S-Glass	PRD-49
Fiber orientation	100% @ ± 450	100% @ ± 45° + 1 ply #113	100% @ 30°
Resin volume/weight	.500/317	.500/.317	.500/.443
Thickness, in.	.0382	.0382	.0600
Tube (Rod) No. 1			
Material	E-glass*	E-glass*	E-glass*
Fiber orientation	100% @ 0°	100% @ 0°	100% @ 0°
Resin volume/weight	.432/.270	.432/.270	.432/.270
Tube No. 2			
Material	S-glass	S-glass	S-glass
Fiber orientation	16% @ 90° 63.8% @ ±45° 20.2% @ 0°*	16% @ 90° 63.8% @ ±45° 20.2% @ 0°*	16% @ 90° 63.8% @ ±30° 20.2% @ 0°*
Resin volume/weight	.420/.251	.420/.251	.420/.251
Tubes No. 3 and 4			
Material	S-glass	S-glass	S-glass
Fiber orientation	80% @ ±45° 20% @ 90°	80% @ ±45° 20% @ 90°	80% @ ±30° 20% @ 90°
Resin volume/weight	.420/.251	.420/.251	.420/.251

*Polyester resin system

TABLE VI - CONTINUED

Unit	Rotor Blade Units S/N 001	S/N 002	S/N 003
Tubes No. 5 through 9			
Material	S-glass	S-glass	S-glass
Fiber orientation	66.6% @ ±45° 33.4% @ 90°	66.6% @ ±45° 33.4% @ 90°	66.6% @ ±30° 33.4% @ 90°
Resin volume/weight	.420/.251	.420/.251	.420/.251
Leading Edge Fill			
Material	E-glass	S-glass	S-glass
Resin volume/weight	.500/.311	.500/.317	.500/.317
Trailing Edge Fill			
Material	S-glass	S-glass	PRD-49
Resin volume/weight	.500/.317	.500/.317	.500/.443
Foam Fill			
Material	PVC	PVC	PVC
Density, lb/ft^3	3.0	3.0	3.0
Root-End Reinforcing			
Material	E-glass**	E-glass**	E-glass**
Resin volume/weight	.550/.356	.550/.356	.550/.356

**One ply 181 fabric @ ±45° to four plies of 143 fabric @ 0° to spanwise direction of blade.

TABLE VII. SUMMARY OF ROTOR BLADE PROPERTIES AT STA. 85.25

Property	Criteria	S/N 001	S/N 002	S/N 003
W , lb/in.	.6	.6013	.5991	.5915
CG , in.	5.25	5.2939	5.3025	5.3066
NA , in.	4.9	4.935	4.7896	5.2488
EA , 10^6 lb	47.0	29.41	31.70	41.0
EI_x, 10^6 lb-in.^{2}	30.0	13.86	15.27	20.79
EI_y, 10^6 lb-in.^{2}	1,500.0	1,091.4	1,116.2	1,539.7
KG , 10^6 lb-in.^{2}	31.0	13.52*	13.52*	15.77*

* Due to a computer programming error in torsional stiffness calculation, the blades were improperly designed for torsional stiffness relative to the criteria. This error was not discovered until after fabrication of the blades.

TABLE VIII. ROTOR BLADE CROSS-SECTIONAL PROPERTIES AT STATION 85.25, S/N 001

ROTOR BLADE SKIN CROSS-SECTION PROPERTIES

N	XO	YO	TS	XI	YI	RHOS	ES	GS
1	0.0000	0.0000	.0668	.0659	0.0000	.0659	2.105E+06	1.624E+06
2	.1500	.3000	.0668	.1500	.1843	.0659	2.105E+06	1.624E+06
3	.3000	.4240	.0668	.3000	.3433	.0659	2.105E+06	1.624E+06
4	.5000	.5370	.0668	.5000	.4630	.0659	2.105E+06	1.624E+06
5	.8000	.6630	.0668	.8000	.5920	.0659	2.105E+06	1.624E+06
6	1.2000	.7900	.0668	1.2000	.7211	.0659	2.105E+06	1.624E+06
7	2.0000	.9660	.0668	2.0000	.8982	.0659	2.105E+06	1.624E+06
8	3.0000	1.1070	.0668	3.0000	1.0398	.0659	2.105E+06	1.624E+06
9	4.0000	1.1930	.0668	4.0000	1.1261	.0659	2.105E+06	1.624E+06
10	5.2310	1.2470	.0668	5.2310	1.1802	.0659	2.105E+06	1.624E+06
11	6.0000	1.2590	.0668	6.0000	1.1922	.0659	2.105E+06	1.624E+06
12	6.5000	1.2600	.0382	6.5000	1.2218	.0714	1.834E+06	1.889E+06
13	7.5000	1.2460	.0382	7.5000	1.2078	.0714	1.834E+06	1.889E+06
14	8.5000	1.2150	.0382	8.5000	1.1768	.0714	1.834E+06	1.889E+06
15	9.5000	1.1690	.0382	9.5000	1.1307	.0714	1.834E+06	1.889E+06
16	10.5000	1.1120	.0382	10.5000	1.0737	.0714	1.834E+06	1.889E+06
17	11.5000	1.0440	.0382	11.5000	1.0057	.0714	1.834E+06	1.889E+06
18	12.5000	.9660	.0382	12.5000	.9277	.0714	1.834E+06	1.889E+06
19	13.5000	.8810	.0382	13.5000	.8427	.0714	1.834E+06	1.889E+06
20	14.5000	.7890	.0382	14.5000	.7506	.0714	1.834E+06	1.889E+06
21	15.5000	.6890	.0382	15.5000	.6506	.0714	1.834E+06	1.889E+06
22	16.5000	.5840	.0382	16.5000	.5456	.0714	1.834E+06	1.889E+06
23	17.5000	.4720	.0382	17.5000	.4335	.0714	1.834E+06	1.889E+06
24	18.5000	.3530	.0382	18.5000	.3145	.0714	1.834E+06	1.889E+06
25	19.0000	.2920	.0382	19.0000	.2535	.0714	1.834E+06	1.889E+06
26	19.5000	.2280	.0382	19.5000	.1895	.0714	1.834E+06	1.889E+06
27	20.0000	.1630	.0382	20.0000	.1245	.0714	1.834E+06	1.889E+06
28	21.0000	.0270	.0382	21.0000	0.0000	.0714	1.834E+06	1.889E+06

CGS= 8.[illegible]622
AS= 1.[illegible]9.0
WS= .1374
SIx= 1.7083
SK= 10.1339
EAS= 3.8743E+06
EIx= 3.3542E+06
GSK= 9.2795E+06

TABLE VIII - CONTINUED

N	RO	RI	T	XT	ET	GT	RHOT
ROTOR BLADE TUBE CROSS-SECTION PROPERTIES							
1	.2500	0.0000	.2500	.3320	6.1380E+06	0.	.0716
2	.7050	0.0000	.7050	1.3040	3.2280E+06	1.6100E+06	.0599
3	1.0200	.7700	.2500	3.0390	2.4820E+06	1.8840E+06	.0697
4	1.1620	1.1000	.0620	5.2310	2.4820E+06	1.8840E+06	.0697
5	1.0750	1.0627	.0123	7.7190	2.5590E+06	1.6830E+06	.0867
6	.9650	.9527	.0123	10.0080	2.5590E+06	1.6830E+06	.0867
7	.8450	.8327	.0123	12.0470	2.5590E+06	1.6830E+06	.0867
8	.6760	.6637	.0123	13.7970	2.5590E+06	1.6830E+06	.0867
9	.5440	.5317	.0123	15.2670	2.5590E+06	1.6830E+06	.0867

N	AT	WT	TIX	EAT	ETIX	GTK
1	.1963	.0141	.0031	1.2052E+05	1.8831E+04	0.
2	1.5614	.1091	.1940	5.0404E+05	6.2630E+05	6.2474E+05
3	1.4059	.0980	.5740	3.4893E+05	1.4248E+06	2.1630E+06
4	.4406	.0307	.2820	1.0935E+05	6.9993E+05	1.0626E+06
5	.0826	.0072	.0472	2.1138E+05	1.2075E+05	1.5883E+05
6	.0741	.0064	.0341	1.8963E+05	8.7176E+04	1.1467E+05
7	.0648	.0056	.0228	1.6590E+05	5.8372E+04	7.6779E+04
8	.0518	.0045	.0116	1.3247E+05	2.9723E+04	3.9097E+04
9	.0416	.0036	.0060	1.0637E+05	1.5387E+04	2.0240E+04

CGT= 3.2580
AT= 3.9191
WT= .2792
TIX= .3081
TK= .6163
EAT= 1.1634E+07
ETIX= 3.0813E+06
GTK= 4.2600E+06

TABLE VIII - CONTINUED

ROTOR BLADE FILL CROSS-SECTION PROPERTIES

XF=	5.2310
CGFI=	2.9294
AFI=	2.1884
WFI=	.1464
FIX=	1.3468
EAFI=	1.2035E+07
EFIX=	7.4076E+06
EF=	5.5000E+06
RHOFI=	.0669

ROTOR BLADE FOAM CROSS-SECTION PROPERTIES

CGFO=	12.1888
AFO=	11.2785
WFO=	.0196
RHOFO=	.001736

ROTOR BLADE TIP CROSS-SECTION PROPERTIES

CGTP=	20.0000
ATP=	.2842
WTP=	.0187
RHOTP=	.0659
TPIX=	.0023
EATP=	1.8617E+06
ETPIX=	1.4854E+04
ETP=	6.5500E+06
XB=	19.5000

ROTOR CROSS-SECTIONAL PROPERTIES

CG=	5.2939
W=	.5013
EA=	2.9941E+07
FIX=	1.3656E+07
GK=	1.352E+07
EINA=	1.0914E+09
CNA=	4.9350

TABLE IX. ROTOR BLADE CROSS-SECTIONAL PROPERTIES AT STATION 85.25, S/N 002

ROTOR BLADE SKIN CROSS-SECTION PROPERTIES

N	XO	YO	TS	XI	YI	RHOS	ES	GS
1	0.0000	0.0000	.0668	.0668	0.0000	.0659	2.105E+06	1.624E+06
2	.1500	.3000	.0668	.1500	.1843	.0659	2.105E+06	1.624E+06
3	.3000	.4240	.0668	.3000	.3433	.0659	2.105E+06	1.624E+06
4	.5000	.5370	.0668	.5000	.4630	.0659	2.105E+06	1.624E+06
5	.8000	.6630	.0668	.8000	.5920	.0659	2.105E+06	1.624E+06
6	1.2000	.7900	.0668	1.2000	.7211	.0659	2.105E+06	1.624E+06
7	2.0000	.9660	.0668	2.0000	.8982	.0659	2.105E+06	1.624E+06
8	3.0000	1.1070	.0668	3.0000	1.0398	.0659	2.105E+06	1.624E+06
9	4.0000	1.1930	.0668	4.0000	1.1261	.0659	2.105E+06	1.624E+06
10	5.2310	1.2470	.0668	5.2310	1.1802	.0659	2.105E+06	1.624E+06
11	6.0000	1.2590	.0668	6.0000	1.1922	.0659	2.105E+06	1.624E+06
12	6.5000	1.2600	.0382	6.5000	1.2218	.0714	1.834E+06	1.889E+06
13	7.5000	1.2460	.0382	7.5000	1.2078	.0714	1.834E+06	1.889E+06
14	8.5000	1.2150	.0382	8.5000	1.1768	.0714	1.834E+06	1.889E+06
15	9.5000	1.1690	.0382	9.5000	1.1307	.0714	1.834E+06	1.889E+06
16	10.5000	1.1120	.0382	10.5000	1.0737	.0714	1.834E+06	1.889E+06
17	11.5000	1.0440	.0382	11.5000	1.0057	.0714	1.834E+06	1.889E+06
18	12.5000	.9660	.0382	12.5000	.9277	.0714	1.834E+06	1.889E+06
19	13.5000	.8810	.0382	13.5000	.8427	.0714	1.834E+06	1.889E+06
20	14.5000	.7890	.0382	14.5000	.7506	.0714	1.834E+06	1.889E+06
21	15.5000	.6890	.0382	15.5000	.6506	.0714	1.834E+06	1.889E+06
22	16.5000	.5840	.0382	16.5000	.5456	.0714	1.834E+06	1.889E+06
23	17.5000	.4720	.0382	17.5000	.4335	.0714	1.834E+06	1.889E+06
24	18.5000	.3530	.0382	18.5000	.3145	.0714	1.834E+06	1.889E+06
25	19.0000	.2920	.0382	19.0000	.2535	.0714	1.834E+06	1.889E+06
26	19.5000	.2280	.0382	19.5000	.1895	.0714	1.834E+06	1.889E+06
27	20.0000	.1630	.0382	20.0000	.1245	.0714	1.834E+06	1.889E+06
28	21.0000	.0270	.0382	21.0000	0.0000	.0714	1.834E+06	1.889E+06

CGS= 8.9622
AS= 1.9890
WS= .1374
SIX= 1.7083
SK= 10.1339
EAS= 3.8743E+06
EIX= 3.3542E+06
GSK= 9.2795E+06

TABLE IX - CONTINUED

ROTOR BLADE TUBE CROSS-SECTION PROPERTIES

N	RO	RI	T	XT	ET	GT	PHOT
1	.2500	0.0000	.2500	.3320	6.1380E+06	0.	.0716
2	.7050	0.0000	.7050	1.3040	3.2280E+06	1.6100E+06	.0699
3	1.0200	.7700	.2500	3.0390	2.4820E+06	1.8840E+06	.0697
4	1.1620	1.1000	.0620	5.2310	2.4820E+06	1.8840E+06	.0697
5	1.0750	1.0627	.0123	7.7180	2.5590E+06	1.6830E+06	.0867
6	.9650	.9527	.0123	10.0080	2.5590E+06	1.6830E+06	.0867
7	.8450	.8327	.0123	12.0470	2.5590E+06	1.6830E+06	.0867
8	.6760	.6637	.0123	13.7970	2.5590E+06	1.6830E+06	.0867
9	.5440	.5317	.0123	15.2670	2.5590E+06	1.6830E+06	.0867

N	AT	WT	TIX	EAT	ETIX	GTK
1	.1963	.0141	.0031	1.2052E+06	1.8831E+04	0.
2	1.5614	.1091	.1940	5.0404E+06	6.2630E+05	6.2474E+05
3	1.4059	.0980	.5740	3.4893E+06	1.4248E+06	2.1630E+06
4	.4406	.0307	.2820	1.0935E+06	6.9993E+05	1.0626E+06
5	.0826	.0072	.0472	2.1138E+05	1.2075E+05	1.5883E+05
6	.0741	.0064	.0341	1.8963E+05	8.7176E+04	1.1467E+05
7	.0648	.0056	.0228	1.6590E+05	5.8372E+04	7.6779E+04
8	.0518	.0045	.0116	1.3247E+05	2.9723E+04	3.9097E+04
9	.0416	.0036	.0060	1.0637E+05	1.5387E+04	2.0240E+04

CGT= 3.2580
AT= 3.9191
WT= .2792
TIX= .3081
TK= .6163
EAT= 1.1634E+07
ETIX= 3.0813E+06
GTK= 4.2600E+06

TABLE IX - CONTINUED

ROTOR BLADE FILL CROSS-SECTION PROPERTIES

XF=	5.2310
CGFI=	2.9294
AFI=	2.1884
WFI=	.1442
FIX=	1.3468
EAFI=	1.4334E+07
EFIX=	8.8218E+06
EF=	6.5500E+06
RHOFI=	.0659

ROTOR BLADE FOAM CROSS-SECTION PROPERTIES

CGFO=	12.1888
AFO=	11.2785
WFO=	.0196
RHOFO=	.001736

ROTOR BLADE TIP CROSS-SECTION PROPERTIES

CGTP=	20.0000
ATP=	.2842
WTP=	.0187
RHOTP=	.0659
TPIX=	.0023
EATP=	1.8617E+06
ETPIX=	1.4854E+04
ETP=	6.5500E+06
XB=	19.500

ROTOR CROSS-SECTIONAL PROPERTIES

CG=	5.3025
W=	.5991
EA=	3.170E+07
EIX=	1.527E+07
GK=	1.352E+07
EINA=	1.1162E+09
CNA=	4.7896

TABLE X. ROTOR BLADE CROSS-SECTIONAL PROPERTIES AT STATION 85.25, S/N 003

ROTOR BLADE SKIN CROSS-SECTION PROPERTIES

N	XO	YO	TS	XI	YI	RHOS	ES	GS
1	0.0000	0.0000	.0668	.0668	0.0000	.0548	3.997E+06	1.292E+06
2	.1500	.3000	.0668	.1500	.1843	.0548	3.997E+06	1.292E+06
3	.3000	.4240	.0668	.3000	.3433	.0548	3.997E+06	1.292E+06
4	.5000	.5370	.0668	.5000	.4630	.0548	3.997E+06	1.292E+06
5	.8000	.6630	.0668	.8000	.5920	.0548	3.997E+06	1.292E+06
6	1.2000	.7900	.0668	1.2000	.7211	.0548	3.997E+06	1.292E+06
7	2.0000	.9660	.0668	2.0000	.8982	.0548	3.997E+06	1.292E+06
8	3.0000	1.1070	.0668	3.0000	1.0398	.0548	3.997E+06	1.292E+06
9	4.0000	1.1930	.0668	4.0000	1.1261	.0548	3.997E+06	1.292E+06
10	5.2300	1.2470	.0668	5.2300	1.1802	.0548	3.997E+06	1.292E+06
11	6.0000	1.2590	.0668	6.0000	1.1922	.0548	3.997E+06	1.292E+06
12	6.5000	1.2600	.0600	6.5000	1.2000	.0539	2.975E+06	1.975E+06
13	7.5000	1.2460	.0600	7.5000	1.1860	.0539	2.975E+06	1.975E+06
14	8.5000	1.2150	.0600	8.5000	1.1550	.0539	2.975E+06	1.975E+06
15	9.5000	1.1690	.0600	9.5000	1.1089	.0539	2.975E+06	1.975E+06
16	10.5000	1.1120	.0600	10.5000	1.0519	.0539	2.975E+06	1.975E+06
17	11.5000	1.0440	.0600	11.5000	.9838	.0539	2.975E+06	1.975E+06
18	12.5000	.9660	.0600	12.5000	.9058	.0539	2.975E+06	1.975E+06
19	13.5000	.8810	.0600	13.5000	.8208	.0539	2.975E+06	1.975E+06
20	14.5000	.7890	.0600	14.5000	.7287	.0539	2.975E+06	1.975E+06
21	15.5000	.6890	.0600	15.5000	.6287	.0539	2.975E+06	1.975E+06
22	16.5000	.5840	.0600	16.5000	.5236	.0539	2.975E+06	1.975E+06
23	17.5000	.4720	.0600	17.5000	.4116	.0539	2.975E+06	1.975E+06
24	18.5000	.3530	.0600	18.5000	.2926	.0539	2.975E+06	1.975E+06
25	19.0000	.2920	.0600	19.0000	.2315	.0539	2.975E+06	1.975E+06
26	19.7500	.1960	.0600	19.7500	.1355	.0539	2.975E+06	1.975E+06
27	20.0000	.1630	.0600	20.0000	.1025	.0539	2.975E+06	1.975E+06
28	21.0000	.0270	.0600	21.0000	0.0000	.0539	2.975E+06	1.975E+06

CGS= 10.0199
AS= 2.6128
WS= .1416
SIX= 2.1588
SK= 14.0883
EAS= 8.6270E+06
EIX= 7.2563E+06
GSK= 1.2159E+06

TABLE X - CONTINUED

ROTOR BLADE TUBE CROSS-SECTION PROPERTIES

N	RO	RI	T	XT	ET	GT	RHOT
1	.2500	0.0000	.2500	.3320	6.1380E+06	0.	.0716
2	.7050	0.0000	.7050	1.3040	4.2910E+06	1.4310E+06	.0699
3	1.0200	.7700	.2500	3.0390	3.9740E+06	1.5820E+06	.0697
4	1.1620	1.1000	.0620	5.2310	3.9740E+06	1.5820E+06	.0697
5	1.0750	1.0627	.0123	7.7180	3.8020E+06	1.4320E+06	.0867
6	.9650	.9527	.0123	10.0080	3.8020E+06	1.4320E+06	.0867
7	.8450	.8327	.0123	12.0470	3.8020E+06	1.4320E+06	.0867
8	.6760	.6637	.0123	13.7970	3.8020E+06	1.4320E+06	.0867
9	.5440	.5317	.0123	15.2670	3.8020E+06	1.4320E+06	.0867

N	AT	WT	TIX	EAT	ETIX	GTK
1	.1963	.0141	.0031	1.2052E+06	1.8831E+04	0.
2	1.5614	.1091	.1940	6.7002E+06	8.3254E+05	5.5528E+05
3	1.4059	.0980	.5740	5.5869E+06	2.2813E+06	1.8163E+06
4	.4406	.0307	.2820	1.7509E+06	1.1207E+06	8.9226E+05
5	.0826	.0072	.0472	3.1406E+05	1.7940E+05	1.3514E+05
6	.0741	.0064	.0341	2.8174E+05	1.2952E+05	9.7566E+04
7	.0648	.0056	.0228	2.4648E+05	8.6725E+04	6.5329E+04
8	.0518	.0045	.0116	1.9682E+05	4.4161E+04	3.3266E+04
9	.0416	.0036	.0060	1.5804E+05	2.2862E+04	1.7221E+04

CGT= 3.2580
AT= 3.9191
WT= .2792
TIX= .4716
TK= .9432
EAT= 1.6440E+07
ETIX= 4.7160E+06
GTK= 3.6124E+06

TABLE X - CONTINUED

ROTOR BLADE FILL CROSS-SECTION PROPERTIES

XF=	5.2300
CGFI=	2.9279
AFI=	2.1861
WFI=	.1441
FIX=	1.3458
EAFI=	1.4319E+07
EFIX=	8.8151E+06
EF=	6.5500E+06
RHOFI=	.0659

ROTOR BLADE FOAM CROSS-SECTION PROPERTIES

CGFO=	12.2028
AFO=	10.7768
WFO=	.0187
RHOFO=	.001736

ROTOR BLADE TIP CROSS-SECTION PROPERTIES

CGTP=	20.1667
ATP=	.1694
WTP=	.0080
RHOTP=	.0470
TPIX=	.0007
EATP=	1.6514E+06
ETPIX=	6.7383E+03
ETP=	9.7500E+06
XB=	19.7500

ROTOR CROSS-SECTIONAL PROPERTIES

CG=	5.3066
W=	.5915
EA=	4.104E+07
EIX=	2.079E+07
GK=	1.577E+07
EINA=	1.5397E+09
CNA=	5.2448

TABLE XI. INSPECTION REPORT, S/N 001

Tool Drawing Dimension (in.)	Actual Dimension (in.)	Remarks
263.75	263.87	
41.70	42.20	
31.20	31.55	
22.20	22.60	
15.40	15.70	
10.50	10.51	
.62 (Typ)	.600 - .620	
7.50		Unable to inspect
12.20		Unable to inspect
18.00	18.08	
21.00	21.06	
5.70	5.77	
1.05	1.08	
7.75	7.795	
12.00	11.10	
12.50	12.30	
35.00	34.25	
38.50	38.88	
43.00	43.25	
47.40	47.80	
52.00	52.22	
56.20	56.70	
61.00	61.20	
1.00R (Typ)	1.0 to 1.2	
Reference sheet 8, Section F-F 2.520	2.59 to 264	
Weight	214.4	

TABLE XII. INSPECTION REPORT, S/N 002

Tool Drawing Dimension	Actual Dimension
263.75 ± .12 length	263.75 in.
21.0 width	19.98 to 21.06 in.
Reference sheet 3, section A-A 4.50 ± .06 "Z"	4.46 to 4.64 in.
1.906 ± .06 "Z"	1.865 to 2.065 in.
Reference sheet 8, section F-F 2.520	2.518 in.
Weight	210.4 lb

TABLE XIII. INSPECTION REPORT, S/N 003

Tool Drawing Dimension	Actual Dimension
263.75 ± .12 length	263.63 in.
21.0 width	21.110 in. at root-end
21.0 width	20.940 in. at center
21.0 width	21.00 in. at r.h. eop
Reference sheet 3, section A-A 4.500 ± .060 "Z"	Tapers from 4.710 in. at eop to 4.787 in.
1.906 ± .060 "Z"	Tapers from 2.088 to 2.203 in.
Total weight	2.16.3 lb
Reference sheet 8, section F-F 2.520	2.540 in.

TABLE XIV. WEIGHT AND CENTER-OF-GRAVITY MEASUREMENTS SUMMARY

Configuration	Weight (lb)	Chordwise CG (in.)	Spanwise CG (in.)
Metal blade	204.4	5.43	115.59
S/N 001	214.4	5.80	109.44
S/N 002	210.4	5.70	111.82
S/N 003	216.3	6.17	109.09

TABLE XV. NATURAL FREQUENCY MEASUREMENTS

Condition	Metal Blade	Actual	Calculated	S/N 003
1st beamwise, cps	1.20	1.05	.95	1.14
2nd beamwise, cps	8.69	6.66	5.51	6.66
1st chordwise, cps	6.25	5.26	7.78	5.70
Torsional, cps	5.00	4.50	3.65	3.60

TABLE XVI. COMPUTER PROGRAM (CROSS-SECTIONAL PROPERTIES OF TUBULAR-REINFORCED COMPOSITE ROTOR BLADE)

```
RUN VERSION 2.3 --PSR LEVEL 312--

                     PROGRAM ROTOR(INPUT,OUTPUT,TAPE5=INPUT,TAPE6=OUTPUT)
000003               DIMENSION XO(30),YO(30),XI(30),YI(30),TS(30),RHOS(30),ES(30),GS(30
                    1),AO(30),AI(30),RO(15),RI(15),T(15),XT(15),RHOT(15),ET(15),GT(15),
                    2AT(15),WT(15),TIX(15),EAT(15),ETIX(15),GTK(15)
000003             1 READ(5,2)M,L,MM,LL,II
000021             2 FORMAT(5I5)
              C      M=NO. SKIN COORDINATE POINTS
              C      L=NO. TUBES
              C      MM=SKIN STATION NUMBER CORRESPONDING TO XF
              C      LL=TUBE NUMBER CORRESPONDING TO XF
              C      II=SKIN STATION NUMBER CORRESPONDING TO XB
000021             3 DO 10 N=1,M
000023               READ(5,5)XO(N),YO(N),TS(N),RHOS(N),ES(N),GS(N)
000042             5 FORMAT(4F10.0,2E12.3)
000042            10 CONTINUE
000045            11 DO 15 N=1,L
000047               READ(5,12)RO(N),T(N),XT(N),RHOT(N),ET(N),GT(N)
000066            12 FORMAT(4F10.0,2E12.3)
000066            15 CONTINUE
000071            14 READ(5,16)RHOFI,RHOFO,RHOTP,EF,EFO,ETP,GF,GFO,GTP
000117            16 FORMAT(3F10.0/3E12.3/3E12.3)
              C      CALCULATE INSIDE SKIN COORDINATES
000117            17 CONTINUE
000117               XF=XO(MM)
000121               XB=XO(II)
000123               XI(1)=XO(1)+TS(1)
000125               YI(1)=0.
000126               K=M-1
000130               DO 20 N=2,K
000132               PSI=ATAN((XO(N+1)-XO(N-1))/(YO(N+1)-YO(N-1)))
000141               IF (PSI)18,19,19
000143            18 PSI=-PSI
000144            19 CONTINUE
000144               XI(N)=XO(N)
000146               YI(N)=YO(N)-TS(N)/SIN(PSI)
000154            20 CONTINUE
000157               XI(M)=XO(M)
000161               YI(M)=0.
              C      CALCULATE SKIN CROSS-SECTIONAL AREA AND STIFFNESS
000162               AO(2)=XO(2)*YO(2)
000164               AI(2)=(XI(2)-XI(1))*YI(2)
000167               AS=AO(2)-AI(2)
000171               WS=AS*RHOS(2)
000173               AX=AO(2)*XO(2)*2./3.-AI(2)*(XI(1)+(XI(2)-XI(1))*2./3.)
000202               EAS=AS*ES(2)
000205               DO 25 N=3,M
000206               AO(N)=(XO(N)-XO(N-1))*(YO(N)+YO(N-1))
000214               AI(N)=(XI(N)-XI(N-1))*(YI(N)+YI(N-1))
000222               AS=AS+AO(N)-AI(N)
000225               EAS=EAS+(AO(N)-AI(N))*ES(N)
              C      CALCULATE SKIN WEIGHT/IN. AND CG.
000232               AX=AX+((AO(N)-AI(N))*(XO(N)+XO(N-1))/2.)
000241               WS=WS+(AO(N)-AI(N))*RHOS(N)
000246            25 CONTINUE
```

TABLE XVI - CONTINUED

```
RUN VERSION 2.3 --PSR LEVEL 312--                                ROTOR

000251            CGS=AX/AS
             C    CALCULATE SKIN CROSS-SECTIONAL MOMENT OF INERTIA ABOUT X-X AXIS
             C    AND STIFFNESS
000252            SIX=(XO(2)*YO(2)**3-(XI(2)-XI(1))*YI(2)**3)/6.
000261            ESIX=SIX*ES(2)
000263            DO 35 N=3,M
000265            SIX=SIX+(XO(N)-XO(N-1))*((YO(N)+YO(N-1))**3-(YI(N)+YI(N-1))**3)/12
                 1.
000301            ESIX=ESIX+(XO(N)-XO(N-1))*((YO(N)+YO(N-1))**3-(YI(N)+YI(N-1))**3)/
                 112.*ES(N)
000316         35 CONTINUE
             C    CALCULATE SKIN CROSS-SECTION TORSIONAL CONSTANT
000321            SL=0.
000321            AL=0.
000322            SC=0.
000324            DO 40 N=2,M
000325            SL=SL+(((XO(N)-XO(N-1))**2+(YO(N)-YO(N-1))**2)**.5+((XI(N)-XI(N-1)
                 1)**2+(YI(N)-YI(N-1))**2)**.5)/(    TS(N))
000354            AL=AL+(AO(N)+AI(N))/2.
000361            SC=SC+(((XO(N)-XO(N-1))**2+(YO(N)-YO(N-1))**2)**.5+((XI(N)-XI(N-1)
                 1)**2+(YI(N)-YI(N-1))**2)**.5)/(    TS(N))/GS(N)
000411         40 CONTINUE
000414            SK=4.*AL**2/SL
000417            GSK=4.*AL**2/SC
             C    WRITE SKIN PROPERTIES
000422         50 WRITE(6,52)
000426         52 FORMAT(1H1,5X,41HROTOR BLADE SKIN CROSS-SECTION PROPERTIES///)
000426            WRITE(6,54)
000432         54 FORMAT(9X,92HN         XO            YO            TS            XI
                 1    YI             RHOS         ES            GS/)
000432            DO 60 N=1,M
000434            WRITE(6,56)N,XO(N),YO(N),TS(N),XI(N),YI(N),RHOS(N),ES(N),GS(N)
000461         56 FORMAT(5X,I5,6F12.4,2E12.3)
000461         60 CONTINUE
000464            WRITE(6,62)CGS,AS,WS,SIX,SK,EAS,ESIX,GSK
000507         62 FORMAT(//5X,4HCGS=F10.4/6X,3HAS=F10.4/6X,3HWS=F10.4/5X,4HSIX=F10.4
                 1/6X,3HSK=F10.4/5X,4HEAS=E12.4/5X,4HEIX=E12.4/5X,4HGSK=E12.4)
             C    CALCULATE TUBE AREA, WEIGHT AND CG.
000507            AB=0.
000510            WB=0.
000510            WBX=0.
000512            DO 200 N=1,L
000513            RI(N)=RO(N)-T(N)
000516            AT(N)=3.14159*(RO(N)**2-RI(N)**2)
000522            AB=AB+AT(N)
000524            WT(N)=AT(N)*RHOT(N)
000527            WB=WB+WT(N)
000531            WBX=WBX+WT(N)*XT(N)
000534        200 CONTINUE
000536            CGT=WBX/WB
             C    CALCULATE TUBE CROSS-SECTIONAL MOMENT OF INERTIA ABOUT X-X AXIS
000540            DO 210 N=1,L
000542            TIX(N)=3.14159/4.*(RO(N)**4-RI(N)**4)
000547        210 CONTINUE
             C    CALCULATE TUBE CROSS-SECTIONAL STIFFNESS
```

TABLE XVI - CONTINUED

```
RUN VERSION 2.3 --PSR LEVEL 312--                              ROTOR

000551          EAB=0.
000551          EBIX=0.
000552          GBK=0.
000554          DO 215 N=1,L
000555          EAT(N)=AT(N)*ET(N)
000560          EAB=EAB+EAT(N)
000562          ETIX(N)=TIX(N)*ET(N)
000564          EBIX=EBIX+ETIX(N)
000566          GTK(N)=2.*TIX(N)*GT(N)
000571          GBK=GBK+GTK(N)
000574      215 CONTINUE
000576          E=10000000.
000577          BIX=EBIX/E
000600          BK=2.*BIX
          C     BIX= MOMENT OF INERTIA ABOUT X-X AXIS OF ALL THE TUBES
          C     WRITE TUBE PROPERTIES
000602      220 WRITE(6,222)
000606      222 FORMAT(1H1,5X,41HROTOR BLADE TUBE CROSS-SECTION PROPERTIES///)
000606          WRITE(6,225)
000612      225 FORMAT(9X,89HN          RO            RI             T              XT
               1       ET            GT              RHOT/)
000612          DO 230 N=1,L
000614          WRITE(6,227)N,RO(N),RI(N),T(N),XT(N),ET(N),GT(N),RHOT(N)
000637      227 FORMAT(5X,I5,4F12.4,2E15.4,1F12.4)
000637      230 CONTINUE
000642          WRITE(6,235)
000645      235 FORMAT(///9X,75HN          AT             WT            TIX          EAT
               1          ETIX           GTK//)
000645          DO 240 N=1,L
000647          WRITE(6,237)N,AT(N),WT(N),TIX(N),EAT(N),ETIX(N),GTK(N)
000670      237 FORMAT(5X,I5,3F12.4,3E15.4)
000670      240 CONTINUE
000673          WRITE(6,250)CGT,AB,WB,BIX,BK,EAB,EBIX,GBK
000716      250 FORMAT(//5X,4HCGT=F10.4/6X,3HAT=F10.4/6X,3HWT=F10.4/5X,4HTIX=F10.4
               1/6X,3HTK=F10.4/5X,4HEAT=E12.4/4X,5HETIX=E12.4/5X,4HGTK=E12.4)
          C     CALCULATE FILL AREA
000716          AS=0.
000717          DO 115 N=2,MM
000721          AS=AS+AI(N)
000723      115 CONTINUE
000725          AF=0.
000725          KK=LL-1
          C     KK= NO. COMPLETE TUBES ACTING WITH FILL MATERIAL
000730          DO 120 N=1,KK
000731          AF=AF+3.14159*RO(N)**2
000734      120 CONTINUE
000737          AFI=AS-AF-3.14159*RO(LL)**2/2.
          C     CALCULATE FILL WEIGHT/IN. AND CG
000744          WFI=AFI*RHOFI
000746          AX=AI(2)*(XI(1)+(XI(2)-XI(1))*2./3.)
000753          DO 125 N=3,MM
000755          DX=XI(N)-XI(N-1)
000757          AX=AX+DX*(YI(N-1)*2.)*(XI(N)-DX/2.)+(YI(N)-YI(N-1))*DX*(XI(N)-DX/3
               1.)
000777      125 CONTINUE
```

```
RUN VERSION 2.3 --PSR LEVEL 312--                                    ROTOR

001002            ATX=0.
001003            DO 130 N=1,KK
001004            ATX=ATX+3.14159*RO(N)**2*XT(N)
001010        130 CONTINUE
001013            ATX=ATX+3.14159/2.*RO(LL)**2*(XF-.4244*RO(LL))
001023            CGFI=(AX-ATX)/AFI
           C      CALCULATE FILL CROSS-SECTIONAL MOMENT OF INERTIA ABOUT X-X AXIS
001025            FIX=(XI(2)-XI(1))*YI(2)**3/4.5
001032            DO 135 N=3,MM
001033            FIX=FIX+(YI(N)+YI(N-1))**3*(XI(N)-XI(N-1))/12.
001043        135 CONTINUE
001046            DO 140 N=1,KK
001047            FIX=FIX-3.14159/4.*RO(N)**4
001053        140 CONTINUE
001055            FIX=FIX-3.14159/4.*RO(LL)**4./2.
           C      CALCULATE FILL CROSS-SECTIONAL STIFFNESS
001065            EAFI=AFI*EF
001067            EFIX=FIX*EF
           C      WRITE FILL PROPERTIES
001071        150 WRITE(6,152)
001075        152 FORMAT(1H1,5X,41HROTOR BLADE FILL CROSS-SECTION PROPERTIES///)
001075            WRITE(6,154)XF,CGFI,AFI,WFI,FIX,EAFI,EFIX,EF,RHOFI
001123        154 FORMAT(6X,3HXF=F10.4/4X,5HCGFI=F10.4/5X,4HAFI=F10.4/5X,4HWFI=F10.4
                 1/5X,4HFIX=F10.4/4X,5HEAFI=E12.4/4X,5HEFIX=E12.4//6X,3HEF=E12.4/3X,
                 26HRHOFI=F10.4)
           C      CALCULATE FOAM AREA, WEIGHT AND CG.
001123            AS=0.
001124            ASX=0.
001124            JJ=MM+1
           C      JJ= SKIN STATION NUMBER CORRESPONDING TO XF + 1
001127            DO 310 N=JJ,II
001130            AS=AS+AI(N)
001132            ASX=ASX+AI(N)*(XI(N)+XI(N-1))/2.
001137        310 CONTINUE
001142            AB=3.14159/2.*RO(LL)**2
001144            ABX=AB*(XT(LL)+4.*RO(LL)/(3.*3.14159))
001152            JK=LL+1
           C      JK= TUBE NUMBER CORRESPONDING TO XF + 1
001154            DO 315 N=JK,L
001155            AB=AB+3.14159*RO(N)**2
001160            ABX=ABX+3.14159*RO(N)**2*XT(N)
001164        315 CONTINUE
001167            AFO=AS-AB
001171            CGFO=(ASX-ABX)/AFO
001174            WFO=AFO*RHOFO
           C      WRITE FOAM PROPERTIES
001176        325 WRITE(6,327)
001202        327 FORMAT(///,5X,41HROTOR BLADE FOAM CROSS-SECTION PROPERTIES//)
001202            WRITE(6,330)CGFO,AFO,WFO,RHOFO
001216        330 FORMAT(4X,5HCGFO=F10.4/5X,4HAFO=F10.4/5X,4HWFO=F10.4/3X,6HRHOFO=F1
                 12.6)
           C      CALCULATE TIP AREA WEIGHT, MOMENT OF INERTIA ABOUT X-X AXIS AND CG
001216            ATP=(XI(M)-XB)*YI(II)
001222            WTP=ATP*RHOTP
001224            CGTP=XB+(XI(M)-XB)/3.
```

TABLE XVI - CONTINUED

```
RUN VERSION 2.3 --PSR LEVEL 312--                          ROTOR

001230          EATP=ETP*ATP
001232          TPIX=(XI(M)-XB)*(YI(II)*2.)**3/36.
001241          ETPIX=TPIX*ETP
          C     WRITE TIP PROPERTIES
001244          WRITE(6,450)
001247      450 FORMAT(///,5X,40HROTOR BLADE TIP CROSS-SECTION PROPERTIES//)
001247          WRITE(6,455)CGTP,ATP,WTP,RHOTP,TPIX,EATP,ETPIX,ETP,XB
001275      455 FORMAT(4X,5HCGTP=F10.4/5X,4HATP=F10.4/5X,4HWTP=F10.4/3X,6HRHOTP=F1
               10.4/4X,5HTPIX=F10.4/4X,5HEATP=E12.4/3X,6HETPIX=E12.4/5X,4HETP=E12.
               24/6X,3HXB=F10.4)
          C     ROTOR BLADE CROSS-SECTIONAL PROPERTIES
001275          W=WS+WFI+WB +WFO+WTP
001302          CG=(WS*CGS+WFI*CGFI+WB*CGT+WFO*CGFO+WTP*CGTP)/W
001314          EA=EAS+EAFI+EAB+EATP
001320          EIX=ESIX+EFIX+EBIX+ETPIX
001324          GK=GSK+GBK
001326          CNA=(EAS*CGS+EAFI*CGFI+EAB*CGT+EATP*CGTP)/EA
          C     EINA SKIN
001337          EINA=(CNA-2./3.*XO(2))**2*AO(2)-(CNA-XI(1)-2./3.*(XI(2)-XI(1)))**2
               1*AI(2)
001351          EINA=EINA*ES(2)
001353          DO 460 N=3,M
001354          EINA=EINA+((CNA-(XO(N)+XO(N-1))/2.)**2*(AO(N)-AI(N))+(XO(N)-XO(N-1
               1))**2*(AO(N)-AI(N))/12.)*ES(N)
001373      460 CONTINUE
          C     EINA FILL
001375          EINA=EINA+(CNA-XI(1)-2./3.*(XI(2)-XI(1)))**2*AI(2)*EF
001405          DO 470 N=3,MM
001407          DX=XI(N)-XI(N-1)
001411          EINA=EINA+((CNA-XI(N)+DX/2.)**2*(DX*YI(N-1)*2.)+(CNA-XI(N)+DX/3.)*
               1(DX*(YI(N)-YI(N-1)))+(2.*YI(N-1)*DX**3/12.)+(2.*(YI(N)-YI(N-1))*DX
               2**3/36.))*EF
001445          EINA=EINA+((CNA-(XI(N)+XI(N-1))/2.)**2*(AI(N))+(XI(N)-XI(N-1))**2*
               1AI(N)/12.)*EF
001461      470 CONTINUE
001464          DO 475 N=1,KK
001466          EINA=EINA-((CNA-XT(N))**2*3.14159*RO(N)**2+3.14159/4.*RO(N)**4)*EF
001477      475 CONTINUE
001502          EINA=EINA-((CNA-XF-.4244*RO(LL))**2*3.14159*RO(LL)**2/2.+.1098*RO(
               1LL)**4)*EF
          C     EINA TUBES
001516          DO 480 N=1,L
001520          EINA=EINA+((CNA-XT(N))**2*AT(N)+TIX(N))*ET(N)
001527      480 CONTINUE
          C     EINA TIP
001532          EINA=EINA+((CNA-(XB+(XI(M)-XB)/3.))**2*ATP+(XI(M)-XB)**3*2.*YI(II)
               1/36.)*ETP
001547          WRITE(6,500)
001553      500 FORMAT(///,5X,32HROTOR CROSS-SECTIONAL PROPERTIES//)
001553          WRITE(6,502)CG,W,EA,EIX,GK,EINA,CNA
001575      502 FORMAT(6X,3HCG=F10.4/7X,2HW=F10.4/6X,3HEA=E12.3/5X,4HEIX=E12.3/6X,
               13HGK=E12.3/4X,5HEINA=E12.4/5X,4HCNA=F10.4//)
001575      600 GO TO 1
001576          END
```

APPENDIX I
SECTION PROPERTY COMPUTER PROGRAM

This appendix contains the computer program used in calculating the cross-sectional properties of the tubular-reinforced rotor blade. Table XVI shows the computer program for the cross-sectional properties of the tubular-reinforced composite rotor blade.

Controls Nomenclature

II	skin station number corresponding to XB
JJ	skin station number corresponding to XF+1
JK	tube number corresponding to XF+1
KK	number of complete tubes acting with fill
L	number of tubes
LL	tube number corresponding to XF
M	number of skin coordinate points
MM	skin station number corresponding to XF

Skin Nomenclature

AI(N)	inside skin cross-sectional area, $in.^2$
AO(N)	outside skin cross-sectional area, $in.^2$
ES(N)	skin modulus of elasticity, psi
GS(N)	modulus of rigidity, psi
RHOS(N)	density, psi
TS(N)	thickness, in.
XI(N)	inside skin coordinate, in.
XO(N)	outside skin coordinate, in.
YI N)	inside skin coordinate, in.
YO(N)	outside skin coordinate, in.
AL	mean area enclosed by skin, $in.^2$
AS	total skin cross-sectional area, $in.^2$
AX	summation of delta areas times X dimension, $in.^3$
CGS	X dimension to skin cg
EAS	spanwise stiffness, lb
ESIX	bending stiffness about x axis, $lb\text{-}in.^2$

Skin Nomenclature - Continued

GSK	torsional stiffness, lb-in.^{2}
PSI	angle between cross-section and line drawn normal to skin surface, radians
SC	mean skin perimeter divided by shear modulus, in.^{3}/lb
SIX	moment of inertia about x axis
SK	torsional constant, in.^{4}
SL	mean skin perimeter, in.
WS	weight, lb
XB	X dimension to beginning of tip fill, in.
XF	X dimension to end of nose fill, in.

Tube Nomenclature

AT(N)	tube cross-sectional area, in.^{2}
EAT(N)	spanwise stiffness, lb
ET(N)	modulus of elasticity, psi
ETIX(N)	bending stiffness about x axis, lb-in.^{2}
GT(N)	shear modulus, psi
GTK(N)	torsional stiffness, lb-in.^{2}
RHOT(N)	tube density, lb/in.^{3}
RI(N)	inside tube radius, in.
RO(N)	outside tube radius, in.
T(N)	tube wall thickness, in.
TIX(N)	moment of inertia about x axis, in.^{4}
WT(N)	tube weight, lb
XT(N)	tube coordinate, in.
AB	cross-sectional area of tubes, in.^{2}
CGT	X dimension to cg of tubes, in.

Tube Nomenclature - Continued

EAB	total spanwise stiffness, lb
E	control modulus, 10.0×10^6 psi
EBIX	total bending stiffness about x axis, lb-in.^{2}
GBK	total torsional stiffness, lb-in.^{2}
BIX	total moment of inertia, in.^{4}
BK	total torsional constant, in.^{4}
WB	total weight, lb/in.
WBX	total weight times X dimension, lb-in.

Foam Nomenclature

AI(N)	inside skin cross-sectional area, in.^{2}
RO(N)	outside tube radius, in.
XI(N)	inside skin coordinate, in.
XT(N)	tube coordinate, in.
AB	tube area, in.^{2}
ABX	tube area times X dimension, in.^{3}
AFO	area, in.^{2}
AS	area inside the skin, in.^{2}
ASX	area inside the skin times X dimension, in.^{3}
CGFO	X dimension to foam cg, in.
RHOFO	density, lb/in.^{3}
WFO	weight, lb

Fill Nomenclature

AI(N)	inside skin cross-sectional area, in.^{2}
RO(N)	outside tube radius, in.
XI(N)	inside skin coordinate, in.

Fill Nomenclature - Continued

XT(N)	tube coordinate, in.
YI(N)	inside skin coordinate, in.
AFI	fill cross-sectional area, $in.^2$
AS	area inside of skin (fill area), $in.^2$
ATX	tube area times X dimension, $in.^3$
AF	tube area (fill area), $in.^2$
AX	inside skin area times X dimension, $in.^3$
CGFI	X dimension to fill cg, in.
EAFI	spanwise stiffness, lb
EF	fill modulus of elasticity, psi
EFIX	bending stiffness about x axis, $lb\text{-}in.^2$
FIX	moment of inertia about x axis, $in.^4$
RHOFI	fill density, $lb/in.^3$
WFI	fill weight, lb/in.
XF	dimension to end of fill material

Tip Nomenclature

XI(N)	inside skin coordinate, in.
YI(N)	inside skin coordinate, in.
ATP	tip area, $in.^2$
CGTP	X dimension to tip cg, in.
EATP	spanwise stiffness, lb
ETP	modulus of elasticity, psi
ETPIX	bending stiffness about x axis
II	skin station number corresponding to XB
RHOTP	tip density, $lb/in.^3$
XB	X dimension to start at tip, in.

Tip Nomenclature - Continued

TPIX moment of inertia about x axis

WTP tip weight, lb

Composite Nomenclature

EINA bending stiffness about neutral axis (Y axis), lb-in.^2

CG X dimension to rotor cross-section cg, in.

W cross-section weight, lb/in.

EA rotor cross-section spanwise stiffness, lb

EIX rotor cross-section bending stiffness about x axis

GK rotor cross-section torsional stiffness, lb-in.^2

CNA X dimension to rotor neutral axis, in.

APPENDIX II
DRAWINGS

This appendix contains the engineering drawings for the composite UH-1D main rotor blade.

QTY REQD	PART NO	DESCRIPTION	MATERIAL	SPECIFICATION	ZONE	ITEM NO.
[illegible]	[illegible]	TUBE ADAPTER				32
[illegible]	[illegible]					31
[illegible]	[illegible]					30
[illegible]	[illegible]					29
[illegible]	[illegible]					28
[illegible]	[illegible]					27
[illegible]	[illegible]					26
[illegible]	[illegible]					25
[illegible]	[illegible]	TUBE ADAPTER				24
[illegible]	[illegible]	[illegible] END FITTING				23
AR		REINFORCEMENT [illegible]		[illegible]		22
AR		FILLER [illegible]	E GLASS	[illegible]		21
AR		FOAM SYNTHETIC		[illegible]		20
[illegible]		SPAR [illegible]	[illegible]	[illegible]		19
[illegible]		SKIN - OUTSIDE	S GLASS	[illegible]		18
[illegible]	[illegible]	CAP				17
[illegible]	[illegible]	FILLER				16
[illegible]	[illegible]	[illegible]				15
[illegible]	[illegible]	TUBE				14
[illegible]	[illegible]	TUBE				13
[illegible]	[illegible]	TUBE				12
[illegible]	[illegible]	TUBE				11
[illegible]	[illegible]	TUBE				10
[illegible]	[illegible]	TUBE				9
[illegible]	[illegible]	TUBE				8
[illegible]	[illegible]	TUBE				7
[illegible]	[illegible]	[illegible]				6
						5
						4
						3
[illegible]	-3	ASSEMBLY		[illegible]		2
[illegible]	—	ASSEMBLY		[illegible]		1

LIST OF MATERIALS

LIST OF MATERIALS

[illegible]

NOTES:

[illegible]

FIBER SCIENCE, INC.
GARDENA, CALIFORNIA

TITLE: HELICOPTER BLADE ARMY UH-1D

SIZE: D | CODE IDENT NO: 32500 | DWG NO: 48-XB-001

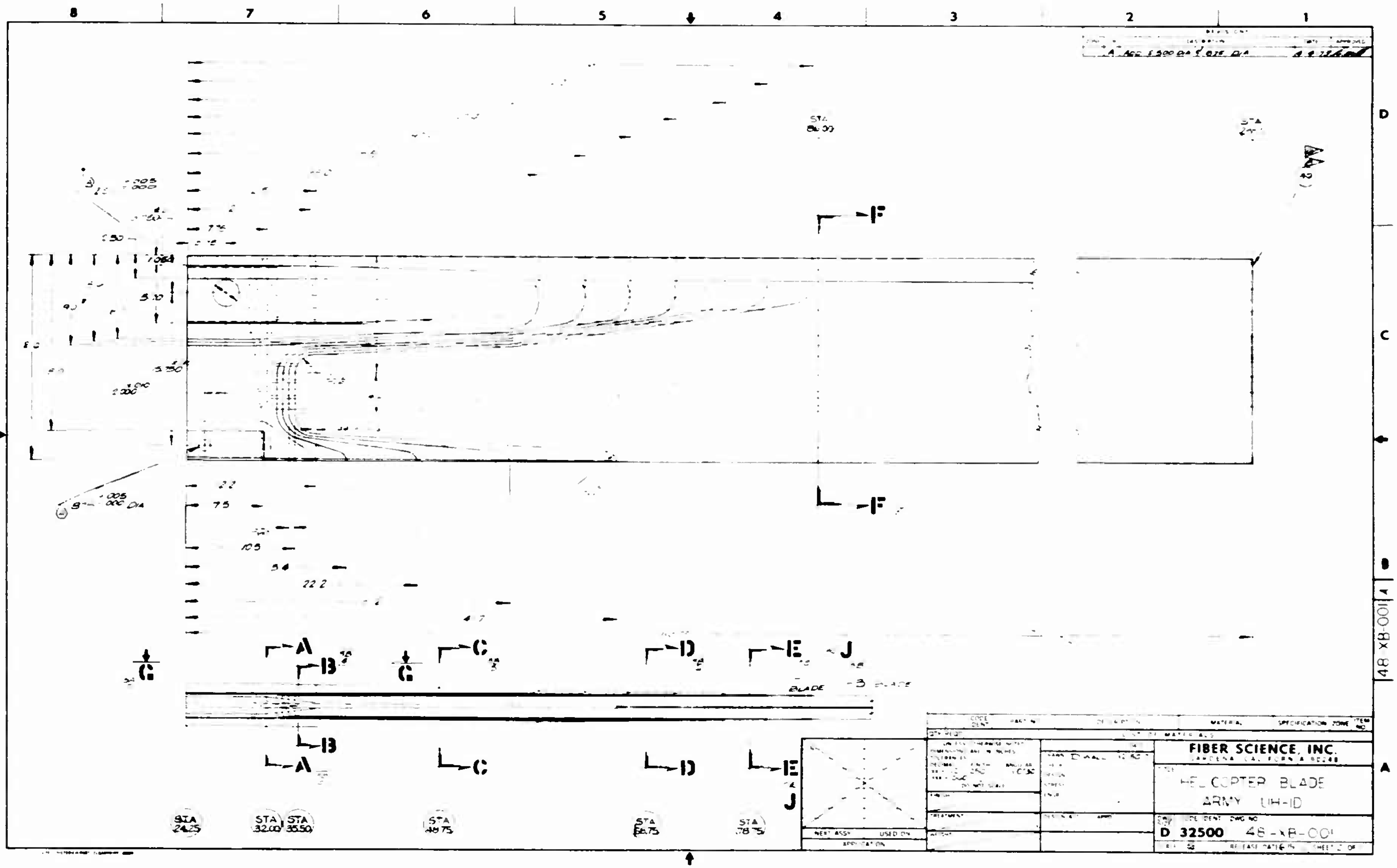
FIBER SCIENCE, INC.
HELICOPTER BLADE
ARMY UH-1D
D 32500
48-XB-001
STA 24.25
STA 32.00
STA 35.50
STA 48.75
STA 66.75
STA 78.75
STA 86.00
BLADE

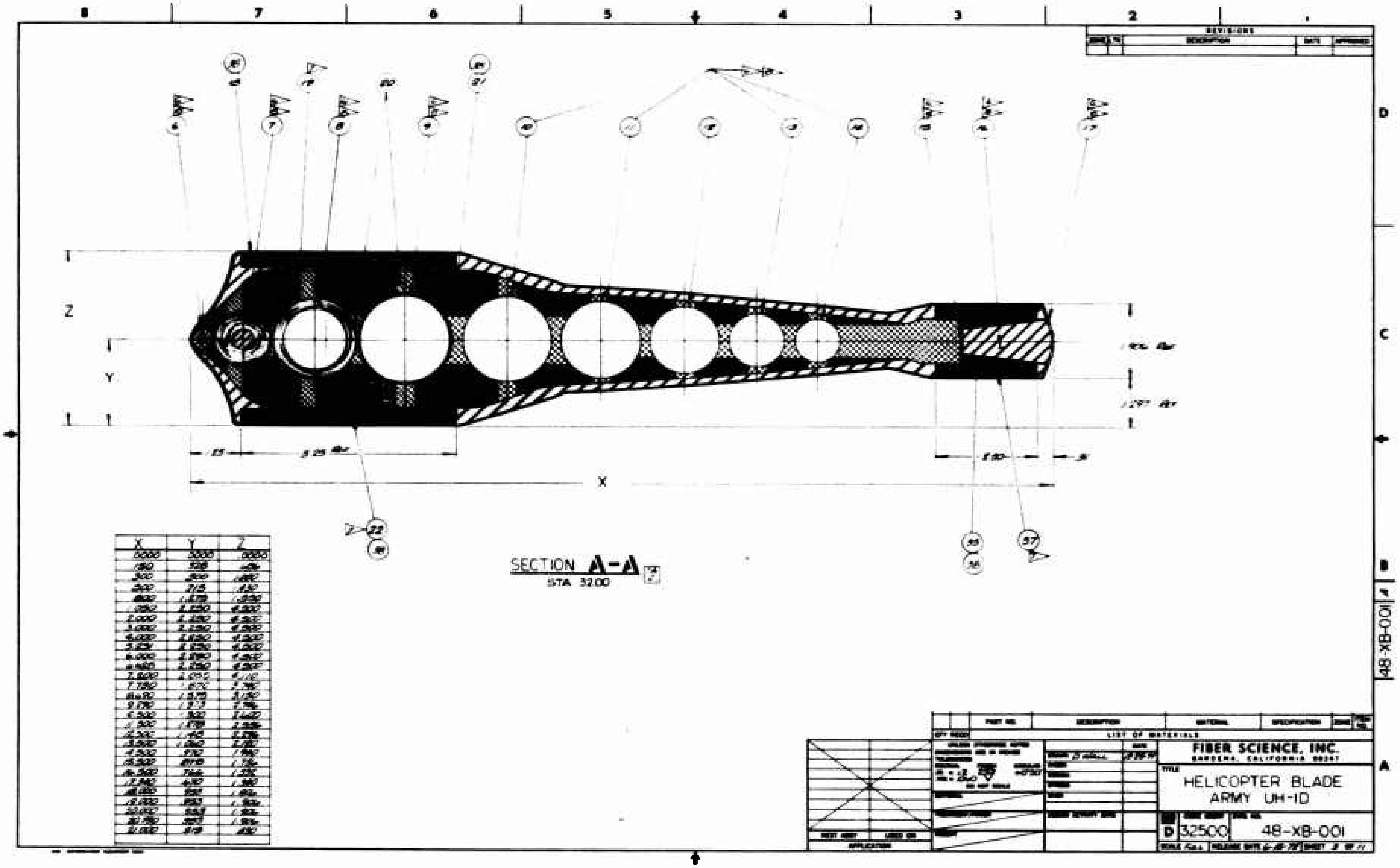

X	Y	Z
.0000	.0000	.0000
.150	[illegible]	[illegible]
.300	.200	.680
.200	.715	.830
.800	1.070	1.030
1.050	1.250	4.000
2.000	2.250	4.500
3.000	2.250	4.500
4.000	2.050	4.200
5.2[illegible]	2.250	4.000
6.000	2.050	4.200
6.450	2.250	4.200
7.000	2.095	4.110
7.750	1.875	3.750
8.450	1.575	3.150
9.750	1.373	2.7[illegible]
10.500	1.300	2.600
11.500	1.178	2.356
12.500	1.145	2.2[illegible]
13.500	1.060	2.120
14.500	.950	1.940
15.500	.875	1.750
16.500	.766	1.532
17.240	.630	1.260
18.000	.830	1.6[illegible]
19.000	.853	1.[illegible]
20.000	.833	1.[illegible]
20.750	.873	1.[illegible]
21.000	.819	.830

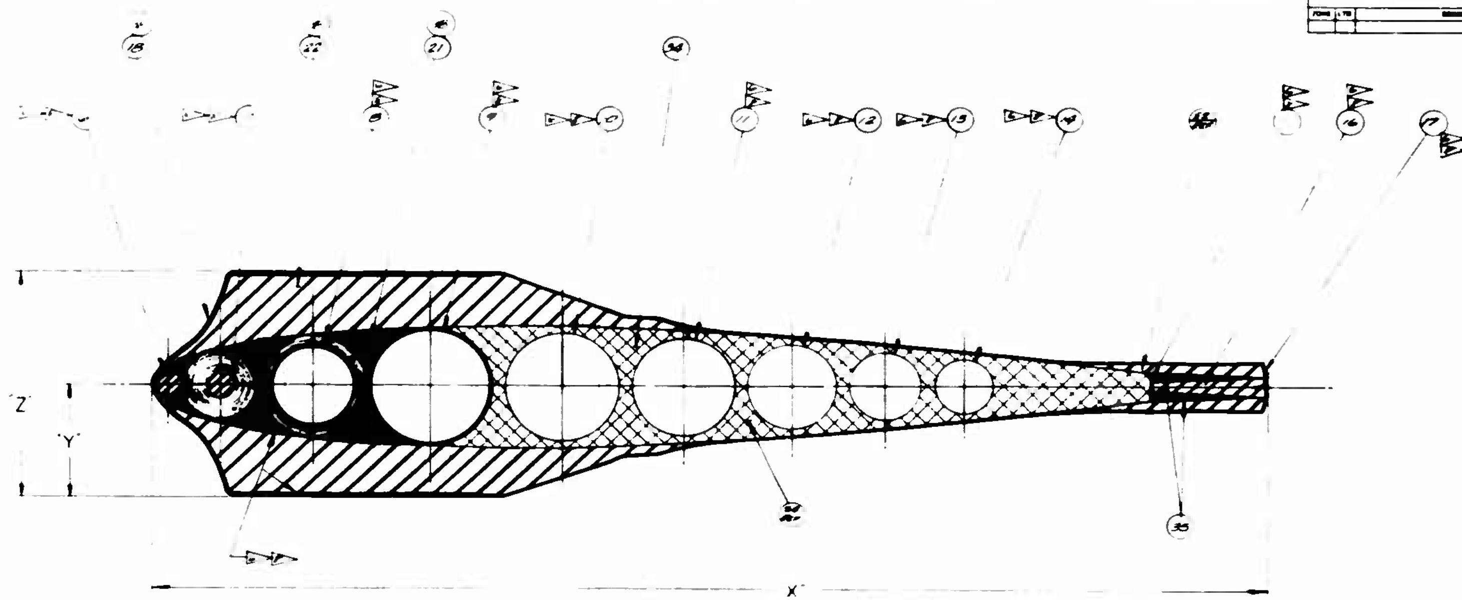

SECTION 13-13
STA 35.50

X	Y	Z
.000	.300	.000
.50	.328	.656
.300	.500	1.300
.500	.688	1.375
.600	.936	1.872
1.400	2.250	4.500
2.000	2.250	4.500
3.000	2.250	4.500
4.000	2.250	4.500
5.131	2.250	4.500
[illegible]	2.250	4.500
6.625	2.250	4.500
7.200	2.028	4.056
7.730	1.845	3.690
8.405	1.598	3.196
9.005	1.395	2.790
9.478	1.375	2.750
10.610	1.110	2.220
11.500	1.044	2.088
12.500	.966	1.932
13.500	.881	[illegible]
14.200	.787	1.576
15.500	.657	1.276
[illegible]	[illegible]	1.080
18.000	.490	.980
18.790	.500	[illegible]
19.8[illegible]	.474	.948
20.916	.440	[illegible]
21.000	.215	.43

FIBER SCIENCE, INC.
GARDENA, CALIFORNIA

HELICOPTER BLADE
ARMY UH-1D

D 32500 48-XB-001

SCALE FULL

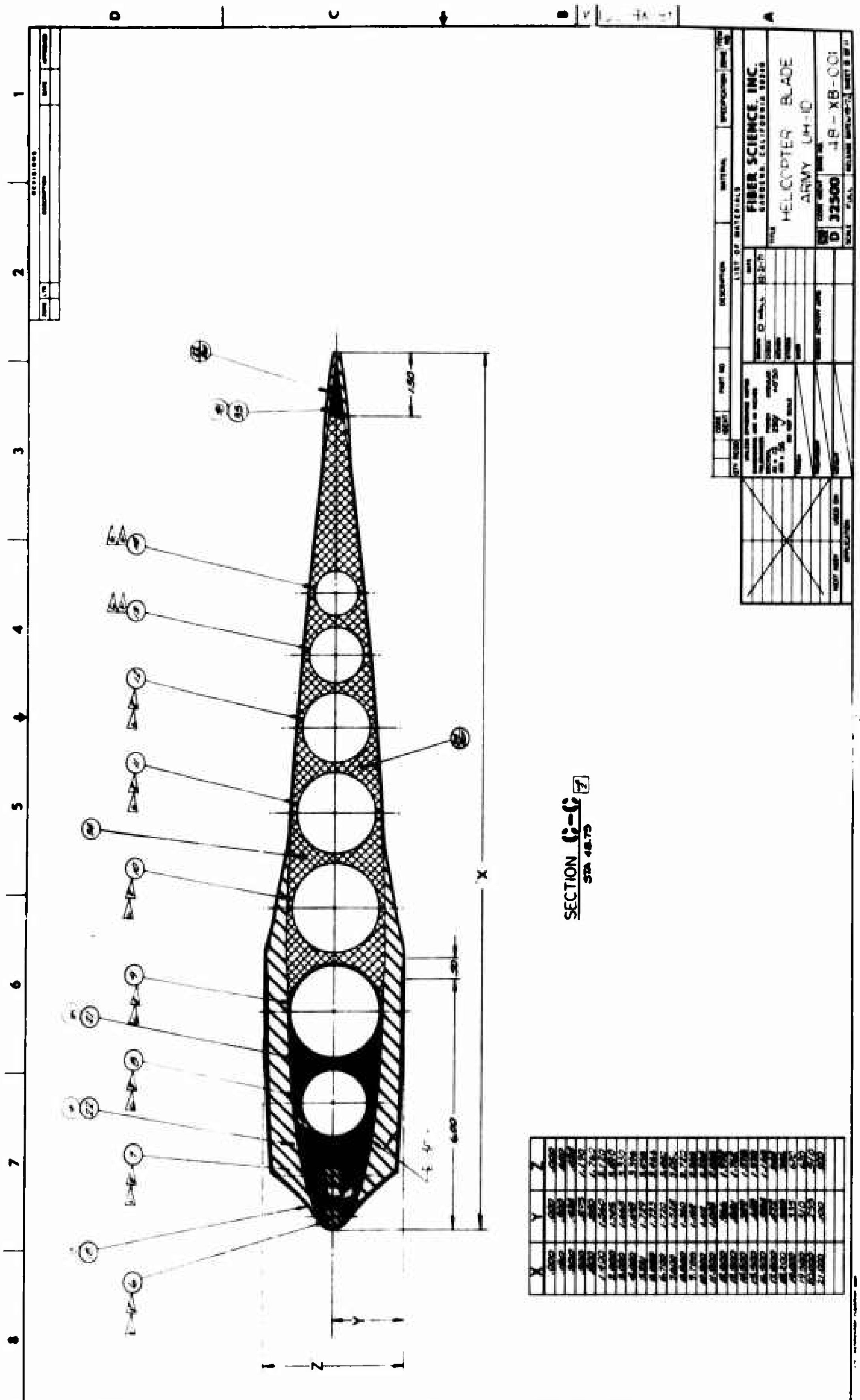
FIBER SCIENCE, INC.
HELICOPTER BLADE
ARMY UH-1D
D 32500
18-XB-001
FULL
SECTION C-C
STA 48.75
X
Y
Z
1.50

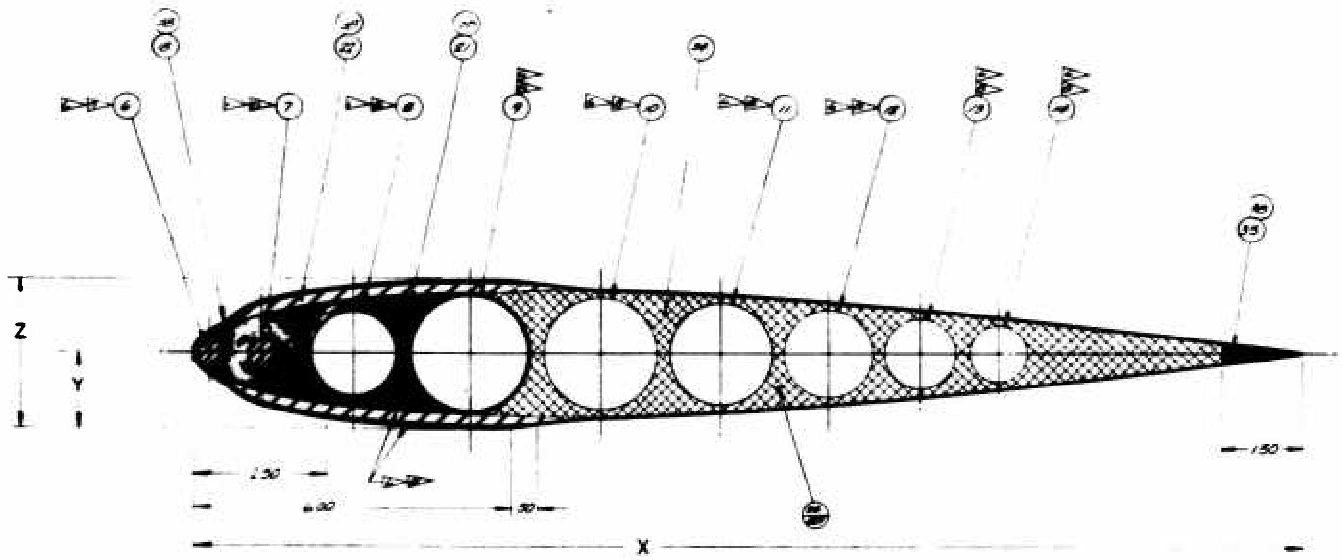

X	Y	Z
.000	.000	.000
.05	.350	.600
.300	.424	.858
.600	.537	1.074
.800	.750	1.500
1.30	.993	1.950
2.000	1.172	2.344
3.000	1.318	2.646
4.000	.798	2.788
5.251	1.457	2.878
5.479	1.462	2.880
6.500	1.350	1.370
7.750	1.248	2.496
8.500	1.218	2.430
9.500	1.165	2.336
10.500	1.112	2.224
11.500	1.048	2.096
12.500	.946	1.974
13.500	.884	1.766
14.500	.789	1.578
15.500	.687	1.378
16.500	.584	1.168
17.500	.472	.944
18.500	.353	.706
19.000	.232	.464
20.000	.125	.306
21.000	.027	.254

SECTION D-D
STA 68.75

FIBER SCIENCE, INC.
GARDENA, CALIFORNIA 90248

HELICOPTER BLADE
ARMY UH-1D

D 32500 48-XB-001

SCALE FULL

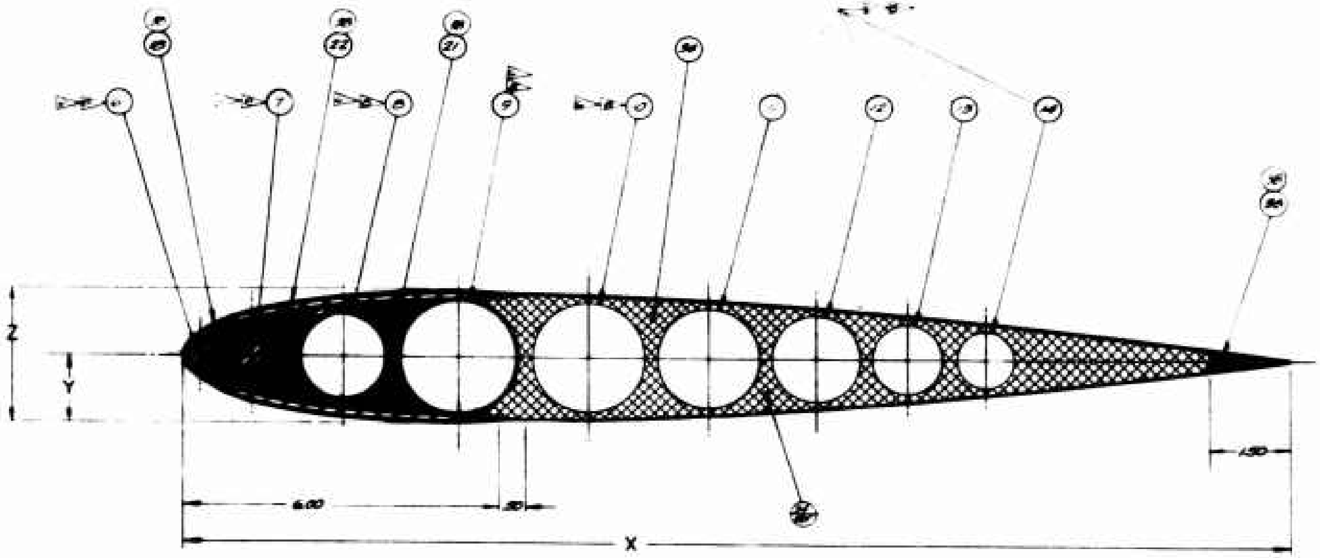

SECTION E-E
STA 78.75

X	Y	Z
.000	.000	.000
.150	.300	.460
.300	.431	.548
.600	.560	1.120
.800	.720	1.440
1.220	.810	1.620
2.000	1.050	2.130
3.000	[illegible]	[illegible]
4.000	1.278	2.556
5.281	1.320	2.640
6.150	1.320	2.640
[illegible]	[illegible]	[illegible]
7.500	[illegible]	[illegible]
[illegible]	[illegible]	[illegible]
[illegible]	[illegible]	[illegible]
[illegible]	[illegible]	[illegible]
[illegible]	[illegible]	[illegible]
[illegible]	[illegible]	[illegible]
[illegible]	[illegible]	[illegible]
[illegible]	[illegible]	[illegible]
[illegible]	[illegible]	[illegible]
[illegible]	[illegible]	[illegible]
[illegible]	[illegible]	[illegible]
[illegible]	[illegible]	[illegible]
[illegible]	[illegible]	[illegible]
[illegible]	[illegible]	[illegible]

LIST OF MATERIALS

FIBER SCIENCE, INC.
GARDENA CALIFORNIA 90248

TITLE
HELICOPTER BLADE
ARMY UH-ID

DRAWN D WALL

SIZE D | CODE IDENT 32500 | DWG NO 48-XB-001

SCALE FULL | SHEET 7 OF 11

NEXT ASSY | USED ON
APPLICATION

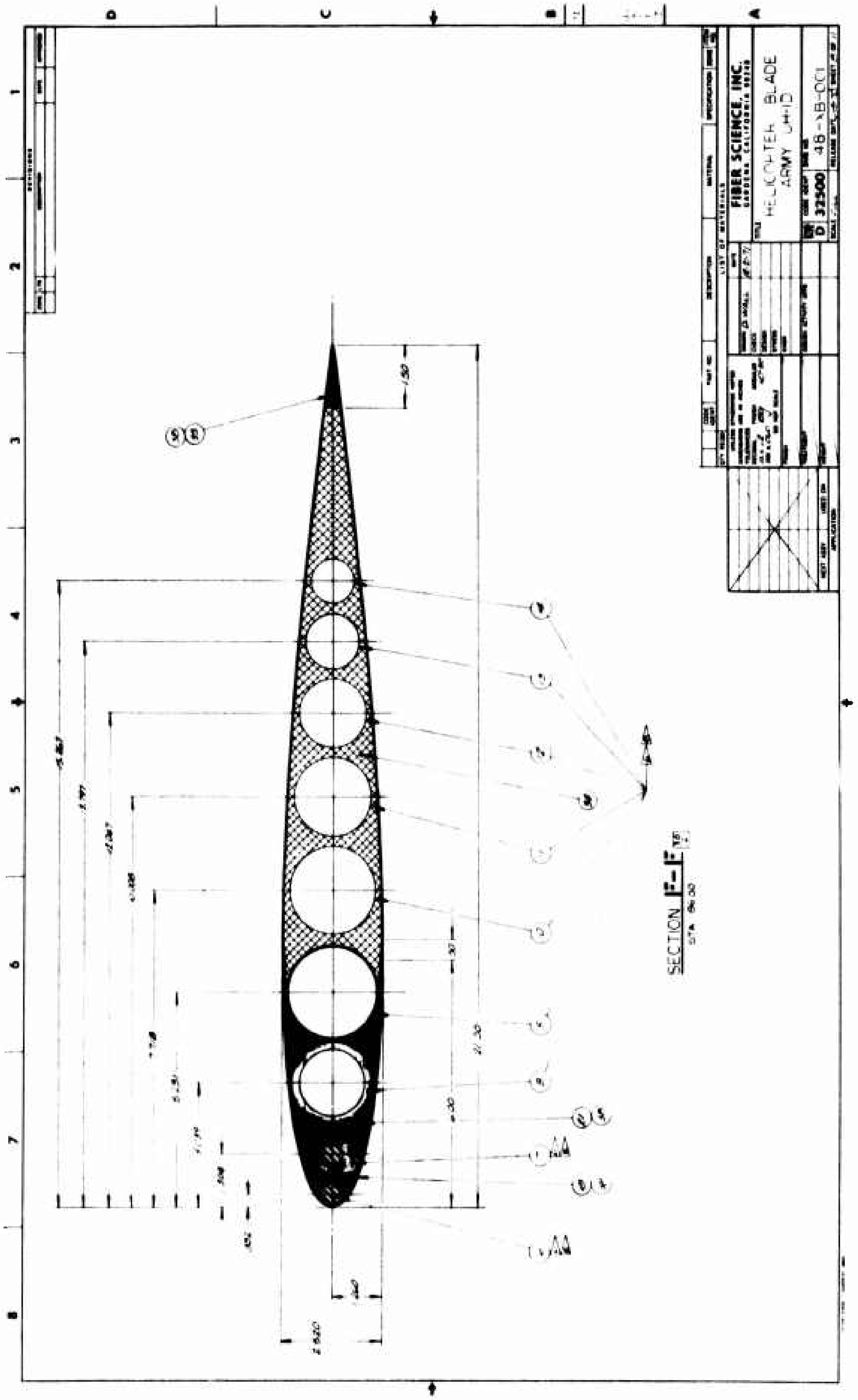
FIBER SCIENCE, INC.
GARDENA, CALIFORNIA
HELICOPTER BLADE
ARMY UH-1D
D 32500 4B-XB-001
SECTION F-F
STA 86.00

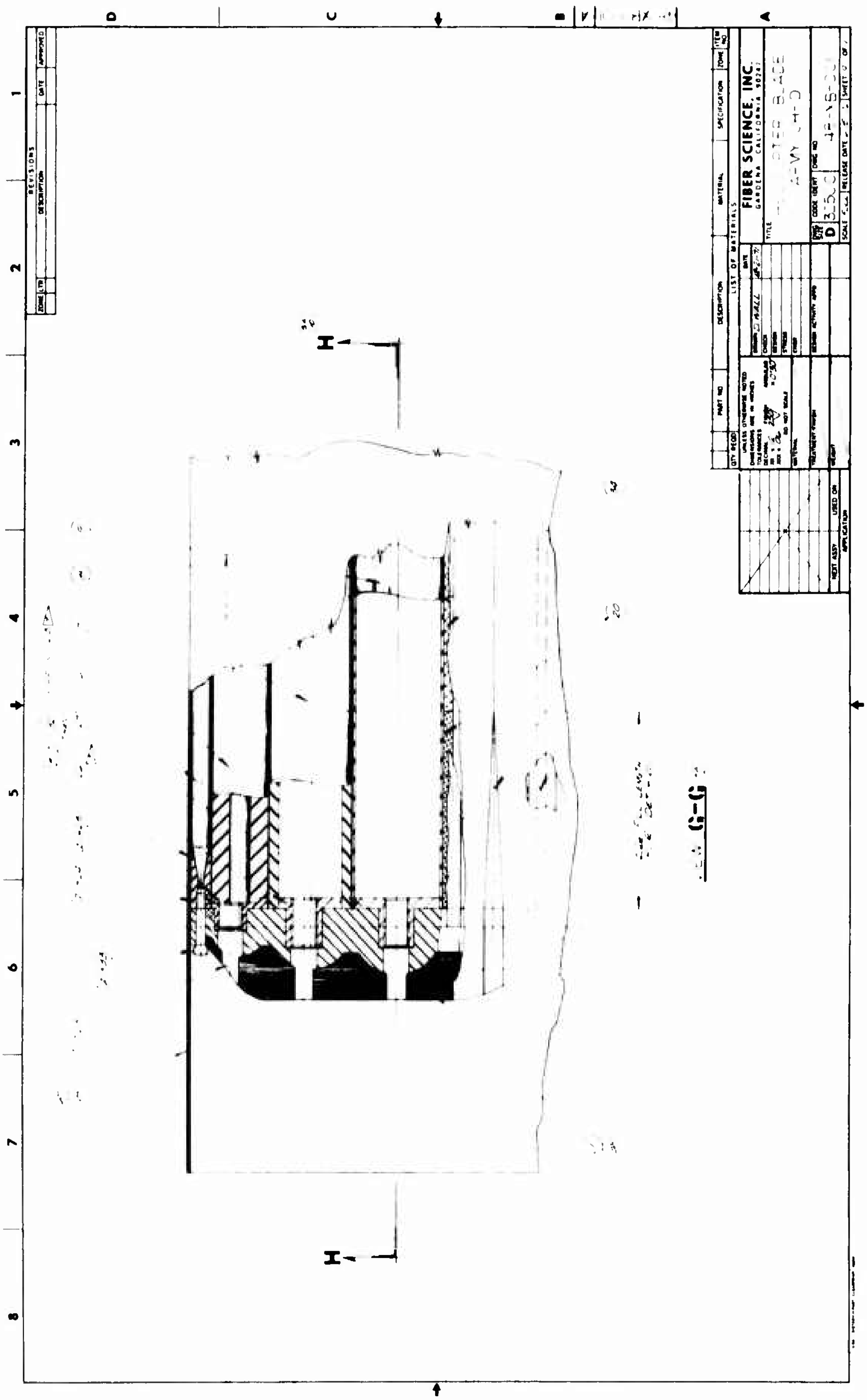
REVISIONS
LIST OF MATERIALS
FIBER SCIENCE, INC.

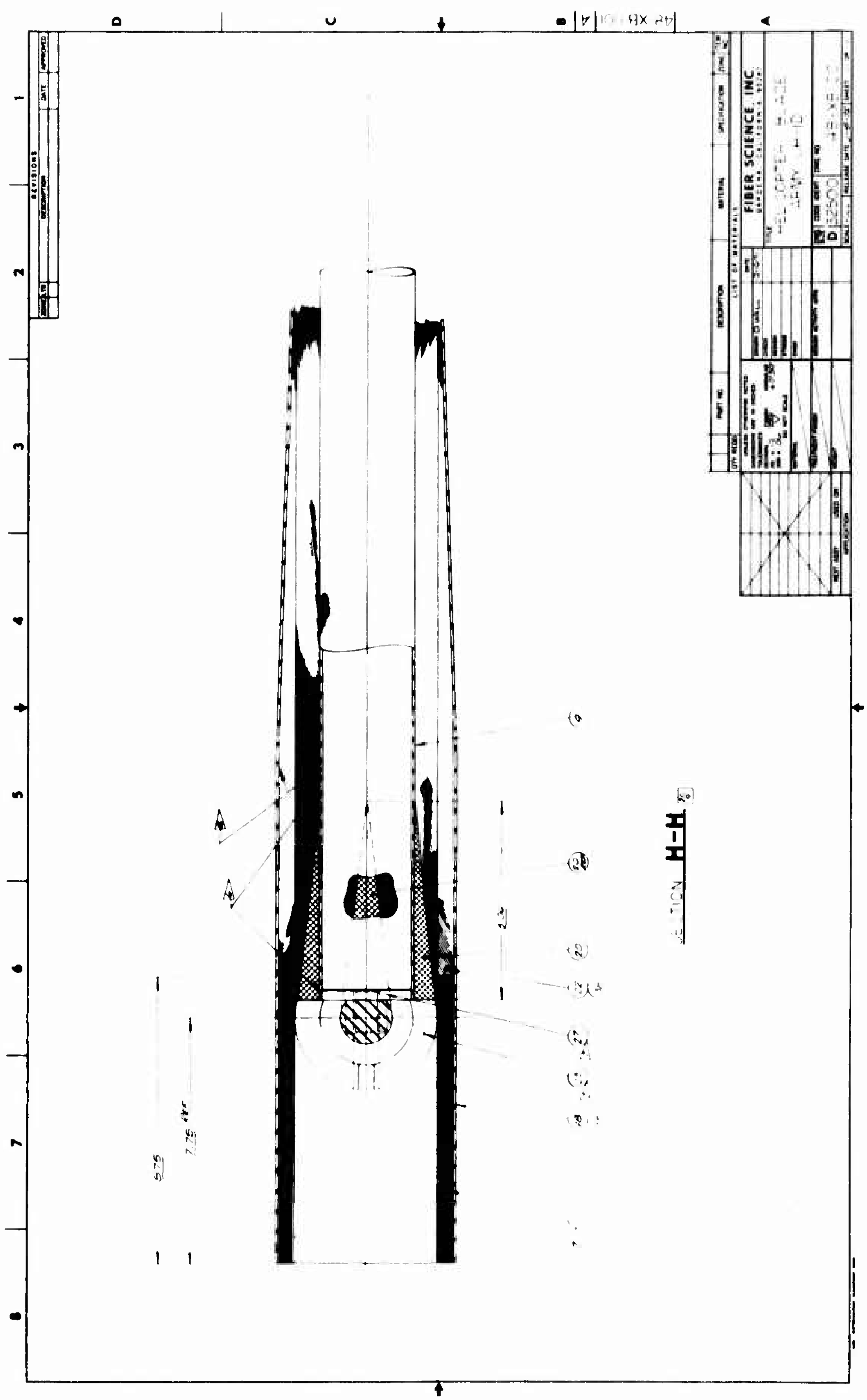
FIBER SCIENCE, INC.
H-H

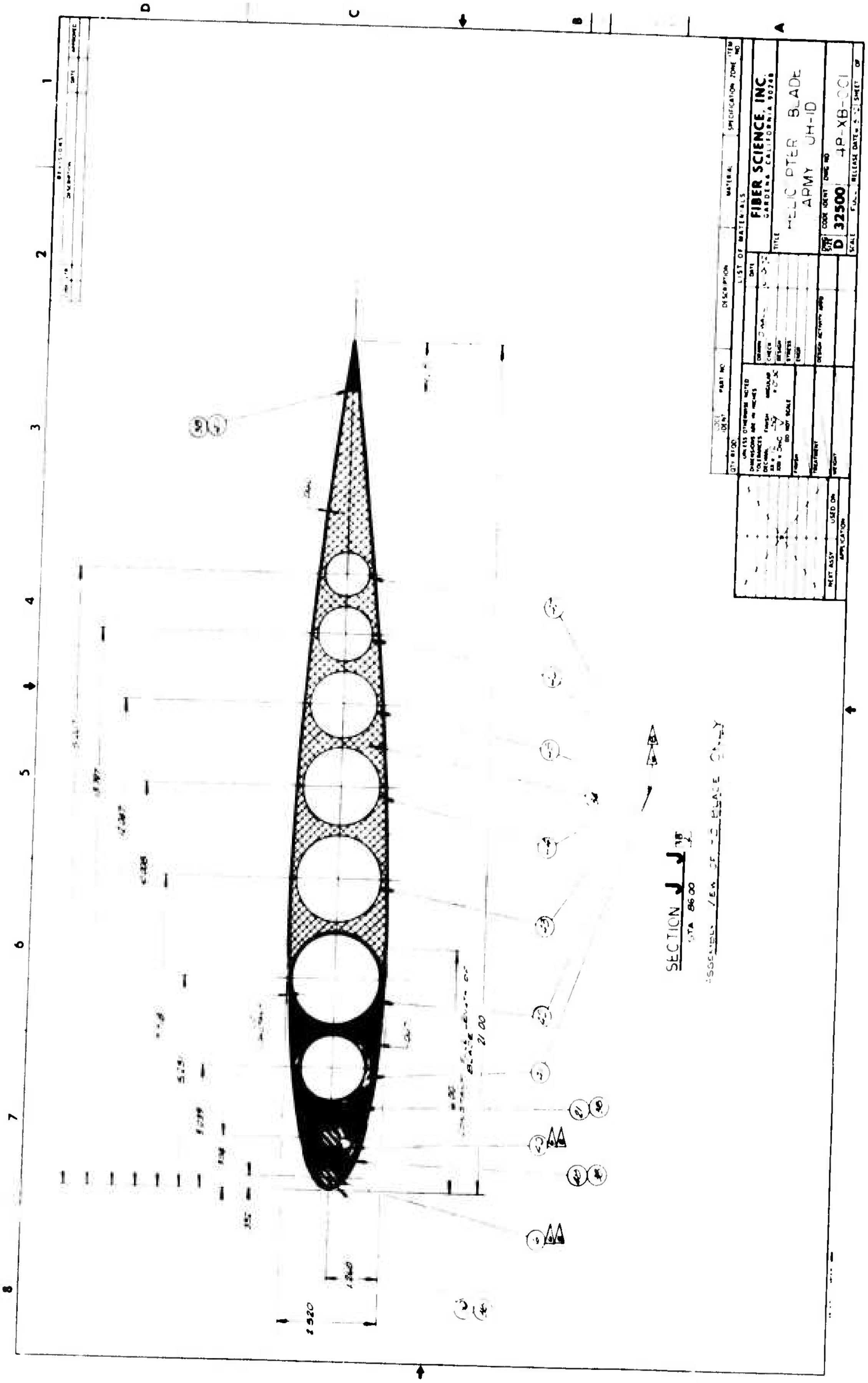
FIBER SCIENCE, INC.
32500
SECTION J J

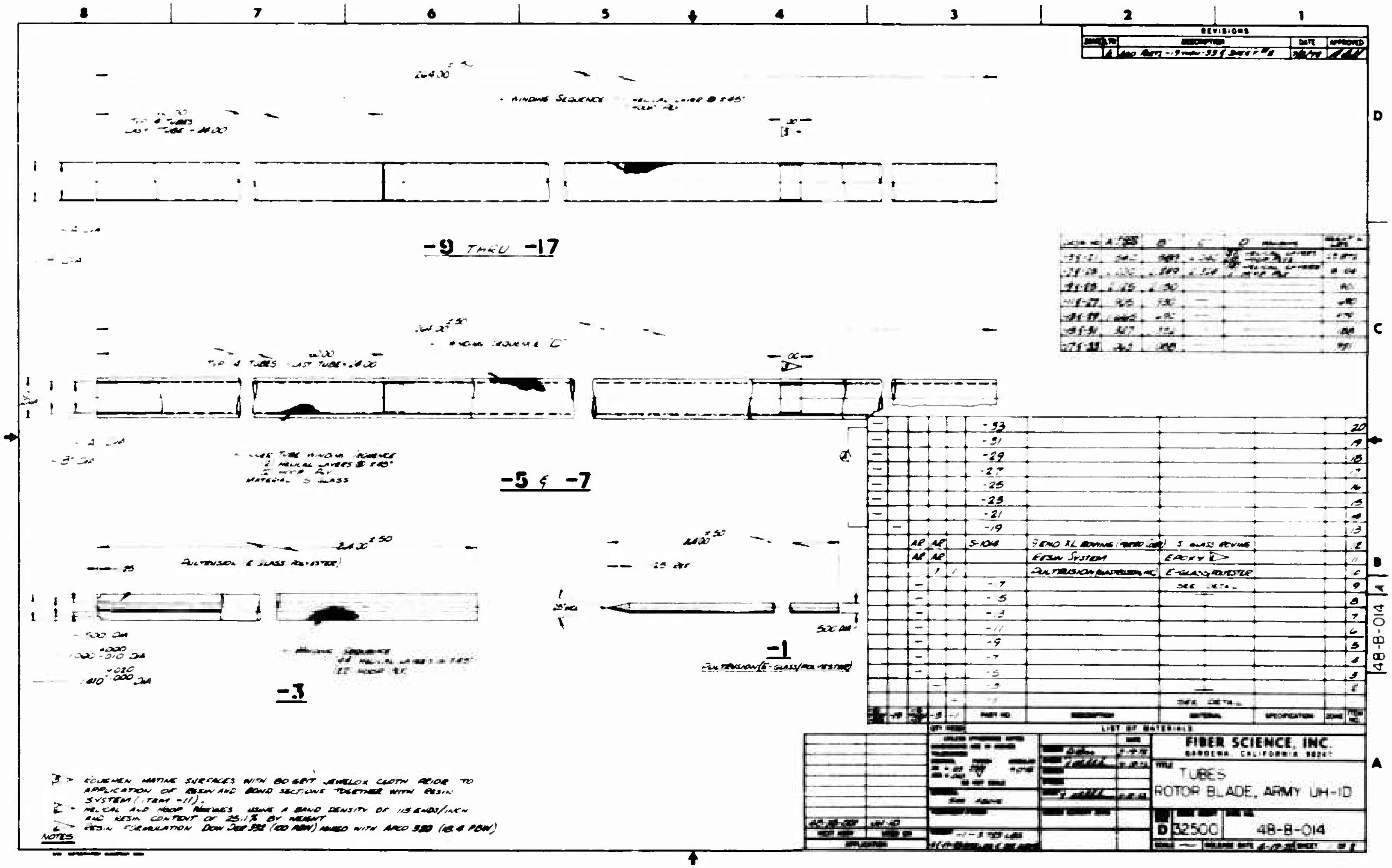
-9 THRU -17
-5 & -7
-3
-1
PULTRUSION (E-GLASS/POLYESTER)
WINDING SEQUENCE
PULTRUSION E GLASS POLYESTER
NOTES
ROUGHEN MATING SURFACES WITH 80 GRIT JEWELOX CLOTH PRIOR TO APPLICATION OF RESIN AND BOND SECTIONS TOGETHER WITH RESIN SYSTEM (ITEM -11).
HELICAL AND HOOP WINDINGS USING A BAND DENSITY OF 115 ENDS/INCH AND RESIN CONTENT OF 25.1% BY WEIGHT
RESIN FORMULATION DOW DER 332 (100 PBW) MIXED WITH APCO 380 (18.4 PBW)
S-1014
9 END XL ROVING
S GLASS ROVING
RESIN SYSTEM
EPOXY
PULTRUSION
E-GLASS/POLYESTER
SEE DETAIL
LIST OF MATERIALS
REVISIONS
FIBER SCIENCE, INC.
GARDENA, CALIFORNIA
TUBES
ROTOR BLADE, ARMY UH-1D
D 32500 48-B-014
48-B-014

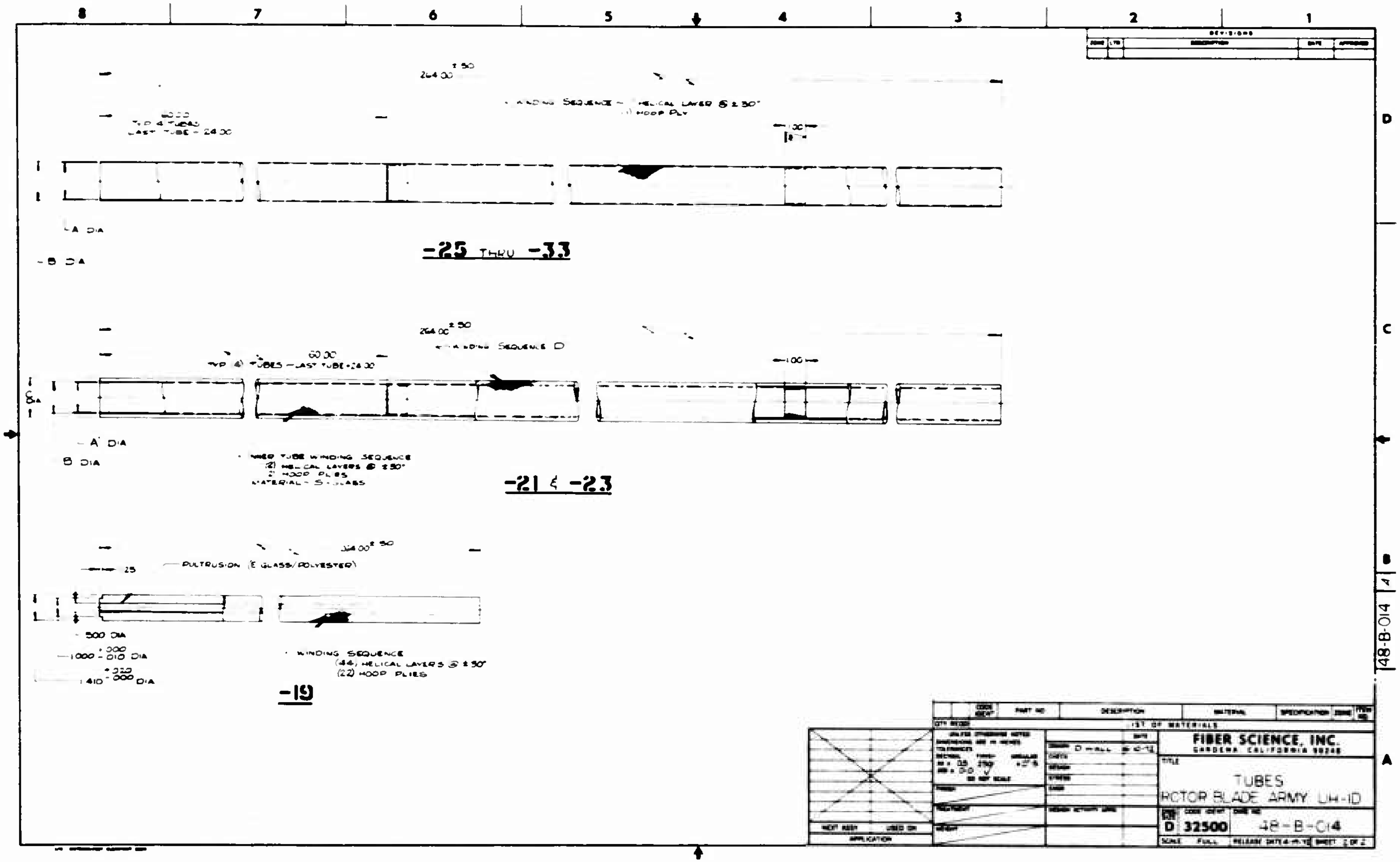

264.00 ± .50
60.00
TYP 4 TUBES
LAST TUBE - 24.00
WINDING SEQUENCE - HELICAL LAYER @ ± 30°
(1) HOOP PLY
1.00
A DIA
B DIA
-25 THRU -33
264.00 ± .50
WINDING SEQUENCE D
60.00
TYP (4) TUBES - LAST TUBE - 24.00
1.00
A DIA
B DIA
WINDING SEQUENCE
(2) HELICAL LAYERS @ ± 30°
HOOP PLIES
MATERIAL - S-GLASS
-21 & -23
264.00 ± .50
.25
PULTRUSION (E GLASS/POLYESTER)
.500 DIA
1.000 +.000 -.010 DIA
1.410 +.020 -.000 DIA
WINDING SEQUENCE
(44) HELICAL LAYERS @ ± 30°
(22) HOOP PLIES
-19
REVISIONS
LIST OF MATERIALS
FIBER SCIENCE, INC.
GARDENA, CALIFORNIA 90248
D HALL
TUBES
ROTOR BLADE ARMY UH-1D
D 32500
48-B-014
SCALE FULL
SHEET 2 OF 2
48-B-014

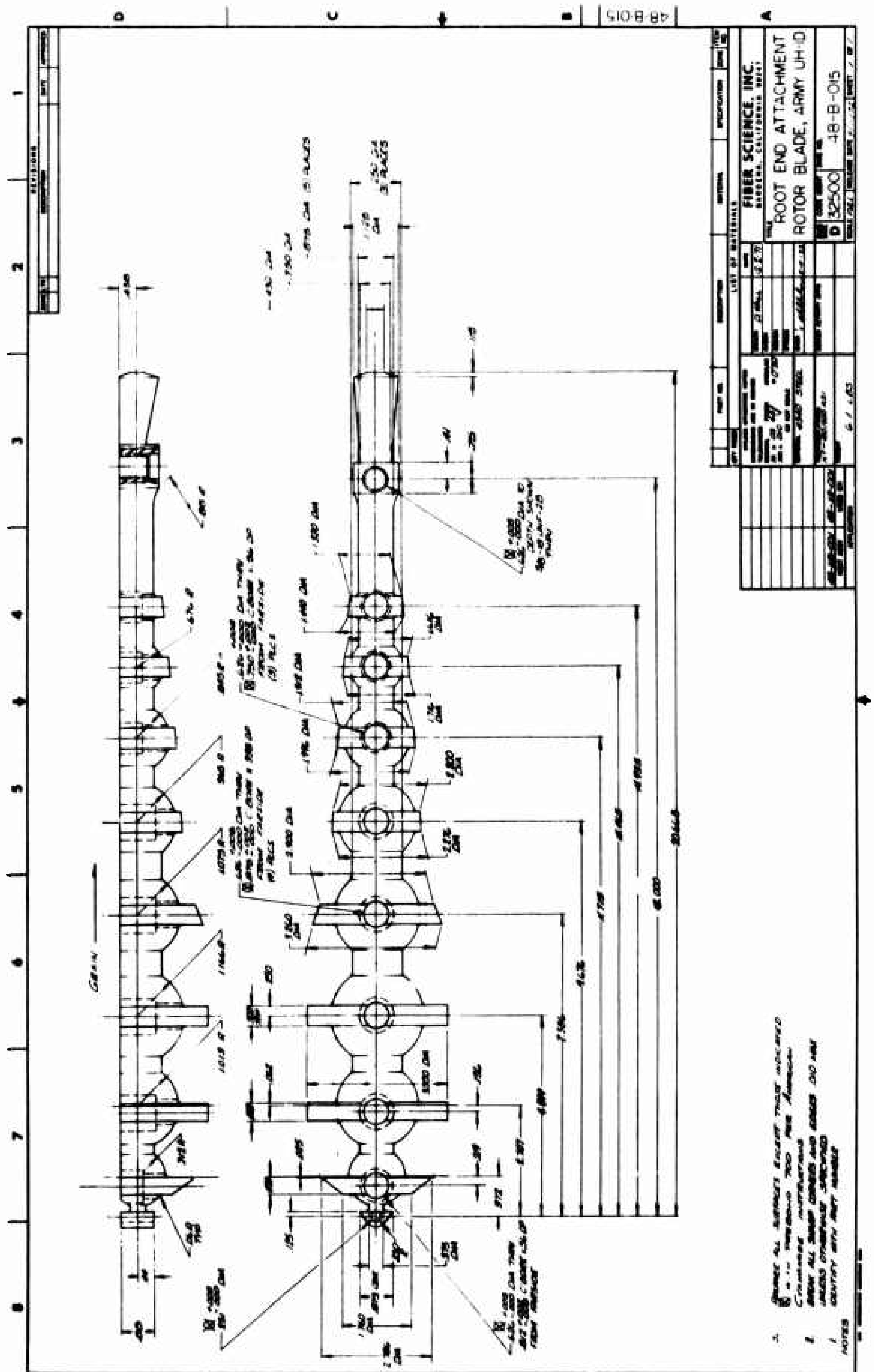
FIBER SCIENCE, INC.
ROOT END ATTACHMENT
ROTOR BLADE, ARMY UH-1D
D
32500
48-B-015
LIST OF MATERIALS
GRAIN
NOTES

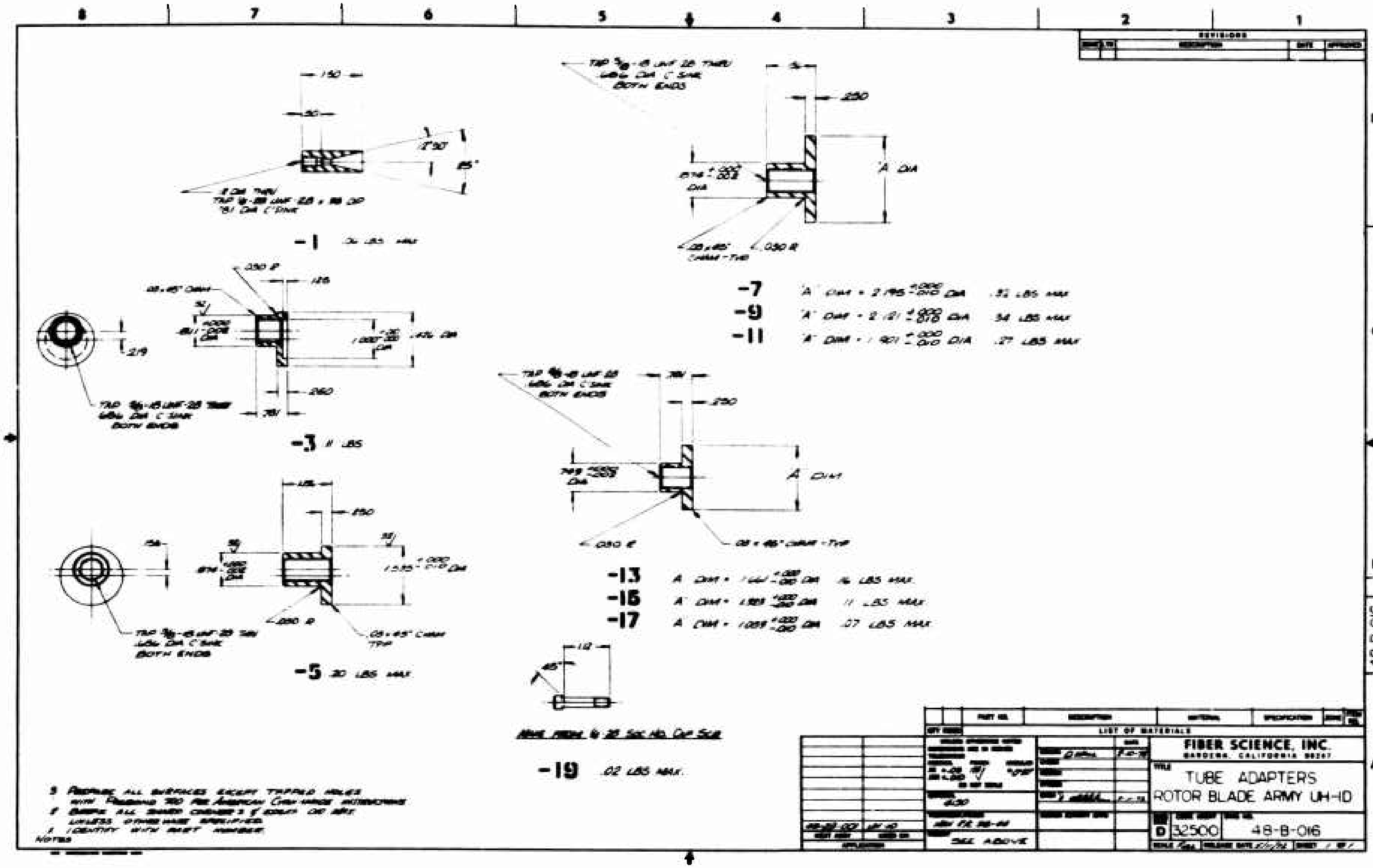
FIBER SCIENCE, INC.
TUBE ADAPTERS
ROTOR BLADE ARMY UH-1D
D 32500
48-B-016
-1
-3
-5
-7
-9
-11
-13
-15
-17
-19 .02 LBS MAX.
NOTES

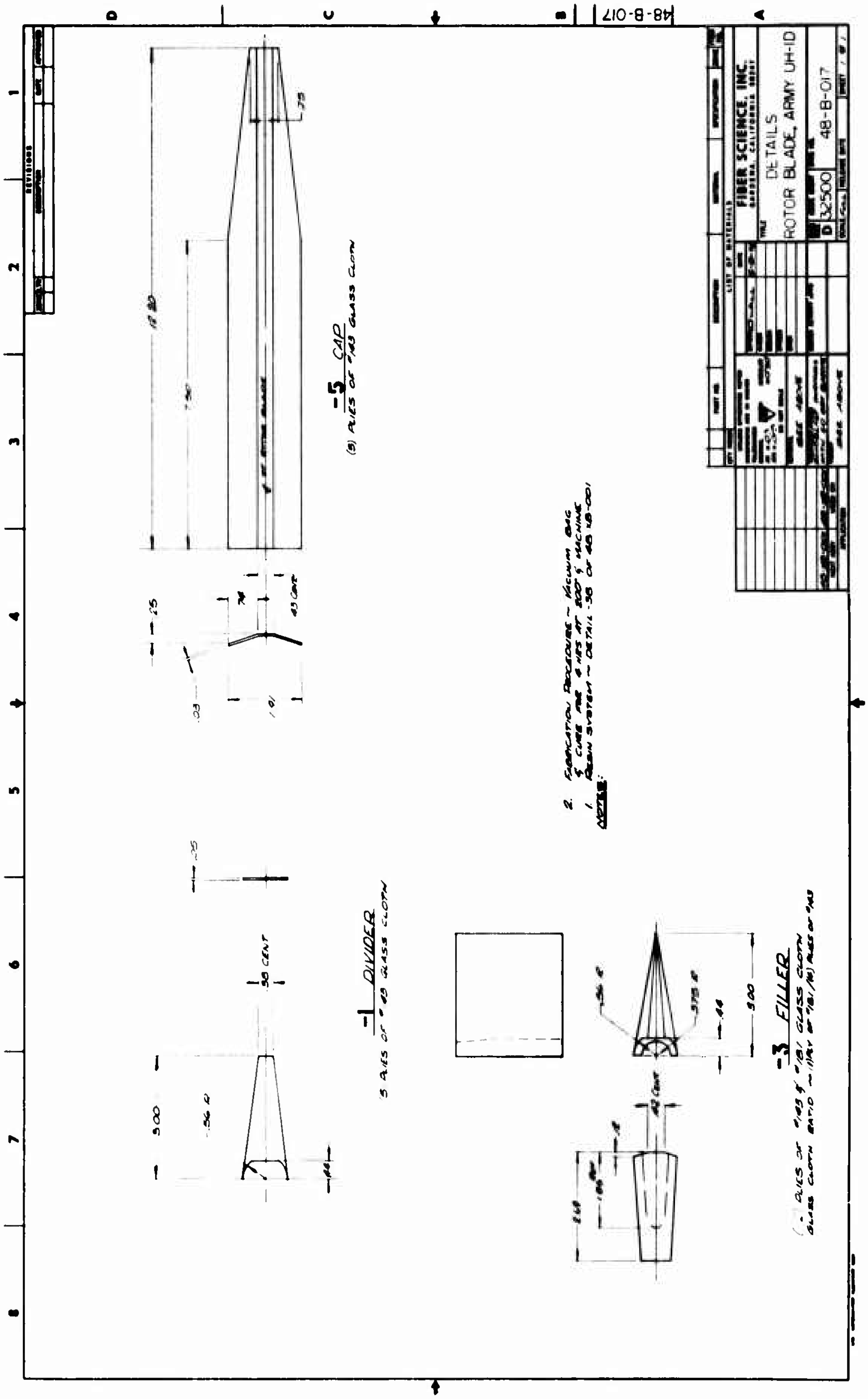
FIBER SCIENCE, INC.
DETAILS
ROTOR BLADE, ARMY UH-1D
D 32500
48-B-017
-5 CAP
-1 DIVIDER
-3 FILLER
NOTES:

APPENDIX III
STRESS ANALYSIS

This appendix contains the stress analysis for the composite UH-1D main rotor blade.

Leading Edge Longo Material

The maximum stresses in the nose fill material are:

$$\left.\begin{aligned} E &= 5.500 \times 10^6 \text{ psi} \\ c &= 1.1922 \text{ in.} \\ EI_x &= 13.86 \times 10^6 \text{ lb-in.}^2 \\ AE &= 29.41 \times 10^6 \text{ lb} \end{aligned}\right\} \text{See Table VIII}$$

$$\sigma = \frac{PE}{AE} \pm \frac{M_b cE}{EI_x}$$

Condition	$\frac{PE}{AE}$	$\frac{M_b cE}{EI_x}$	σ (psi)
1	+ 9,818	$\pm$ 21,289	+ 31,107 - 11,471
2	+ 9,818	$\mp$ 14,193	- 4,375 + 24,011
3	+ 17,018	$\pm$ 11,827	+ 28,845 + 5,191
4	+ 17,018	$\pm$ 9,462	+ 26,480 + 7,556

The single-cycle tensile strength of the nose fill material is

$$F_{tu} = .50 \times 250{,}000 + .50 \times 10{,}000 = 130{,}000 \text{ psi}$$

The estimated endurance limit of nose fill material is

$$F_{tu} = .3 \times 130{,}000 = 39{,}000 \text{ psi}$$

$$MS = \frac{39{,}000}{31{,}107} - 1 = .25$$

Trailing-Edge Longo Material

The maximum stresses in the tip fill material are:

$$\left.\begin{aligned} E &= 6.650 \times 10^6 \text{ psi} \\ c &= 21.0 - 4.935 = 16.065 \text{ in.} \\ EI_y &= 1{,}091.4 \times 10^6 \text{ lb-in.}^2 \end{aligned}\right\} \text{See Table VIII}$$

$$EA = 29.41 \times 10^6 \text{ lb}$$

$$\sigma = \frac{PE}{AE} - \frac{M_c cE}{EI_y}$$

Condition	$\frac{PE}{AE}$	$\frac{M_c cE}{EI_y}$	σ (psi)
1	+ 11,870	- 32,302	- 20,432
2	+ 11,870	+ 9,984	+ 21,854
3	+ 20,576	- 35,728	- 15,152
4	+ 20,576	+ 9,299	+ 29,875

The single-cycle tensile strength of the tip fill material is

$$F_{tu} = .50 \times 325{,}000 + .50 \times 10{,}000 = 167{,}500 \text{ psi}$$

The estimated endurance limit of the tip fill material is

$$F_{tu} = .3 \times 167{,}500 = 50{,}250 \text{ psi}$$

$$MS = \frac{50{,}250}{29{,}825} - 1 = .68$$

Tubes

The average transverse shear stress in the tubes, neglecting the skin and PVC foam load paths, is calculated as follows:

Tube area excluding the two "pultrusion" rods,

$$A = 1.5614 - .1963 + 1{,}4059 + .4406 + .0826$$

$$+ .0741 + .0648 + .0518 + .0416 = 3.5265 \text{ in.}^2$$

$$\tau = \frac{V_b}{A} = \frac{1{,}400}{3.5265} = 397 \text{ psi}$$

The estimated endurance limit shear strength of the tubes is

$$F_{su} = 10{,}000 \text{ psi}$$

$$MS = \frac{10{,}000}{397} - 1 = 24.19^*$$

*NOTE: The bending and axial load stresses have not been included.

Skin

The stresses in the skin are checked at X = 6.5 inches and at X = 19.5 inches aft from the rotor blade nose.

X = 6.5 in.

$t = .0382$ in.

$c_b = 1.260$ in.

$E = 1.834 \times 10^6$ psi

$EI_x = 13.86 \times 10^6$ lb-in.^{2}

$EI_y = 1{,}091.4 \times 10^6$ lb-in.^{2}

$EA = 29.41 \times 10^6$ lb-in.^{2}

$$EQ = 1.8617 \times 10^6 \ (20.00 - 4.935) + (21.0 - 6.5)\ .0382 \times 2 \times 1.835 \times 10^6 \left(21.00 - 4.935 - \frac{21.00 - 6.5}{2}\right)$$

$$= 45.956 \times 10^6 \text{ lb-in.}$$

$$\tau = \frac{V_c EQ}{2tEI_y}$$

$$\sigma = \frac{PE}{AE} \pm \frac{M_b c_b E}{EI_x}$$

Condition	$\frac{PE}{AE}$	$\frac{M_b c_b E}{EI_x}$	σ (psi)	τ (psi)
1	3,274	$\pm$ 7,502	+ 10,776 - 4,228	2,227
2	3,274	$\mp$ 5,001	- 1,727 + 8,275	397
3	5,675	$\pm$ 4,168	+ 9,861 + 1,507	2,618
4	5,675	$\mp$ 3,334	+ 2,341 + 9,009	772

The estimated endurance limit for the skins in tension and shear is:

$$F_{tu} = 15{,}000 \text{ psi}$$

$$F_{su} = 15{,}000 \text{ psi}$$

$$MS = \frac{1}{\sqrt{\left(\frac{10{,}776}{15{,}000}\right)^2 + \left(\frac{2{,}227}{15{,}000}\right)^2}} - 1 = .36$$

<u>X = 19.5 in.</u>

$$c_c = 19.5 - 4.935 = 14.565 \text{ in.}$$

$$EQ = 1.8617 \times 10^6\ (20.0 - 4.935) + (21.0 - 19.5) \times .0382 \times 2 \times 1.834 \times 10^6 \left(21.0 - 4.935 - \frac{21.0 - 19.5}{2}\right) = 31.265 \times 10^6 \text{ lb-in.}$$

$$\tau = \frac{V_c EQ}{2tEI_y}$$

$$\sigma = \frac{PE}{AE} - \frac{M_c c_c E}{EI_y}$$

Condition	$\frac{PE}{AE}$	$\frac{M_c c_c E}{EI_y}$	σ (psi)	τ (psi)
1	3,274	- 8,076	- 4,802	1,514
2	3,274	+ 2,496	+ 5,770	270
3	5,675	- 8,933	- 3,258	1,781
4	5,675	+ 2,325	+ 8,000	535

$$MS = \frac{1}{\sqrt{\left(\frac{8{,}000}{15{,}000}\right)^2 + \left(\frac{525}{15{,}000}\right)^2}} - 1 = .87$$

The loads on the attachment pins are calculated for the loading conditions shown in Table IV.

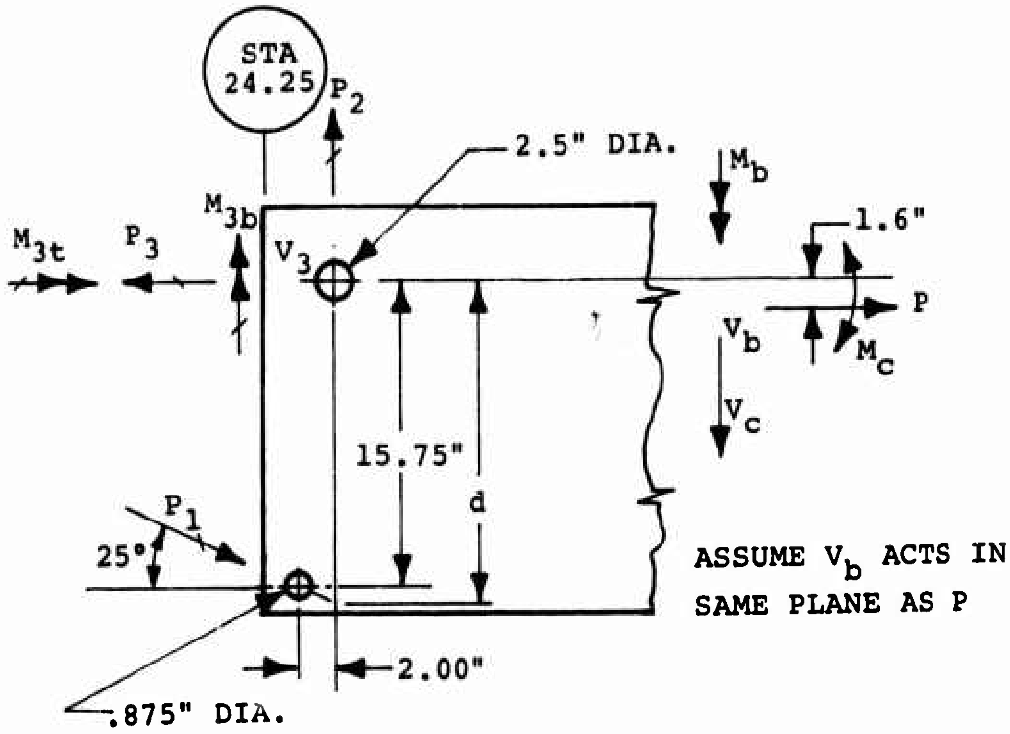

$$d = 15.75 + 2.00 \tan 25° = 16.6826 \text{ in.}$$

$$P_1 = \frac{M_c - 1.6\ P}{d \cos 25°}$$

$$P_2 = P_1 \sin 25° + V_c$$

$$P_3 = \frac{M_c + P\ (15.75 - 1.6) - 2.00 \times P_2}{15.75}$$

$$M_{3b} = M_b$$

$$M_{3t} = 1.60 \times V_b$$

$$V_3 = V_b$$

Condition	P_1 (lb)	P_2 (lb)	P_3 (lb)	M_{3b} (in.-lb)	M_{3t} (in.-lb)	V_3 (lb)
1	27,064	15,508	87,011	250,000	9,008	5,630
2	-19,564	- 7,708	45,197	-175,000	6,736	-4,210
3	25,477	16,167	125,404	145,000	5,936	3,710
4	-20,821	- 7,229	83,930	-180,000	-9,488	-5,930

The shear load on the main attachment pin is calculated as follows:

$$V = \left(\frac{P_3}{2} \pm \frac{M_{3b}}{4.5}\right) + \left(\frac{P_2}{2} \pm \frac{M_{3t}}{4.5}\right)$$

Condition	V (lb)
1	99,540
2	61,719
3	95,388
4	82,164

The main pin will bear against steel shims which are sandwiched between the GRP layers as well as a fitting which bolts to the root-end fitting that the GRP fill material wraps around.

The bearing stress in the steel shims (Σt - .104), assuming that all the load except "P_3" feeds into the shims, is

$$P = 99{,}540 - \frac{87{,}011}{2} = 56{,}034 \text{ lb}$$

$$\sigma = \frac{56{,}034}{2.5 \times .105} = 213{,}462 \text{ psi}$$

The steel shims are made of AM-355 or an equivalent,

$$F_{tu} \approx 200{,}000 \text{ psi}$$

$$F_{bru} \approx 320{,}000 \text{ psi}$$

$$MS = \frac{320{,}000}{213{,}462} - 1 = .50$$

The shear stress in the 2.5-inch-diameter pin is

$$\tau = \frac{99{,}540}{\pi \times 1.25^2} = 20{,}277 \text{ psi}$$

The aft (.875-in.-dia) pin will feed all its load into the steel shims. The bearing stress in the steel and the shear stress on the pin are:

$$\sigma = \frac{27{,}064}{.875 \times .105 \times 2} = 147{,}086 \text{ psi}$$

$$MS = \frac{320{,}000}{147{,}086} - 1 = 1.75$$

$$\tau = \frac{27{,}064}{2 \times \pi \times .4325^2} = 22{,}556 \text{ psi}$$

NOTE: The 2.5- and .875-inch-diameter pins are subjected to the same bearing stresses as the shims; therefore, they should be case-hardened on their surface.

DISTRIBUTION

Director of Defense Research & Engineering	1
Assistant Secretary of the Army (R&D)	1
Assistant Chief of Staff for Force Development, DA	1
Deputy Chief of Staff for Logistics, DA	1
Chief of Research & Development, DA	1
Army Aviation Systems Command	2
Hq, Army Air Mobility R&D Laboratory	2
Systems Research Integration Office, AMRDL	1
Ames Directorate, Army Air Mobility R&D Laboratory	1
Eustis Directorate, Army Air Mobility R&D Laboratory	33
Langley Directorate, Army Air Mobility R&D Laboratory	2
Lewis Directorate, Army Air Mobility R&D Laboratory	2
Army Aviation Systems Test Activity	2
Army R&D Group (Europe)	2
Army Scientific & Technical Information Team(Europe)	1
Army Advanced Materiel Concepts Agency	1
Army Ballistic Research Laboratories	1
Army Fuels & Lubricants Laboratory	1
Army Research Office	1
Army Materials & Mechanics Research Center	2
Army Plastics Technical Evaluation Center	1
Army Materiel Systems Analysis Agency	1
USACDC Aviation Agency	1
Picatinny Arsenal	2
Army Aviation School	1
Army Agency for Aviation Safety	1
Army Field Office, AFSC	1
Air Force Office of Scientific Research	1
Air Force Flight Test Center	2
Air Force Materials Laboratory	1
Air Force Flight Dynamics Laboratory	1
Naval Air Systems Command	3
Chief of Naval Research	2
Naval Air Development Center	2
Ames Research Center, NASA	1
Langley Research Center, NASA	2
Lewis Research Center, NASA	1
Scientific & Technical Information Facility, NASA	2
Eastern Region Library, FAA	1
Federal Aviation Administration, Washington	1
Government Printing Office	1
Defense Documentation Center	12